



JUSCELINA ARCANJO DOS SANTOS

**FISIOLOGIA DE FLORESTAS PLANTADAS NO BRASIL: EFEITOS CLIMÁTICOS
E GENÉTICOS**

**LAVRAS – MG
2022**

JUSCELINA ARCANJO DOS SANTOS

**FISIOLOGIA DE FLORESTAS PLANTADAS NO BRASIL: EFEITOS CLIMÁTICOS
E GENÉTICOS**

Tese apresentada à Universidade Federal de Lavras, como parte das exigências do Programa de Pós-Graduação em Engenharia Florestal, área de concentração em Silvicultura e genética florestal, para a obtenção do título de Doutor.

Dr. Otavio Camargo Campoe
Orientador

**LAVRAS – MG
2022**

**Ficha catalográfica elaborada pelo Sistema de Geração de Ficha Catalográfica da Biblioteca
Universitária da UFLA, com dados informados pelo(a) próprio(a) autor(a).**

Santos, Juscelina Arcanjo dos.

Fisiologia de florestas plantadas no Brasil: efeitos climáticos e genéticos / Juscelina Arcanjo dos Santos. - 2022.

101 p.

Orientador(a): Otávio Camargo Campoe.

Tese (doutorado) - Universidade Federal de Lavras, 2022.
Bibliografia.

1. Silvicultura. 2. ecofisiologia. 3. fotossíntese. I. Campoe, Otávio Camargo. II. Título

JUSCELINA ARCANJO DOS SANTOS

**FISIOLOGIA DE FLORESTAS PLANTADAS NO BRASIL: EFEITOS CLIMÁTICOS
E GENÉTICOS**

**ECOPHYSIOLOGY OF PLANTED FORESTS IN BRAZIL: CLIMATE AND
GENETIC EFFECTS**

Tese apresentada à Universidade Federal de Lavras, como parte das exigências do Programa de Pós-Graduação em Engenharia Florestal, área de concentração Silvicultura e genética florestal, para a obtenção do título de Doutor.

APROVADA em 03 de março de 2022
Dr. Otávio Camargo Campoe UFLA
Dr. Joannès Guillemot CIRAD
Dr. Clayton Alcarde Alvares Empresa SUZANO
Dr. Túlio Barroso Queiroz Empresa Bracell
Dra. Dra. Ana Carolina Maioli Campo UFLA

Prof. Dr. Otavio Camargo Campoe
Orientador

**LAVRAS – MG
2022**

*A minha minha mãe, minha irmã e meus amados
sobrinhos, por todo amor e carinho.*

AGRADECIMENTOS

Agradeço a Deus pela vida, paciência, sabedoria e pela oportunidade de realizar este grande sonho.

À Universidade Federal de Lavras pela oportunidade de viver momentos maravilhosos que ficarão pra sempre em meu coração, por todo suporte e estrutura para realizar minha pesquisa e pelos conhecimentos adquiridos durante esses quatro anos.

Ao Programa de Pós-Graduação em Engenharia Florestal, pelo aprendizado e oportunidade. À Coordenação de Aperfeiçoamento de Pessoal de Nível Superior (CAPES), pela concessão da bolsa, código de financiamento 001.

A minha mãe Santa e a minha irmã Mara por todo amor e dedicação nessa caminhada e aos meus amados sobrinhos Enzo e Sarah por todo amor, carinho e alegrias

Ao meu orientador, Otávio Camargo Campoe por todo apoio e orientação neste trabalho, por me ensinar a pensar grande e por ser inspiração profissional.

Aos membros da banca pelo aceite em contribuir com o trabalho.

Ao meu amigo Cléber Rodrigo de Souza por toda parceria, ensinamentos, ajuda imprescindível no desenvolvimento deste trabalho, paciência e pela amizade. Seu profissionalismo e dedicação é admirável Cléber!

Ao pesquisador Michael Aspinwall da Universidade de Alburn pelas sugestões, correções e *insights* que contribuiram para a melhoria deste trabalho.

Ao Instituto de Pesquisas e Estudos Florestais (IPEF), pela parceria na concessão dos dados obtidos nos diversos projetos como TECHS, BEPP, PPPIB, EUCFLUX e ao CIRAD.

A minha grande amiga Mariana Morelli por todo carinho, amizade, apoio e incentivo profissional nesses mais de 10 anos de Engenharia Florestal e de amizade

Ao Paulo André Trazzi, por compartilhar esse período da vida comigo, pelas trocas de experiências e por todo amor, carinho e paciência.

As colegas de trabalho Anny e Lorena, que se tornaram grandes amigas, obrigada pelo incentivo, companheirismo e parceria durante este período.

Aos amigos que o doutorado me apresentou, em especial agradeço a: Fernanda Leite, Douglas Gonçalves, Lucas Rocha, Vitor Abreu, Daniel Dantas, Fabrina e Denys Souza pelas longas conversas, almoços no RU, cafés da tarde, tornando essa caminhada mais alegre e mais leve.

Agradeço aos docentes do Departamento de Ciências Florestais em especial a professora Dulcinéia de Carvalho e ao professor Gilvano Ebling Brondani pelos ensinamentos, paciência oportunidades de trabalho e convivência.

Agradeço aos colegas de trabalho e professores do laboratório de estudos em Silvicultura e Restauração Florestal (LASERF) pela convivência, pelas conversas e por compartilharem o dia a dia comigo, em especial ao professor Lucas Amaral por ser exemplo de trabalho e dedicação, pelos diálogos, ensinamento e disposição em ajudar, a professora Soraia e aos amigos Rodolfo, Anatoly, Clarissa, Bruna e Mariana.

Ao núcleo de Estudos em Silvicultura (NES) pelas trocas de experiência, aprendizados e pelos bons momentos compartilhados.

Aos demais colegas e amigos que tive a oportunidade de conhecer, conviver e trocar experiências, que direta ou diretamente contribuíram com a minha formação e realização deste trabalho.

Enfim, Muito obrigada a todos!!!

“Quanto mais me aprofundo na Ciência mais me aproximo de Deus”.

Albert Einstein

RESUMO

A fotossíntese e a condutância estomática são processos essenciais no funcionamento dos ecossistemas. A fotossíntese é o processo chave no ciclo do carbono, sendo que essa troca de carbono e água pela planta é regulada pelos estômatos, processo que é responsável por equilibrar a captação fotossintética de CO₂ contra a necessidade de controlar a perda de água das folhas. Estes processos influenciam a eficiência do uso da água das plantas, o crescimento, a distribuição da vegetação no ecossistema e a produtividade das florestas. Entender como estes processos fisiológicos são influenciado por fatores ambientais e genéticos, fornece informações para melhorar a simulação da produtividade das florestas e também para entender como as plantas irão se comportar em cenários futuros de mudanças climáticas. Dentro deste contexto, este trabalho tem o objetivo de modelar a capacidade fotossintética e a condutância estomática das florestas de eucalipto e pinus no Brasil em dois artigos. No primeiro artigo utilizamos o modelo de Farquhar et al. (1980) para obter os parâmetros V_{cmax} , J_{max} e J_{max}/V_{cmax} , e analisamos a influência da idade, das variáveis temperatura de crescimento, isto é, a temperatura média da média diária aos 10 e 30 dias antes da medição de fotossíntese e precipitação total aos 10 e 30 dias, além de avaliar a influencia dos grupos climáticos de eucalipto e das diferentes espécies de pinus nestes parâmetros. Nossos resultados mostram que a capacidade fotossintética das florestas apresenta diferenças entre os grupos funcionais, as variáveis temperatura de crescimento e precipitação aos 10 e 30 dias antes da coleta de dados influenciou os parâmetros fotossintéticos, sugerindo aclimação da fotossíntese foliar. A idade da população influenciou a capacidade fotossintética ao longo do crescimento. Florestas mais velhas possuem maior J_{max} . Não houve diferenças entre os grupos climáticos subtropical e tropical, demonstrando uma adaptação dos genótipos as condições ambientais do Brasil, O segundo artigo investiga o desempenho de três modelos de condutância estomática (BB, BBL e USO) para identificar o melhor modelo, além de analisar como a condutância estomática e a eficiência do uso da água varia entre os grupos funcionais e entre genótipos nas plantações florestais brasileiras. Nossos resultados, revelaram que os modelo BBL e USO tiveram melhor desempenho nos dados das florestas do Brasil. As espécies do grupo pinus tiveram o maior parâmetro de resposta da condutância estomática (g_1) e, conseqüentemente, a menor eficiência no uso da água quando comparado aos genótipos do grupo eucalipto. Dentro do grupo de eucalipto, os genótipos de apresentaram diferenças nas respostas estomática, indicando que além das características do genótipo, as condições climáticas locais também podem ter influenciado a variação em g_1 . Encontramos nestes dois artigos parâmetros fotossintéticos V_{cmax} , J_{max} , J_{max}/V_{cmax} e parâmetro de resposta estomática (g_1) modelado pelos três modelos de g_s , mais utilizados nos modelos de vegetação global e modelos baseados em processos para vários genótipos de eucalipto e pinus. Nosso estudo ampliará o banco de dados de parâmetros fisiológicos para as florestas plantadas do Brasil possibilitando o uso em estudos de modelagem global da vegetação.

Palavras-chave: Fotossíntese, condutância estomática, modelagem ecofisiológica, eucalipto, pinus

ABSTRACT

Photosynthesis and stomatal conductance are essential processes in the functioning of ecosystems. Photosynthesis is the key process in the carbon cycle, and this exchange of carbon and water by the plant is regulated by the stomata, a process that is responsible for balancing the photosynthetic uptake of CO₂ against the need to control the loss of water from the leaves. These processes influence the water use efficiency of plants, growth, the distribution of vegetation in the ecosystem and the productivity of forests. Understanding how these physiological processes are influenced by environmental and genetic factors provides information to improve the simulation of forest productivity and also to understand how plants will behave in future climate change scenarios. Within this context, this work aims to model the photosynthetic capacity and stomatal conductance of eucalypt and pine forests in Brazil in two articles. In the first article, we used the model by Farquhar et al., (1980) to obtain the parameters V_{cmax} , J_{max} and J_{max}/V_{cmax} , and we analyzed the influence of age, growth temperature, this is, at the average temperature of the daily average 10 and 30 days before the photosynthetic measurement, and precipitation variables, and climatic groups on these parameters for the two functional groups (pine and eucalypt). Our results show that the photosynthetic capacity of forests presents a difference between the functional groups, the variables growth temperature and precipitation at 10 and 30 days before data collection influenced photosynthetic parameters, suggesting acclimatization of foliar photosynthesis. Age of stand influenced photosynthetic capacity throughout the rotation. Older forests have higher J_{max} . There were no differences between the subtropical and tropical climate groups, demonstrating an adaptation of the genotypes to the environmental conditions of Brazil. The second article investigates the performance of three stomatal conductance models (BB, BBL and USO) to identify the best model, in addition to to analyze how stomatal conductance and water use efficiency vary between functional groups and between eucalypt genotypes in Brazilian forest plantations. Our results revealed that the BBL and USO models performed better in the Brazilian forestry data. The species of the pine group had the highest stomatal conductance response parameter (g_1) and, consequently, the lowest efficiency in water use when compared to the genotypes of the eucalypt group. Within the eucalypt group, the genotypes showed differences in stomatal responses, indicating that in addition to the genotype characteristics, local climatic conditions may also have influenced the variation in g_1 . We found in these two articles photosynthetic parameters V_{cmax} , J_{max} , J_{max}/V_{cmax} and stomatal response parameter (g_1) modeled by the three g_s models, most used in global vegetation models and process-based models for various eucalyptus and pine genotypes. Our study will expand the physiological parameters database for planted forests in Brazil, making it possible to use them in global vegetation modeling studies.

Keywords: Photosynthesis, stomatal conductance, ecophysiological modeling, eucalypt, pine

LISTA DE SIGLAS

Aci	Curvas de resposta da fotossíntese às concentrações de CO ₂
Amax	Taxa máxima de assimilação de CO ₂
Anet	Taxa líquida de assimilação de CO ₂
APAR	Radiação fotossinteticamente ativa absorvida
BB	Modelo de Ball-Woodrow-Berry
BBL	Modelo de Ball-Berry-Leuning
Ca	Concentração ambiente de CO ₂
Ci	Concentração de CO ₂ nos espaços intercelulares
ESMs	Modelos de Sistema terrestre
FvCB	Modelo de fotossíntese de Farquhar, von Caemmerer & Berry 1980
GPP	Produção primária bruta
GVMs	Modelos de vegetação global
g1	Parâmetro de inclinação do modelo de condutância estomática
Jmax/Vcmax	Relação entre Jmax:Vcmax
Jmax	Taxa potencial máxima de transporte de elétrons
Jmax ₂₅	Taxa potencial máxima de transporte de elétrons padronizada a 25°
LAI	Índice de área foliar
LUE	Eficiência do uso da luz
PBMs	Modelos baseados em processos
PFTs	Tipos funcionais de plantas
PPFD	Densidade de fluxo de fótons fotossintéticos
Prec ₁₀	Precipitação total aos 10 dias antes da coleta de dados
Prec ₃₀	Precipitação total aos 30 dias antes da coleta de dados
RMSE	Erro quadrático médio
Rubisco	Enzima ribulose-1,5-bisfosfato carboxilase
T growth	Temperatura de crescimento
T _{mean10}	Média da temperatura média diária 10 dias antes da coleta de dados
T _{mean30}	Média da temperatura média diária 30 dias antes da coleta de dados
TBMs	Modelos da biosfera terrestre

TPU	Taxa de utilização da triose fosfato
USO	Modelo unificado de otimização estomática
V _{cm} ^{max}	Taxas máximas de carboxilação de Rubisco
V _{cm} ^{max25}	Taxas máximas de carboxilação de Rubisco padronizada a 25°
VPD	Déficit de pressão de vapor
V _{pd} L	Déficit de pressão de vapor entre a folha e ar
WUE	Eficiência do uso da água

SUMÁRIO

	PRIMEIRA PARTE	1
1	INTRODUÇÃO.....	2
2	REFERENCIAL TEÓRICO	4
2.1	Modelagem da fotossíntese.....	4
2.2	Modelagem da condutância estomática	8
2.2.1	Modelo de Ball-Woodrow-Berry (BWB)	9
2.2.2	Modelo de Ball - Berry -Leuning (BBL)	11
2.2.3	Modelo unificado de otimização estomática (USO)	14
	REFERÊNCIAS.....	18
	SEGUNDA PARTE- ARTIGOS	24
	ARTIGO 1 - CLIMATIC VARIABLES AND STAND AGE INFLUENCE PHOTOSYNTHETIC CAPACITY OF FOREST PLANTATIONS IN BRAZIL	24
1.	Introduction.....	25
2.	Material and Methods	29
3.	Results	37
4.	Discussion	42
5.	Conclusion	48
6.	Acknowledgements	49
7.	References.....	49
8.	Supplementary material.....	56
	ARTIGO 2 - COMPARING OF STOMATAL CONDUCTANCE MODELS IN BRAZILIAN FOREST PLANTATIONS.....	60
1.	Introduction.....	61
2.	Material and Methods	64
3.	Results	69
4.	Discussion	78
5.	Conclusion	83
6.	Acknowledgements	83
7.	References.....	83
3.	CONSIDERAÇÕES FINAIS.....	88

PRIMEIRA PARTE

1 INTRODUÇÃO

A fotossíntese é o processo chave associado ao crescimento das plantas, portanto o estudo de seus principais mecanismos e sua resposta complexa a diversos fatores é fundamental para entender como as plantas funcionam sob condições de estresse e esclarecer se há espaço para melhorar produtividade florestal (LI, et al., 2013; NADAL; FLEXAS, 2019; SANDS; LANDSBERG, 2002). A troca de carbono e água realizada pela planta é regulada pelos estômatos, processo que é responsável por equilibrar a captação de CO₂, contra a necessidade de controlar a perda de água das folhas (HÉROULT et al., 2013). É este processo que influencia a eficiência do uso da água (WUE) das plantas, o crescimento, a distribuição da vegetação no ecossistema e a produtividade das florestas (WANG et al., 2018)

Avaliar estes processos fisiológicos e os fatores ambientais e genéticos que podem influenciar a capacidade fotossintética das plantas, podem fornecer informações para melhorar a simulação da produtividade das florestas e também para entender como as plantas irão se comportar em cenários futuros de mudanças climáticas. Entender sobre as limitações fotossintéticas também são úteis em estratégias de melhoramento de espécies florestais tendo em vista que um objetivo chave da silvicultura é desenvolver genótipos com alta capacidade fotossintética e maior eficiência do uso da água o que é influenciado pela taxa de fotossíntese líquida e condutância estomática (YANG et al., 2018).

Modelar a capacidade fotossintética e a condutância estomática é fundamental para prever as respostas da vegetação e assim desenvolver estratégias para adoção de espécies e genótipos na silvicultura em cenários atuais e futuros. Uma forma de estimar as respostas fotossintéticas e determinar os fatores e os parâmetros importantes que podem promover limitações na fotossíntese máxima é a utilização de dados de trocas gasosas. Medições de trocas gasosas foliares (CO₂ e H₂O) desempenham um papel central na ecofisiologia vegetal uma vez que contribuem para o entendimento das diferentes respostas nas taxas de fotossíntese e transpiração entre as espécies. Estas medições também são utilizadas para modelar a resposta das plantas às mudanças no meio ambiente como alterações na temperatura, umidade do ar e luminosidade (DUURSMA, 2015).

Para entender os fatores que influenciam a capacidade fotossintética, modelos de fotossíntese são utilizados para obter parâmetros que limitam o processo bioquímico: V_{cmax} (taxas máximas de carboxilação de Rubisco), J_{max} (taxa potencial máxima de transporte de elétrons) e TPU (utilização da triose fosfato) e modelos de condutância estomática aplicados

para entender o comportamento dos estômatos nas diferentes condições ambientais, além de fornecer o parâmetro que explica o comportamento estomático (g_1), proxy padronizado para comparar a eficiência no uso da água (WUE) dos diferentes tipos funcionais de planta (PFTs). Os parâmetros V_{cmax} e J_{max} e g_1 são amplamente utilizados para parametrização de modelos de sistema terrestre (ESMS) os quais são ferramentas usadas para prever o balanço de carbono (C) da vegetação terrestre futuro e modelos baseados em processos (PBMs) que simulam processos fisiológicos que influenciam o crescimento e como esses processos são influenciados pelo ambiente (FRANKS et al., 2018; MEDLYN et al., 2011).

Estudos que investigam a capacidade fotossintética e o comportamento estomático visando obter parâmetros fisiológicos ainda são incipientes no Brasil. Portanto investigar a ecofisiologia das florestas plantadas é necessário e fundamental para ampliar o conhecimento sobre o comportamento das plantas diante das condições ambientais, além de fornecer parâmetros úteis em modelagem global da vegetação. Dentro deste contexto, este trabalho tem o objetivo de modelar a capacidade fotossintética e condutância estomática das florestas de eucalipto e pinus no Brasil em dois artigos. No primeiro artigo, utilizamos o modelo de Farquhar et al. (1980) para obter os parâmetros V_{cmax} , J_{max} e a relação J_{max}/V_{cmax} e analisamos a influência da idade, da temperatura de crescimento e precipitação aos 10 e 30 dias antes da coleta de dados, além de avaliar a influencia dos grupos climáticos de eucalipto e das diferentes espécies de pinus nestes parâmetros fotossintéticos e o segundo artigo investiga o desempenho de três modelos de condutância estomática (BB, BBL e USO) além de analisar como a condutância estomática e a WUE varia entre os diferentes genótipos nas plantações florestais brasileiras.

2 REFERENCIAL TEÓRICO

2.1 Modelagem da fotossíntese

A fotossíntese é o processo chave no ciclo do carbono terrestre (PRENTICE et al., 2001; DE KAWUE et al., 2015) e a modelagem deste processo de forma precisa é fundamental para entender o funcionamento dos ecossistemas vegetais e também para projetar a resposta da biosfera às mudanças ambientais (FRIEDLINGSTEIN et al., 2014). Diversos fatores influenciam a fotossíntese, podendo citar a temperatura, a concentração de CO₂, variação na radiação absorvida e as características bioquímicas das células (TAIZ; ZEIGER, 2013; DE PURY; FARQUHAR, 1997). A fotossíntese é composta por processos biológicos interconectados localizados em diferentes compartimentos da célula (SHARKEY et al., 2007).

Existem três principais processos que controlam o resposta da fotossíntese, nomeadamente processos bioquímicos, respiratório e estomático (LIN et al., 2012) Estes processos incluem o transporte de CO₂ através dos estômatos, os quais incluem o componente difusional que compreende a trajetória do CO₂ da atmosfera (C_a) até a cavidade subestomática (C_i) e finalmente no cloroplasto (C_c) (NADAL; FLEXAS, 2019). O componente bioquímico é caracterizado pela assimilação fotossintética por meio da fixação do CO₂ no ciclo de Calvin (SHARKEY, 2016; NADAL; FLEXAS, 2019). As variáveis ambientais tais como a intensidade da luz e da temperatura, podem ter efeitos diferentes em cada um destes processos (SHARKEY et al., 2007; LARCHER, 2006).

A maioria dos esforços tem se concentrado nos processos bioquímicos que influenciam a fotossíntese (LIN et al., 2012). O modelo de fotossíntese de Farquhar, von Caemmerer e Berry foi desenvolvido em 1980 (modelo FvCB) para descrever os processos bioquímicos da fotossíntese e tem sido o modelo mais utilizado para entender as respostas da fotossíntese à variação ambiental (FARQUHAR; VON CAEMMERER; BERRY, 1980). Este modelo permite que medições de trocas gasosas sejam interpretadas em termos de processos bioquímicos e biofísicos (SHARKEY, 2016). O modelo FvCB fornece métricas comparáveis da capacidade fotossintética, prevendo a resposta da fotossíntese às mudanças na concentração de CO₂ dentro do espaço aéreo da folha (C_i) (DUURSMA, 2015). As equações que descrevem o modelo seguem abaixo:

(1)

$$A_n = \min (A_c, A_j) - R_d$$

$$A_c = V_{CMAX} \frac{C_i - \Gamma^*}{C_i + K_c(1 + \frac{O_i}{K_o})}$$

$$A_j = J \frac{C_i - \Gamma^*}{4(C_i + 2\Gamma^*)}$$

Onde:

A_c e A_j ($\mu\text{mol m}^{-2} \text{s}^{-1}$): Taxa de assimilação limitada pela atividade da Rubisco e pelo transporte de elétrons (regeneração da ribulose-1,5-bisfosfato, RuBP) respectivamente

R_d ($\mu\text{mol m}^{-2} \text{s}^{-1}$): Respiração mitocondrial sob condição de iluminação

V_{CMAX} ($\mu\text{mol m}^{-2} \text{s}^{-1}$): Atividade catalítica máxima da Rubisco

C_i e O_i : concentrações de CO_2 e O_2 no espaço intercelular respectivamente ($\mu\text{mol mol}^{-1}$)

Γ^* : Ponto de compensação de CO_2 na ausência de respiração mitocondrial

K_c e K_o : São os coeficientes de Michaelis-Menten para CO_2 e O_2 , respectivamente ($\mu\text{mol mol}^{-1}$)

J ($\text{mol m}^{-2} \text{s}^{-1}$): taxa potencial de transporte de elétrons, relacionada à densidade de fluxo de fótons fotossinteticamente ativa incidente (Q) por:

$$\theta J^2 - (\alpha Q + J_{MAX}) J + \alpha Q J_{MAX} = 0 \quad (2)$$

Onde:

J_{MAX} : Taxa potencial de transporte de elétrons ($\mu\text{mol m}^{-2} \text{s}^{-1}$)

θ : Curvatura da curva de resposta à luz (sem unidade)

α : rendimento quântico do transporte de elétrons $\text{mol e}^- \text{mol}^{-1}$

O modelo estima a taxa de fotossíntese com base nas propriedades da enzima ribulose1, 5 bisfosfocarboxilase/oxigenase (Rubisco) em três fases distintas. Na primeira fase a taxa de fotossíntese é limitada pela atividade da rubisco e ocorre quando a concentração de CO_2 é baixa, ou seja, a enzima não atingiu a velocidade máxima (V_{max}) por falta de substrato (TAIZ; ZEIGER, 2013; SANDS; LANDSBERG, 2002). Esta fase ocorre normalmente quando as concentrações de CO_2 são inferiores a 20 Pa (~ 200 ppm) (SHARKEY et al., 2007)

Na fase 2, a fotossíntese é limitada pela capacidade do ciclo de Calvin regenerar a molécula aceptora ribulose – 1,5 bisfosfato (RuBP) que depende do transporte de elétrons (J_{max}) (TAIZ; ZEIGER, 2013; LANDSBERG; SANDS, 2011). A fotossíntese limitada por regeneração de RuBP inclui as condições em que a intensidade da luz limita a taxa de fotossíntese e geralmente ocorre em concentrações de CO_2 superiores a 30 Pa (200 ppm) (SHARKEY et al., 2007; LANDSBERG; SANDS, 2011).

A terceira fase ocorre quando as reações do cloroplasto têm uma capacidade maior que a capacidade da folha de usar os produtos dos cloroplastos, principalmente, mas não exclusivamente, a triose fosfato. Este terceiro estado é chamado de limitação do uso de fosfato de triose (TPU). Nessa condição, a fotossíntese não responde ao aumento de CO_2 , nem é inibida pelo aumento da concentração de oxigênio (SHARKEY et al., 2007).

As curvas de resposta da fotossíntese a diferentes concentrações de CO_2 (A-ci) permitem correlacionar esses três mecanismos que podem limitar a taxa de fotossíntese em diferentes concentrações de CO_2 no mesófilo (SHARKEY, 2016) e são importantes em estudos de ecofisiologia vegetal, pois fornecem informações mecanicistas sobre as limitações bioquímicas subjacentes da assimilação do carbono que podem variar de acordo com o genótipo (STINZIANO et al., 2017). A assimilação de CO_2 é modelada usando a simples suposição de que a taxa de fotossíntese (A) sem as limitações seria 100%, mas é reduzida por essas três condições bioquímicas.

Visando entender como o clima afeta a produtividade das plantas, e também prever como o aquecimento do clima pode influenciar captação de CO_2 , os modelos do sistema terrestre (ESMs) e os modelos baseados em processos (PBMs) geralmente incorporam como componente o modelo de Farquhar para quantificar os fatores limitantes (V_{cmax} , J_{max} e TPU) as taxas de fotossíntese (FRANKS et al., 2018).

Os modelos de sistema terrestre integram processos biogeoquímicos e biogeoquímicos da superfície terrestre com modelos físicos de clima, têm sido amplamente utilizados para demonstrar a importância dos processos da superfície terrestre na determinação do clima e para destacar as grandes incertezas na quantificação dos processos da superfície terrestre (FRIEDLINGSTEIN et al., 2006; LI et al., 2015; FRANKS et al., 2018). Já os modelos baseados em processos basicamente simulam processos fisiológicos que influenciam o crescimento e como esses processos são influenciados pelo ambiente. Esses modelos podem explicar as interações entre as espécies, os processos e as condições ambientais consideradas no modelo (PRETZSCH; FORRESTER; RÖTZER, 2015). Na literatura existem diversos

modelos que se baseiam em processos fisiológicos podendo citar o CABALA (BATTAGLIA et al., 2004), FOREST-BGC (RUNNING; COUGHLAN, 1988; RUNNING; GOWER, 1991), 3-PG (LANDSBERG; WARING, 1997) e o MAESTRO/MAESPA (WANG; JARVIS, 1990; BALDWIN et al., 2001; DUURSMA; MEDLYN, 2012). Estes modelos geralmente utilizam parâmetros específicos para os grupos funcionais de plantas, pois há uma grande variação na resposta fotossintética de cada tipo funcional de planta.

Existem diversos fatores que se correlacionam com as variações nos parâmetros V_{cmax} e J_{max} , por exemplo os fatores morfológicos como a fenologia foliar (WU et al., 2017), ontológicos (idade da folha) (ALBERT et al., 2018), características genéticas das espécies (MEDLYN et al., 2002; LIN et al., 2013), clima de origem das espécies (BERRY; BJÖRKMAN, 1980) e a nutrição das florestas. Esses fatores estão normalmente associados à variação no conteúdo de nitrogênio foliar e ou teor/proporção de clorofila nas folhas (LIN et al., 2013; HASPEN et al., 2017).

A variabilidade entre espécies, dentro do mesmo grupo funcional também foi verificado por Croft et al. (2017). Os autores ainda relataram que a correlação entre o conteúdo de clorofila da folha e o V_{cmax} foi maior que a correlação entre o conteúdo de nitrogênio foliar e o V_{cmax} , sugerindo que a clorofila é um *proxy* mais confiável para estimativas de V_{cmax} em modelos de sistemas terrestres. A menor correlação entre o nitrogênio da folha foi possivelmente devido à dinâmica da partição de nitrogênio que envolve a distribuição de nitrogênio foliar entre *pools* fotossintéticos e não fotossintéticos (HIKOSAKA et al., 1997; CROEF et al., 2017). A partição muda com o tempo e com as espécies, de acordo com a demanda e fatores como otimização do crescimento e fatores ambientais (CROFT et al., 2017).

Com relação aos fatores climáticos, a temperatura de crescimento (temperatura predominante antes da medição de fotossíntese) e umidade do solo são fatores que influenciam na variação de V_{cmax} e J_{max} (SMITH e DUKE, 2018). Lin et al. (2013) encontraram valores de V_{cmax} e J_{max} a uma temperatura padrão (25°) significativamente mais elevadas em espécies de origem mais quente como o *Eucalyptus melliodora* do que em espécies de origem mais fria como *E. dunnii*. Os autores atribuíram estas diferenças no teor de nitrogênio foliar que podem ter sido causadas por diferenças na área foliar do dossel. Espécies de clima quente mantêm uma área foliar por árvore mais baixa do que as espécies de clima frio (BATTAGLIA et al., 1998; LIN et al., 2013).

Estudos avaliando a aclimação e adaptação da fotossíntese forneceram evidências da aclimação da fotossintética à temperatura de crescimento (temperatura média 30 dias antes da

coleta) (KUMARATHUNGE et al., 2019). No estudo de Kumarathunge et al. (2019) a temperatura ótima da fotossíntese mostrou uma tendência de aumento com o aumento da temperatura de crescimento. No entanto, ao avaliar os parâmetros J_{max} e V_{cmax} (25°) nenhuma correlação foi detectável entre a temperatura de crescimento e o V_{cmax} . Já o J_{max} mostrou uma forte diminuição com o aumento da temperatura de crescimento. Por outro lado estudos de Smith e Duke, (2018) revelaram que temperaturas mais altas podem diminuir a capacidade fotossintética, especialmente durante épocas de baixa disponibilidade de água.

Embora a fotossíntese seja altamente sensível a mudanças de temperatura, que é impulsionada pela sensibilidade à temperatura de V_{cmax} e J_{max} e o grande número de pesquisas sobre este assunto, o efeito do aumento da temperatura, tanto a curto como a longo prazo nas limitações bioquímicas da fotossíntese ainda não é totalmente claro ou generalizável (KATTGE; KNORR, 2007; STENFANSKI et al., 2019).

2.2 Modelagem da condutância estomática

Os estômatos tem a função de controlar as trocas de CO_2 e H_2O entre plantas e a atmosfera (BUCKLEY, 2019; BUCKLEY; MOTT, 2013), regulam o processo de fotossíntese e transpiração (TARIN et al., 2019), afetam a produtividade e o potencial hídrico da planta e a eficiência do uso da água (MEDLYN et al., 2017). Diversos fatores bióticos e abióticos afetam a resposta dos estômatos, por exemplo, potencial hídrico da folha, temperatura, radiação e déficit de pressão de vapor (DPV) (TARIN et al., 2019, MEDLYN et al., 2011; TUZET et al., 2013).

A sensibilidade da condutância estomática aos fatores ambientais é uma preocupação constante na fisiologia vegetal, principalmente a sensibilidade ao estresse hídrico (DAMOUR et al. 2010). Diante das mudanças climáticas previstas para as próximas décadas, é fundamental prever os efeitos dos eventos de seca e elevadas concentrações de CO_2 nos ecossistemas terrestres (DAMOUR et al., 2010; MEDLYN et al., 2011).

Diversos modelos ao nível da folha foram desenvolvidos visando modelar a condutância estomática (g_s) em função de fatores ambientais como CO_2 , luz, temperatura (JARVIS, 1976) umidade relativa (BALL et al., 1987), déficit de pressão de vapor (LEUNING, 1995) e potencial hídrico do solo (TUZET et al., 2003). Em uma revisão proposta por Damour et al., (2010) ele destacou mais de 30 modelos de condutância estomática já desenvolvidos. Os modelos de g_s basicamente se dividem em três abordagens: abordagem empírica; mecanicista (baseados em

processos) e a abordagem de otimização econômica (BUCKLEY; MOTT, 2013; LU et al., 2018).

A abordagem empírica é a mais utilizada nos modelos de g_s , por ser a mais simples e fácil de implementar em muitas condições (BUCKLEY; MOTT, 2013; BALL et al., 1987; LEUNING, 1995). O modelo empírico concentrava-se na previsão, em vez de explorar os mecanismos pelos quais os estômatos respondem ao ambiente, porque o conhecimento desses mecanismos na época era bastante limitado (BUCKLEY; MOTT, 2013). Os modelos mecanicistas são mais complexos matematicamente e são mais adequados para investigar os processos celulares e subcelulares envolvidos na detecção ambiental, transdução de sinal e movimentos de íons. Estes modelos foram cruciais para compreender como funcionam os estômatos (BUCKLEY; MOTT, 2013; LU et al., 2018). A terceira abordagem é a otimização econômica baseada na teoria de que as plantas tendem a maximizar a assimilação de CO_2 para uma quantidade fixa de perda de água ou tendem a minimizar a perda de água para uma quantidade fixa de assimilação de CO_2 , desenvolvida por Cowan e Farquhar (1977).

Além de serem utilizados para estudar o comportamento estomático das diferentes espécies nos diferentes ambientes (HEROULT et al., 2013; WANG et al., 2018; ZHOU et al., 2013) os modelos de g_s também são utilizados como componentes de modelos ESMs como o CABLE (DE KAUWE et al., 2015), o modelo “Community Land Model” (BONAN et al., 2014) e os modelos baseados em processos como o modelo de absorção de radiação no dossel-MAESPA (DUURSMA; MEDLYN, 2012).

Os modelos de g_s que mais se destacam são o modelo Ball-Woodrow-Berry- BWB (1987), modelo Ball-Woodrow-Berry modificado por Leuning- BBL (1995) e o modelo de otimização estomática desenvolvido por Medlyn et al. (2011).

2.2.1 Modelo de Ball-Woodrow-Berry (BWB)

O modelo Ball-Woodrow-Berry também conhecido como modelo BWB foi desenvolvido em 1987, e assume que a condutância estomática está fortemente acoplada a taxa de fotossíntese (BALL et al., 1987). Este modelo baseia-se na teoria de que os estômatos ajudam a manter uma concentração intercelular de CO_2 estável, mantendo assim uma relação linear com a fotossíntese líquida, ou seja, o modelo prevê que a condutância estomática é igual a zero quando a fotossíntese líquida é igual à zero (WANG et al., 2018; DAMOUR et al., 2010). Esta relação linear acontece porque os estômatos se abrem e fecham para manter uma relação quase

constante entre a concentração de CO₂ intercelular e ambiental podendo variar em função da umidade do ar (WONG et al., 1979; HOSHIKA et al., 2017).

De forma resumida o modelo de Ball–Woodrow–Berry propõe a resposta da condutância estomática à umidade relativa do ar, ao CO₂ e a fotossíntese (HOSHIKA et al., 2017; DAMOUR et al., 2010), dessa forma todos os fatores que reduzem a taxa de fotossíntese causarão uma redução na condutância estomática. Estes fatores são modelados através da dependência da fotossíntese (BALL et al., 1987).

A expressão empírica desenvolvida para o modelo BWB de g_s segue abaixo:

$$g_s = m + \frac{A_n H_s}{C_s} + g_0 \quad (3)$$

Onde:

A_n : taxa de assimilação líquida de CO₂

H_s : umidade relativa do ar na superfície da folha

C_s : Concentração atmosférica de CO₂ na superfície da folha

g_0 : parâmetro ajustado

m : é a inclinação da relação entre g_s e $(A_n H_s C_s)$ determinados por meio de regressão linear.

O modelo Ball–Woodrow–Berry é um dos modelos de condutância estomática mais utilizado nos diversos estudos de ecofisiologia e são utilizados em tanto em florestas (STIZIANO et al., 2018; HOSHIKA et al., 2015), como em culturas agrícola como arroz (MASUTOMI et al., 2019); tomate (WEI et al., 2018). Este modelo apresenta diversas vantagens, como a facilidade de calcular como a condutância estomática se correlaciona com a capacidade fotossintética e a concentração de CO₂ no ambiente (BALDOCCHI, 2008).

Outra vantagem do modelo é a facilidade de parametrização e implementação em grandes escalas, por exemplo, podem ser utilizados como componentes de modelos ESMs (MEDLYN et al., 2011). O modelo BWB tem sido muito utilizado na escala da folha, mas também pode ser extrapolado para a escala do campo ou da floresta (DAMOUR et al. 2010). Este modelo também é utilizado em estudos que visam avaliar os impactos das mudanças climáticas e os prejuízos causados na produtividade das florestas.

Apesar de ser amplamente utilizado, o modelo BWB também teve algumas críticas por parte dos pesquisadores. As principais críticas ao modelo foram: a primeira é que o modelo não simula corretamente a fotossíntese líquida (A_n) e o g_s quando a concentração de CO₂ na

superfície foliar (C_s) é igual ao CO_2 no ponto de compensação (Γ). Quando o $C_s = \Gamma$, a fotossíntese e o g_s deveriam ser respectivamente igual a 0 e $g\theta$ (LEUNING, 1990; DAMOUR et al. 2010).

A segunda crítica foi o fato de que no modelo proposto por Ball-Woodrow-Berry os estômatos respondem a umidade relativa do ar e não ao déficit de pressão de vapor (DPV) (LEUNING, 1995). Os pesquisadores Aphalo e Jarvis (1991) mostraram que o DPV era mais adequado do que umidade relativa do ar para descrever a resposta de g_s , o que pode ser compreendido, considerando que estas variáveis são relacionadas por uma equação derivada da equação de difusão de vapor de água no ar como é descrita a seguir.

(4)

$$E = \alpha(g_s^{-1} + g_b^{-1})^{-1} \cdot VPD$$

Onde:

g_b : condutância da camada limite ao vapor de água

α e g_b : parâmetros físicos dependentes da pressão atmosférica temperatura, velocidade do vento e arquitetura da planta.

O modelo BWB também foi criticado por apresentar baixo desempenho em espécies de plantas C3 em concentrações sub-ambientais de $[\text{CO}_2]$, quando as taxas de fotorrespiração aumentam (LEUNING 1990; WEBER, GATES, 1990; MINER et al., 2017). Diante dessas críticas contra a primeira versão do modelo de Ball-Woodrow-Berry (1987), o pesquisador LEUNING propôs algumas modificações e o modelo ganhou uma nova versão que ficou conhecida como modelo de Ball-Berry-Leuning (LEUNING, 1990; LEUNING 1995).

2.2.2 Modelo de Ball - Berry -Leuning (BBL)

Estudando o comportamento dos estômatos e da fotossíntese em florestas de *Eucalyptus grandis* na Austrália, Leuning testou o modelo de Ball-Woodrow-Berry (1987) e percebeu que o modelo BWB não poderia ser usado para determinar o comportamento estomático em baixas concentrações de CO_2 e a condutância estomática não podia ser simulada com precisão quando (C_s) atinge o ponto de compensação de CO_2 (LEUNING, 1990).

Diante destas observações ele propôs uma versão modificada com um novo ajuste na equação, a partir da inserção do termo ($C_s - \Gamma$) no denominador, o qual foi denominado de

função de restrição estomática. Essa função mostra que existe um ponto de compensação do CO₂ para assimilação fotossintética, o qual é definido como a concentração de CO₂ na qual há um balanço entre a fotossíntese bruta e respiração, ou seja, não há fotossíntese líquida (LEUNING, 1990).

A nova equação descreveu o g_s sob uma ampla gama de fatores ambientais, melhorando ainda mais a correlação já existente. A expressão modificada foi combinada com o modelo de fotossíntese de Farquhar e von Caemmerer (1980) visando obter um modelo integrado de fotossíntese, CO₂ intercelular e condutância estomática (LEUNING, 1990). Quando as condutâncias estomáticas foram plotadas utilizando o índice estomático modificado verificou-se que os dados foram melhor ajustados quando comparado com a equação original de Ball-Berry (1987), obtendo uma dispersão reduzida e a linearidade melhorada. A equação modificada segundo Leuning (1990) segue abaixo:

(5)

$$g_s = m + \frac{A_n H_s}{C_s - \Gamma} + g_0$$

Onde:

Γ = ponto de compensação do CO₂

A_n = fotossíntese líquida

h_s = umidade relativa do ar na superfície da folha

C_s = Concentração atmosférica de CO₂ na superfície da folha

O uso do termo $(C_s - \Gamma)$ no denominador da equação modificada por Leuning (1990) descreveu melhor a resposta do g_s do que apenas a utilização da variável (C_s) , como proposto na equação de Ball–Woodrow–Berry. Esta modificação melhorou a equação porque possibilita contabilizar corretamente a $A_n \rightarrow 0$ quando $(C_s \rightarrow \Gamma)$ em vez de $(C_s \rightarrow 0)$ (LEUNING, 1990). Esta equação prevê que a condutância estomática aumente em função da taxa de assimilação de CO₂ (A_n) e da umidade relativa do ar na superfície da folha (h_s) quando o (C_s) é mantido constante. A condutância estomática diminuirá com aumento da concentração ambiental de CO₂, desde que a taxa de fotossíntese aumente mais lentamente que o (C_s) (LEUNING, 1990; LEUNING, 1995).

Mais tarde, Leuning (1995) propôs uma nova modificação na equação e argumentou que a abordagem original do modelo Ball–Woodrow–Berry era insuficiente para sua aplicação em experimentos que estavam sendo realizados na Austrália. Ele substituiu a variável umidade relativa (H_s) pela função de Lohammer que utiliza o DPV como uma proxy para a transpiração. A equação de Lohammer foi desenvolvida inicialmente para analisar medições de folhas em campo, causada em grande parte por mudanças na temperatura das folhas, em vez de mudanças na umidade absoluta do ar (LOHAMMER et al., 1980).

Leuning (1995) argumentou que a umidade relativa não é uma variável independente válida, pois as plantas devem responder a um potencial que gere perda de água, como uma diferença de pressão de vapor (DPV) (LEUNING, 1995; BALDOCCHI, 2008). Ele considerou duas formas alternativas para a dependência do DPV, a primeira foi uma dependência por meio de uma função linear e a segunda a partir de uma função hiperbólica. A função hiperbólica proporcionou um melhor ajuste aos dados experimentais em vez da função linear da umidade relativa como formulado originalmente no modelo Ball-Berry (LEUNING, 1995; MEDLYN et al. 2011).

A abordagem proposta por Leuning (1995) assume que a condutância estomática e a taxa de transpiração são linearmente relacionadas (LEUNING, 1995; MOTT; PARKHURST 1991). O modelo resultante proposto por Leuning (1995) também conhecido por BBL (1995) tem o seguinte formato:

(6)

$$g_s = g_0 \frac{mA_n}{(C_s - \Gamma) \left(1 + \frac{D}{D_0}\right)}$$

A principal diferença entre a modificação proposta por Leuning (1990) e Leuning (1995) é que a resposta de umidade na equação 4 é em função da umidade relativa do ar diferente da equação 5 que mostra a resposta em função do déficit de pressão de vapor (DPV) (LEUNING, 1995; DEWAR 2002).

A equação original de Ball–Woodrow–Berry (equação 2) foi muito criticada por que muitos pesquisadores argumentavam que a g_s é dependente do DPV e da transpiração em vez da umidade relativa como proposto no modelo original. No entanto segundo Baldocchi (2008), é possível derivar uma relação entre DPV e umidade relativa, o que torna esta crítica ilusória.

Outra abordagem é que esta crítica parece ser consequência apenas de resultados sob condições de seca no solo e certas condições atmosféricas (BALDOCCHI, 2008).

Estudos realizados por Zhang et al., (2017) confirmaram que a condutância estomática (g_s) pode ser prevista com precisão se os parâmetros no modelo forem ajustados considerando às condições de água no solo e que o declínio nos parâmetros induzido pelas condições de seca deve ser considerado, caso contrário, a g_s pode ser superestimada.

Diversos estudos apresentam resultados diferentes com relação a melhor aplicabilidade dos modelos de condutância estomática (WANG et al., 2016; WANG et al., 2018; HOSHIKA et al., 2017; LU e WANG, 2018). Selecionar um modelo de g_s com base nos dados de pesquisa existente pode ser um problema uma vez que a precisão destes modelos pode ser afetada por diferentes fatores, como as diferentes espécies, regiões de teste, condições ambientais e escalas de tempo (GAO et al., 2016; WANG et al., 2018).

Tanto o modelo de Ball–Woodrow–Berry quanto o modelo Ball-Berry modificado por Leuning mostrou boa concordância com as observações em diversos tipos de vegetação (BALL et al., 1987; LEUNING, 1995; LU e WANG, 2018; MASUTOMI et al., 2019; HOSHIKA et al., 2015; ZHANG et al., 2017). Esses dois modelos são amplamente utilizados porque são fáceis de parametrizar além de apresentarem facilidade de uso, alto poder explicativo e precisão preditiva em várias condições experimentais (MEDLYN et al., 2011; DAMOUR et al., 2010).

O modelo de Ball-Berry-Leuning (1995) também tem sido utilizado em estudos de previsão dos impactos das mudanças climáticas nos ecossistemas. Lu e Wang (2018) estudaram três modelos de g_s , o modelo Ball-Berry-Leuning e dois modelos de otimização (modelo de limitação de Rubisco e modelo de limitação de regeneração da RuBP) com dados obtidos em experimentos sob CO_2 instantâneo, dados de ambiente semi-controlado e dados de experimento- FACE (Experimentos de enriquecimento em larga escala de CO_2 ao ar livre). Os resultados indicaram que o modelo Ball-Berry-Leuning e o modelo de limitação de regeneração da RuBP tiveram desempenho semelhante. O desempenho semelhante destes modelos pode ser explicado porque o modelo RuBP foi derivado estruturalmente do modelo clássico de Ball-Berry, no entanto foi baseado na teoria de otimização da condutância estomática (MEDLYN et al., 2011; LU; WANG, 2018). Os resultados deste trabalho ainda mostraram que outros fatores como os diferentes grupos funcionais (C3 e C4) podem afetar significativamente o desempenho do modelo (LU; WANG, 2018).

2.2. 3 Modelo unificado de otimização estomática (USO)

Uma alternativa aos modelos propostos Ball-Woodrow-Berry (BWB) (1987) e Ball-Berry-Leuning (BBL) (1995) é o modelo unificado de otimização estomática (USO) proposto por Medlyn et al. (2011). O modelo de otimização USO baseia-se na teoria do comportamento estomático ideal desenvolvido por Cowan e Farquhar (1977). A abordagem da otimização dos estômatos postula que os estômatos devem agir para maximizar o ganho de carbono (fotossíntese, A) e ao mesmo tempo, minimizar a perda de água (E , transpiração). Esta teoria foi matematicamente expressa como o custo marginal da água por unidade de ganho de carbono e é obtida quando a seguinte expressão é minimizada:

$$E - \lambda An \tag{7}$$

Onde λ (mol H₂O mol⁻¹C) é um parâmetro que representa o custo marginal da água em relação ao ganho de carbono pela planta. Essa teoria foi posteriormente combinada com o modelo de fotossíntese desenvolvido por Farquhar-von Caemmerer (1980) para obter duas expressões quadráticas para o C_i (carbono interno) ideal (ARNETH et al., 2002). As diferentes expressões são obtidas de acordo com o fator limitante da fotossíntese que pode ser a atividade da enzima Rubisco ou a regeneração da ribulose 1,5-bisfosfato RuBP.

O modelo assume que a fotossíntese é limitada pela regeneração da RuBP conforme está descrito na seguinte equação:

$$A = \frac{J}{4} \frac{C_i - \Gamma^*}{C_i + 2\Gamma^*} - R_d \tag{8}$$

Onde:

J : é a taxa de transporte de elétrons,

Γ : CO₂ no ponto de compensação na ausência de respiração no escuro

R_d : taxa de respiração no escuro

C_i : concentração intercelular de CO₂

E também pode ser limitada pela taxa de carboxilação conforme a equação:

(9)

$$A = V_{cmax} \frac{C_i - \Gamma^*}{C_i + K_m} - R_d$$

V_{cmax} : taxa máxima de atividade da Rubisco

K_m : coeficiente Michaelis-Menten para a cinética da Rubisco

A equação geral do modelo de otimização estomática unificado (USO) foi proposto por Medlyn et al. (2011) conforme a equação 9 (MEDLYN et al., 2011).

(10)

$$g_s^* \approx 1.6 \left(1 + \frac{g_1}{\sqrt{D}} \right) \frac{A}{C_a} + g_0$$

Onde:

A : taxa de assimilação líquida

C_a e D : são a concentração de CO_2 e déficit de pressão de vapor na superfície da folha respectivamente.

O modelo USO combina a abordagem dos modelos empíricos (BWB e BBL) e a abordagem da teoria de otimização dos estômatos em um único modelo, por isso considera-se que este modelo é análogo aos modelos empíricos amplamente utilizados. O parâmetro g_1 do modelo USO é significativo, ou seja, tem implicações biológicas e pode ser útil para descrever estratégias de uso da água pelas plantas (MEDLYN et al., 2011). O g_1 pode ser visto como um proxy padronizado para comparar a eficiência no uso da água WUE dos diferentes tipos funcionais de planta (PFT) e condições ambientais (LIN et al., 2015; MEDLYN et al., 2017).

Este parâmetro pode ser obtido ajustando-se os dados da mesma maneira que normalmente é feito nos modelos empíricos, no entanto no modelo de otimização (USO) o g_1 é proporcional ao termo $\sqrt{\Gamma^*} \lambda$ e aumenta com o custo marginal da água do ganho de carbono (λ) e com o ponto de compensação de CO_2 (Γ) (Equação 9) (HEROULT et al., 2013; MEDLYN et al., 2011; WANG et al., 2018).

(11)

$$g_1 \propto \sqrt{\Gamma^*} \lambda$$

A simulação do comportamento estomático sob diversas condições ambientais é importante para caracterizar os mecanismos de resposta dos ecossistemas vegetais às mudanças climáticas e também para prever os ciclos de carbono e água no contexto das mudanças climáticas (MEDLYN et al., 2011; WANG et al., 2018). A formulação do modelo USO proposto por Medlyn et al. (2011), tem potencial significativo para interpretar e prever diferenças nas estratégias de uso de água das plantas e o comportamento estomático entre as espécies em resposta a diversas condições ambientais, incluindo o aumento de CO₂ na atmosfera contribuindo para melhorar as simulações do ciclo do carbono e o uso da água em grandes escalas (MINER et al., 2017).

Variações climáticas na umidade do solo causadas por períodos de estresse hídrico podem afetar a condutância estomática e conseqüentemente afetam a simulação dos ciclos de carbono e água. Neste contexto, o estudo de modelos de condutância estomática apropriados para condições de seca são importantes para prever os efeitos das mudanças climáticas (MEDLYN et al., 2011; MEDLYN et al., 2017; WANG et al., 2018). O modelo USO foi utilizado em diversos estudos para investigar a resposta das plantas as condições de seca com diversas espécies (HEROULT et al., 2013; ZHOU et al., 2013; WANG et al., 2018; MEDLYN et al., 2017)

Heroult et al. (2013), ao testar a hipótese de que o parâmetro g_1 pode variar entre as espécies, avaliaram quatro espécies de eucalipto originárias de diferentes zonas climáticas e relataram fortes diferenças no comportamento estomático entre as espécies arbóreas, com redução significativa no parâmetro g_1 durante um período de seca em espécies de eucaliptos originárias de zonas úmidas mas não em espécies de origem sub-úmida. No mesmo sentido, estudos conduzidos por Zhou et al. (2013) modelando a resposta estomática e não estomática de diferentes espécies as condições de seca também relataram variação no parâmetro g_1 das espécies.

O modelo USO também é utilizado para estudar a eficiência no uso da água (WUE) das plantas. Tarin et al. (2019), avaliando a resposta do g_1 como *proxy* da WUE em um ecossistema de *Acacia spp.* na Austrália, em várias escalas espaciais e temporais relataram que o parâmetro g_1 obtido tanto por meio da abordagem de medições de fluxo como pelo método de troca de gases foliares são altamente responsivo à disponibilidade de água. Os autores ainda apontam que a variação sazonal e anual no parâmetro g_1 destaca a preocupação de que o uso de forma generalizada de valores constantes de g_1 não é uma opção confiável para parametrizar os modelos climáticos globais.

REFERÊNCIAS

- ALBERT, L. P. et al. Age-dependent leaf physiology and consequences for crown-scale carbon uptake during the dry season in an Amazon evergreen forest. *New Phytologist*, v. 219, n. 3, p. 870-884, 2018. <http://dx.doi.org/10.1111/nph.15056>.
- APHALO P.J.; JARVIS P. G. Do stomata respond to relative humidity? *Plant, Cell And Environment*, v. 14, p. 127–132. 1991.
- ARNETH, A. et al. Response of central Siberian Scots pine to soil water deficit and long-term trends in atmospheric CO₂ concentration. *Global Biogeochemical Cycles*, v.16, n.1 1005, p.1-13, 2002. <https://doi.org/10.1029/2000GB001374>
- BALDOCCHI, D. Lecture 32, Stomatal Conductance, *Biometeorology*, ESPM 129, 2008.
- BALDWIN, V.C. et al. Linking growth and yield and process models to estimate impact of environmental changes on growth of loblolly pine. *Forest Science*, v. 47, n.1, 77–82, 2001.
- BALL, J. T.; WOODROW, I. E.; BERRY, J. A. A model predicting stomatal conductance and its contribution to the control of photosynthesis under different environmental conditions. In *Progress in photosynthesis research* (ed. J Biggins), v. 4, p. 221–224, 1987. Dordrecht, The Netherlands: Kluwer Academic Publishers.
- BATTAGLIA, M. et al. Prediction of leaf area index in eucalypt plantations: effects of water stress and temperature. *Tree Physiology*, v. 18, n. 8-9, p. 521-528, 1998. <http://dx.doi.org/10.1093/treephys/18.8-9.521>.
- BATTAGLIA, et al. CABALA: a linked carbon, water and nitrogen model of forest growth for silvicultural decision support. *Forest Ecology and Management*, v. 193, n.1, p. 251–282, 2004. <https://doi.org/10.1016/j.foreco.2004.01.033>
- BERRY, J.; BJORKMAN, O. Photosynthetic Response and Adaptation to Temperature in Higher Plants. *Annual Review Of Plant Physiology*, v. 31, n. 1, p. 491-543, 1980. *Annual Reviews*. <http://dx.doi.org/10.1146/annurev.pp.31.060180.002423>.
- BONAN, G. B. et al. Modeling stomatal conductance in the earth system: linking leaf water-use efficiency and water transport along the soil-plant atmosphere continuum, *Geoscientific Model Development*, v. 7, p. 2193–2222, doi:10.5194/gmd-7-2193-2014, 2014.
- BUCKLEY, T. N. How do stomata respond to water status? *New Phytologist*, v. 224, n. 1, p. 21-36, 2019. <http://dx.doi.org/10.1111/nph.15899>.
- BUCKLEY, T. N.; MOTT, K. A. Modelling stomatal conductance in response to environmental factors. *Plant, Cell & Environment*, v. 36, n. 9, p.1691-1699, 2013. . <http://dx.doi.org/10.1111/pce.12140>

COWAN I. R, FARQUHAR G. D. Stomatal function in relation to leaf metabolism and environment. In: *Integration of Activity in the Higher Plant* (ed. Jennings DH), pp. 471–505, 1977, Cambridge University Press, Cambridge.

CROFT, H. et al. Leaf chlorophyll content as a proxy for leaf photosynthetic capacity. *Global Change Biology*, v. 23, n. 9, p. 3513-3524, 2017. <http://dx.doi.org/10.1111/gcb.13599>.

DAMOUR, G. et al. An overview of models of stomatal conductance at the leaf level. *Plant, Cell & Environment*, v. 33, p. 1419-1438, 2010. <http://dx.doi.org/10.1111/j.1365-3040.2010.02181.x>.

DE KAUWE, M.G. et al. A test of an optimal stomatal conductance scheme within the CABLE land surface model. *Geoscientific Model Development*, v. 8, p. 431-452, 2015.

DE PURY, D. G. G.; FARQUHAR, G.D. Simple scaling of photosynthesis from leaves to canopies without the errors of big-leaf models. *Plant, Cell and Environment*, v. 20, p. 537-557, 1997.

DEWAR, R. C. The Ball-Berry-Leuning and Tardieu-Davies stomatal models: synthesis and extension within a spatially aggregated picture of guard cell function. *Plant, Cell And Environment*, v. 25, n. 11, p.1383-1398, 2002. <http://dx.doi.org/10.1046/j.1365-3040.2002.00909.x>.

DUURSMA, R. A. Plantecophys - An R Package for Analysing and Modelling Leaf Gas Exchange Data. *Plos One*, v.10, n.11, 2015. <https://doi.org/10.1371/journal.pone.0143346>.

DUURSMA, R. A.; MEDLYN, B. E.; MAESPA: A model to study interactions between water limitation, environmental drivers and vegetation function at tree and stand levels, with an example application to [CO₂] × drought interactions. *Geoscientific Model Development Discussions*. v. 5, n.4, p. 919–940, 2012. <https://doi//10.5194/gmd-5-919-2012>.

FARQUHAR, G. D.; CAEMMERER, S. V.; BERRY, J. A. A biochemical model of photosynthetic CO₂ assimilation in leaves of C₃ species. *Plant*, n. 149, p.78–90, 1980.

FRANKS, P. J. et al. Comparing optimal and empirical stomatal conductance models for application in Earth system models. *Global change biology*, v. 24, n. 12, p. 5708-5723, 2018. <https://doi.org/10.1111/gcb.14445>.

FRIEDLINGSTEIN, P. et al. Uncertainties in CMIP5 Climate Projections due to Carbon Cycle Feedbacks. *Journal Of Climate*, v. 27, n. 2, p. 511-526, 2014. American Meteorological Society. <http://dx.doi.org/10.1175/jcli-d-12-00579.1>.

GAO, G. L. et al. H. Environmental response simulation and the up-scaling of plant stomatal conductance. *Acta Ecol. Sin.* v. 36, p.1491–1500, 2016.

HASPER, T. B. et al. Stomatal CO₂ responsiveness and photosynthetic capacity of tropical woody species in relation to taxonomy and functional traits. *Oecologia*, v. 184, n. 1, p. 43, 2017.

HÉROULT, A. et al. Optimal stomatal conductance in relation to photosynthesis in climatically contrasting Eucalyptus species under drought. *Plant, Cell & Environment*, v. 36, n. 2, p.262-274, 2012. <http://dx.doi.org/10.1111/j.1365-3040.2012.02570.x>.

HIKOSAKA, K. Modelling Optimal Temperature Acclimation of the Photosynthetic Apparatus in C3Plants with Respect to Nitrogen Use. *Annals of Botany*, v. 80, n. 6, p. 721-730, 1997. <http://dx.doi.org/10.1006/anbo.1997.0512>

HOSHIKA, Y. et al. Stomatal conductance models for ozone risk assessment at canopy level in two Mediterranean evergreen forests. *Agricultural And Forest Meteorology*, v. 234-235, p. 212-221, 2017. <https://doi.org/10.1016/j.agrformet.2017.01.005>

HOSHIKA, Y. et al. Ozone-induced stomatal sluggishness changes carbon and water balance of temperate deciduous forests. *Scientific Reports*, v. 5, n. 1, p.1-8, 2015. <http://dx.doi.org/10.1038/srep0987>.

JARVIS, P. G. The Interpretation of the Variations in Leaf Water Potential and Stomatal Conductance Found in Canopies in the Field. *Philosophical Transactions Of The Royal Society B: Biological Sciences*, v. 273, n. 927, p. 593-610, 1976. <http://dx.doi.org/10.1098/rstb.1976.0035>.

KATTGE, J.; KNORR, W. Temperature acclimation in a biochemical model of photosynthesis: a reanalysis of data from 36 species. *Plant, Cell & Environment*. v. 30, n. 9, p. 1176-1190. 2007. <http://dx.doi.org/10.1111/j.1365-3040.2007.01690.x>.

KUMARATHUNGE, D. P. et al. Acclimation and adaptation components of the temperature dependence of plant photosynthesis at the global scale. *New Phytologist*, v. 222, n. 2, p. 768-784, 2019. <http://dx.doi.org/10.1111/nph.15668>.

LANDSBERG, J. J.; WARING, R. H. A generalized model of forest productivity using simplified concepts of radiation-use efficiency, carbon balance and partitioning. *Forest Ecology and Management*, Amsterdam, v. 95, p. 209-228, 1997. [https://doi.org/10.1016/S0378-1127\(97\)00026-1](https://doi.org/10.1016/S0378-1127(97)00026-1)

LANDSBERG, J. J.; SANDS, P. J. *Physiological ecology of forest production: Principles, processes, and models*. London: Academic Press, 2011. 331p.

LARCHER, W. *Ecofisiologia vegetal*. São Carlos: RiMa, 2006. 550 p.

LEUNING, R. A critical appraisal of a combined stomatal– photosynthesis model for C3 plants. *Plant, Cell & Environmental*, v. 18, p. 339–355, 1995.

LEUNING, R. Modelling stomatal behaviour and photosynthesis of *Eucalyptus grandis*. *Australian Journal of Plant Physiology*, v. 17, p.159-175, 1990.

LIN, Y. S. et al. Optimal stomatal behaviour around the world. *Nature Climate Change*, v. 5, n.5, p. 459-464. 2015. <https://doi.org/10.1038/nclimate2550>

- LIN, Y.-S.; MEDLYN, B. E.; ELLSWORTH, D. S. Temperature responses of leaf net photosynthesis: the role of component processes. *Tree physiology*, v. 32, n. 2, p. 219-231, 2012. <http://dx.doi.org/10.1093/treephys/tpr141>
- LIN, Y.-S et al. Biochemical photosynthetic responses to temperature: how do interspecific differences compare with seasonal shifts? *Tree Physiology*, v. 33, n. 8, p. 793-806, 2013. <http://dx.doi.org/10.1093/treephys/tpt047>.
- LOHAMMER, T. et al. Simulation models of gaseous exchange in Scots pine. *Ecological Bulletin*, v. 32, p. 505–523, 1980.
- LU, X.; WANG, L. Evaluating ecohydrological modelling framework to link atmospheric CO₂ and stomatal conductance. *Ecohydrology*, v. 12, n. 1, p.1-11, 2018. <http://dx.doi.org/10.1002/eco.2051>.
- MASUTOMI, Y. et al. Ozone changes the linear relationship between photosynthesis and stomatal conductance and decreases water use efficiency in rice. *Science Of The Total Environment*, v. 655, p. 1009-1016, 2019. <http://dx.doi.org/10.1016/j.scitotenv.2018.11.132>.
- MEDLYN, B. E. et al. How do leaf and ecosystem measures of water-use efficiency compare? *New Phytologist*, v. 216, n. 3, p.758-770, 2017. <http://dx.doi.org/10.1111/nph.14626>.
- MEDLYN, B. E. et al. Temperature response of parameters of a biochemically based model of photosynthesis. II. A review of experimental data. *Plant, Cell & Environment*, v. 25, n. 9, p. 1167-1179, 2002. <http://dx.doi.org/10.1046/j.1365-3040.2002.00891.x>.
- MEDLYN, B. E. et al. Reconciling the optimal and empirical approaches to modelling stomatal conductance. *Global Change Biology*, v. 17, n. 6, p.2134-2144, 2011. <http://dx.doi.org/10.1111/j.1365-2486.2010.02375.x>.
- MINER, G. L.; BAUERLE, W. L.; BALDOCCHI, D. D. Estimating the sensitivity of stomatal conductance to photosynthesis: a review. *Plant, Cell & Environment*, v. 40, n. 7, p.1214-1238, 2017. Wiley. <http://dx.doi.org/10.1111/pce.12871>
- MOTT K. A.; PARKHURST, D. F. Stomatal responses to humidity in air and helox. *Plant, Cell and Environment*, v. 14, n. 5, p. 509-515, 1991. doi:10.1111/j.1365-3040.1991.tb01521.x
- NADAL, M.; FLEXAS, J. Variation in photosynthetic characteristics with growth form in a water-limited scenario: Implications for assimilation rates and water use efficiency in crops, *Agricultural Water Management*, v. 216, p. 457-472, 2019. <https://doi.org/10.1016/j.agwat.2018.09.024>
- PRENTICE, I. C et al. (2001) The carbon cycle and atmospheric carbon dioxide. In: Houghton JT, Ding Y, Griggs DJ, Noguer M, van der Linden PJ, Dai X, Maskell K, Johnson CA, eds. *Climate Change 2001: the scientific basis. Contribution of Working Group I to the third assessment report of the Intergovernmental Panel on Climate Change*. Cambridge, UK: Cambridge University Press, 183–237.

PRETZSCH, H.; FORRESTER, D. I.; RÖTZER, T. Representation of species mixing in forest growth models. A review and perspective. *Ecological Modelling*, v. 313, p.276-292, 2015. <https://doi.org/10.1016/j.ecolmodel.2015.06.044>.

RUNNING, S. W.; COUGHLAN, J. C. A general model of forest ecosystem processes for regional applications. I. Hydrologic balance, canopy gas exchange and primary production processes. *Ecological Modelling*, n. 42, p.125-154, 1988. [https://doi.org/10.1016/0304-3800\(88\)90112-3](https://doi.org/10.1016/0304-3800(88)90112-3)

RUNNING, S.W.; GOWER, S. T. FOREST-BGC, a general model of forest ecosystem processes for regional applications. II. Dynamic carbon allocation and nitrogen budgets. *Tree Physiology*, v. 9, n.1–2, p. 147-160, 1991. <https://doi.org/10.1093/treephys/9.1-2.147>

SANDS, P. J.; LANDSBERG, J. J. Parameterization of 3-PG for plantation grown *Eucalyptus globulus*. *Forest Ecology and Management*, Amsterdam, v. 163, p. 273-292, 2002. [https://doi.org/10.1016/S0378-1127\(01\)00586-2](https://doi.org/10.1016/S0378-1127(01)00586-2)

SHARKEY T. D. What gas exchange data can tell us about photosynthesis. *Plant, Cell and Environment*, v. 39, n.6, p. 1161-1163. 2016. <https://doi.org/10.1111/pce.12641>

SHARKEY, T. D. et al. Fitting photosynthetic carbon dioxide response curves for C3leaves. *Plant, Cell & Environment*, v. 30, n. 9, p. 1035-1040, 2007. <http://dx.doi.org/10.1111/j.1365-3040.2007.01710.x>

SMITH, N. G.; DUKES, J. S. Drivers of leaf carbon exchange capacity across biomes at the continental scale. *Ecology*, v. 99, n. 7, p. 1610-1620, 2018. <http://dx.doi.org/10.1002/ecy.2370>.

STEFANSKI, A. et al. Surprising lack of sensitivity of biochemical limitation of photosynthesis of nine tree species to open-air experimental warming and reduced rainfall in a southern boreal forest. *Global Change Biology*, v. 26, n. 2, p. 746-759, 2019. <http://dx.doi.org/10.1111/gcb.14805>.

STINZIANO, J. R.; BAUERLE, W. L.; WAY, D. A. Modelled net carbon gain responses to climate change in boreal trees: Impacts of photosynthetic parameter selection and acclimation. *Global Change Biology* v. 25, n. 4, p.1445-1465, 2018. <http://dx.doi.org/10.1111/gcb.14530>

TAIZ, L.; ZEIGER, E. *Fisiologia vegetal*.5.ed. Porto Alegre:Artemed, 2013. 954p.

TARIN, T. et al. Water-use efficiency in a semi-arid woodland with high rainfall variability. *Global Change Biology*, p.1-13, 2019. <http://dx.doi.org/10.1111/gcb.14866>.

TUZET, A.; PERRIER, A.; LEUNING, R. A coupled model of stomatal conductance, photosynthesis and transpiration. *Plant Cell Environmental*, v.26, p. 1097–1116, 2003. <http://dx.doi:10.1046/j.1365-3040.2003.01035>.

VON CAEMMERER S.; EVANS J. R. Temperature responses of mesophyll conductance differ greatly between species. *Plant, Cell and Environment*, v.38, p. 629–637, 2015.

WANG, H. Z. et al. Characteristics of stomatal conductance of *Populus pruinosa* and the quantitative simulation. *Sci. Silvae Sin.* v. 52, p. 136–142, 2016. <http://dx.doi.org/10.11707/j.1001-7488.20160116>

WANG, Q.; HE, Q.; ZHOU, G. Applicability of common stomatal conductance models in maize under varying soil moisture conditions. *Science Of The Total Environment*, v. 628-629, p.141-149, 2018. <http://dx.doi.org/10.1016/j.scitotenv.2018.01.291>

WANG, Y.P.; JARVIS, P.G. Description and validation of an array model- MAESTRO. *Agricultural and Forest Meteorology*. v. 51, n 3-4, p. 257–280, 1990. [https://doi.org/10.1016/0168-1923\(90\)90112-J](https://doi.org/10.1016/0168-1923(90)90112-J)

WEBER, J.; GATES, D. Gas exchange in *Quercus rubra* (northern red oak) during a drought: analysis of relations among photosynthesis, transpiration, and leaf conductance. *Tree Physiology*, v.7, p. 215–225. 1990. <http://dx.doi.org/10.1093/treephys/7.1-2-3-4.215>.

WEI, Z. et al. Simulation of Stomatal Conductance and Water Use Efficiency of Tomato Leaves Exposed to Different Irrigation Regimes and Air CO₂ Concentrations by a Modified “Ball-Berry” Model. *Frontiers In Plant Science*, v. 9, p.1-13, 2018. <http://dx.doi.org/10.3389/fpls.2018.00445>.

WONG, S. C, COWAN, I. R, FARQUHAR, G. D. Stomatal Conductance Correlates with photosynthetic capacity. *Nature*, v. 282, p. 424– 426, 1979. <https://doi.org/10.1038/282424a0>.

WU, J. et al. The phenology of leaf quality and its within-canopy variation is essential for accurate modeling of photosynthesis in tropical evergreen forests. *Global Change Biology*, v. 23, n. 11, p. 4814-4827, 2017. <http://dx.doi.org/10.1111/gcb.13725>.

YANG, Y. et al. Photosynthetic characteristics explain the high growth rate for *Eucalyptus camaldulensis*: Implications for breeding strategy. *Industrial Crops And Products*, v. 124, p.186-191, 2018. . <http://dx.doi.org/10.1016/j.indcrop.2018.07.071>

ZHANG, N. et al. Can the Responses of Photosynthesis and Stomatal Conductance to Water and Nitrogen Stress Combinations Be Modeled Using a Single Set of Parameters? *Frontiers In Plant Science*, v. 8, p.1-20, 2017. <http://dx.doi.org/10.3389/fpls.2017.00328>

ZHOU, S. et al. How should we model plant responses to drought? An analysis of stomatal and non-stomatal responses to water stress. *Agricultural and Forest Meteorology*, v. 182-183, p. 204–214. 2013. <https://doi.org/10.1016/j.agrformet.2013.05.009>

SEGUNDA PARTE- ARTIGOS**ARTIGO 1 - CLIMATIC VARIABLES AND STAND AGE INFLUENCE
PHOTOSYNTHETIC CAPACITY OF FOREST PLANTATIONS IN BRAZIL**

Climatic variables and stand age influence photosynthetic capacity of forest plantations in Brazil

Abstract: Realistic representations of plant carbon exchange processes are necessary to understand the growth and productivity of forests and to understand how plants will behave in future climate change scenarios. These processes are known to vary over depending on environmental and genetic factors. Here, we used the model by Farquhar et al., (1980) to obtain the parameters V_{cmax} , J_{max} and J_{max}/V_{cmax} , and we analyzed the influence of age, growth temperature and precipitation variables and climatic groups on these parameters for the two functional groups (pine and eucalypts). Our results show that the photosynthetic capacity of forests has a difference between the functional groups, the variables growth temperature and precipitation at 10 and 30 days before physiological measurements influenced photosynthetic parameters, suggesting its acclimatization to the environment. The age of the stand influenced photosynthetic ability. Older forests showed an increasing trend in J_{max} . There were no differences between the subtropical and tropical climatic groups, demonstrating an adaptation of the genotypes to the environmental conditions of Brazil. The values of V_{cmax} , J_{max} and J_{max}/V_{cmax} parameters provided in this study expand the database of photosynthetic parameters and can be widely used in modeling studies of planted forests in Brazil.

Keywords: gas exchange, genetic variation, photosynthesis, productivity, temperature, acclimation.

1. Introduction

Forest plantations with species of the genera *Eucalyptus* and *Pinus* represent a large percentage of planted forests in the world. *Eucalyptus* forests cover more than 20 million hectares in more than 90 countries around the world, with the majority in Brazil (7.47 million ha), India (3.9 million ha) and China (4.5 million ha) (FERREIRA et al., 2018; IGLESIAS-TRABADO; WILSTERMANN 2009, IBA 2021). These forests play an important role in providing raw material to meet the global demand for wood and also for the conservation of native forests. Projections indicate that this global demand will increase in future scenarios, making it essential to develop better management strategies (PAQUETTE; MESSIER, 2010; CHRISTINA et al., 2015).

For better strategies to be developed, it is important to understand the processes that influence tree growth and development, tree-environment interactions, and forest function at the ecosystem-scale. Photosynthesis is a key determinant of tree carbon (C) uptake and growth, and represents the largest flux of C between vegetation and the atmosphere (DE KAWUE et al., 2015; PRENTICE et al., 2001; BEER et al., 2010, IPCC 2013). Understanding the factors that influence photosynthesis is important in ecophysiological modeling of forests, which aims to understand the factors that influence forest growth through process-based models (PBM) (LANDSBERG; SANDS, 2011; CHRISTINA et al., 2016) and also to study the prediction of photosynthetic fluxes under climate change scenarios (MEDLYN et al., 2011; FRIEDLINGSTEIN et al., 2014; IPCC 2014). The main tools used to predict the carbon C balance of vegetation in future scenarios are the Earth System Models (ESMs) and Global Vegetation Models (GVMs) (KUMARATHUNGE et al., 2019, SMITH; DUKES, 2018).

These models incorporate the biochemical model of photosynthesis proposed by Farquhar *et al.*, (1980), also known as FvCB (DE KAWUE et al., 2015). The FvCB model defines the biochemical limitations of photosynthesis: the maximum rate of Rubisco carboxylation (V_{cmax}), the maximum rate of electron transport for RuBP regeneration (J_{max}), and the rate of triose phosphate utilization (TPU). Net photosynthesis is also determined by stomatal limitations of CO_2 diffusion, mesophyll conductance to CO_2 , and the rate of leaf respiration. The two major biochemical processes thought to limit photosynthesis are V_{cmax} and J_{max} (LIN et al., 2012). TPU limitation is not normally used in models as it rarely limits photosynthesis under field conditions (SHARKEY, 1985; ELLSWORTH et al., 2015; DE KAWUE et al., 2015; KUMARATHUNGE et al., 2019; STEFANSKI et al., 2019). The FvCB model assumes that mesophyll conductance is infinite, and C_i equals the $[CO_2]$ at the site of CO_2 fixation in the chloroplast. Although many studies have shown this assumption to be incorrect, leading to inaccurate estimates of photosynthesis in the field, ‘apparent’ rates of V_{cmax} and J_{max} , which incorporate both biochemical capacity and mesophyll conductance, are still widely used in larger-scale vegetation models (LIN et al., 2013)

Photosynthetic parameters can vary between species and plant growth conditions due to adaptation and acclimation to environmental conditions (KATTGE; KNOOR 2007, SMITH; DUKE, 2018). Adaptation occurs at the population-level and is a long-term evolutionary response to the environment. Differences in temperature adaptation among populations or species are sometimes observed when populations differ in the temperature response of photosynthesis. For example, cool-origin populations sometimes show higher A and V_{cmax} than warm-origin

populations when compared at a common growth and measurement temperature (OLEKSYN et al., 1998, SILIM et al., 2010; ASPINWALL et al., 2017). Acclimation occurs within individuals and can happen within days to weeks (KUMARATHUNGE et al., 2019). Photosynthetic acclimation to an increase in growth temperature is much more diverse than its response to rising CO₂ concentrations and cannot be described in terms of simple up- or down-regulation (WAY; YAMORI 2014). Temperature acclimation can be inferred from several different responses (WAY; YAMORI 2014). Typically, acclimation responses involve at least one of the following: 1) changes in the short-term temperature optimum of net photosynthesis, V_{cmax}, or J_{max}, 2) changes in net photosynthesis at warmer or colder growth temperatures relative to some standard growth temperature, or 3) changes in V_{cmax} or J_{max} at standard temperature (25 °C) with changes in growth temperature. Typically, V_{cmax} or J_{max} at 25 °C decline with increasing growth temperature (SMITH; DUKES, 2018).

Although most land surface models use specific parameters for plant functional groups (PFTs), there is still a misuse of these parameters. In a review prepared by Rogers (2013), when analyzing variation in V_{cmax} for 16 plant functional groups (PFTs) used in 10 ESMs, the author reported that in many cases, parameterization was based on limited data sets and poorly defined coefficients that were used to adjust model parameters and set PFT-specific values for V_{cmax}. An important conclusion of Rogers (2013) is that databases need additional data from a wider range of species (representing different PFTs) and growth conditions to reduce uncertainty in the parameterization of photosynthetic processes in larger-scale models.

The models used to project future climate change are highly sensitive to parameterization, so abiotic responses such as environmental conditions must be accurately represented. Temperature and water availability influence plant physiological performance on multiple spatial and temporal scales (STEFANSKI et al., 2019). However, photosynthesis and respiration are known to respond to environmental conditions on timescales close to weeks, rather than decades (KUMARATHUNGE et al., 2019; SMITH; DUKES, 2018; KATTGE; KNOOR 2007; BATTAGLIA et al., 1998).

Several studies have investigated the influence of growth temperature, i.e. the ambient temperature days before measurements, on the photosynthetic capacity of plants aiming to understand temperature acclimation (MEDLYN et al., 2002, KATTGE; KNOOR 2007; SMITH; DUKES, 2018; KUMARATHUNGE et al., 2019). Smith and Dukes (2018) reported that the previous week's temperature and soil moisture at the time of measurement were a better predictor of photosynthetic capacity than long-term climate (SMITH; DUKES, 2018). The

authors also highlight the plasticity of plant photosynthesis and the rapid acclimatization of photosynthesis to changes in environmental conditions. There is evidence that photosynthetic capacity varies with plant growth temperature, enabling plants to carry out photosynthesis more efficiently (KATTGE; KNOOR, 2007). Aspinwall et al. (2016) also observed that *E. tereticornis* demonstrated acclimation of leaf photosynthesis and respiration to seasonal temperature changes that was consistent under current and + 3°C warmer climate, indicating that observations of thermal acclimation to prevailing seasonal temperature changes may be used to infer photosynthetic and respiratory responses of trees to climate warming.

There is also clear evidence that soil moisture can modulate the effects of climate warming on photosynthesis (REICH et al., 2018). As the seasonal differences in precipitation alters soil moisture availability we evaluate total precipitation as an indicative of soil moisture (ROSENTHAL et al., 2014). In addition to climatic factors, several studies have reported that leaf phenology (WU et al., 2017), ontological factors (leaf age) (ALBERT et al., 2018), genetic characteristics of species (MEDLYN et al., 2002; LIN et al., 2013), climate of origin of species (BERRY; BJÖRKMAN, 1980; ASPINWALL et al., 2017) and forest nutrition (BAHAR et al., 2016) can strongly influence V_{cmax} and J_{max} . It is possible the models could be improved by incorporating information about these factors, especially if they explain significant variation in photosynthetic parameters.

Previous studies on *Pinus* stand shown that photosynthetic capacity does not change with age, but net photosynthesis declines with age because stomatal limitation increases (DRAKE *et al.*, 2010). However, it is known that plants have morphological variations over the growing season, for example, the photosynthetic parameters vary with leaf age (ALBERT *et al.*, 2018), which covaries with leaf traits over the growing season (NIINEMETS, 2012; SONG et al., 2021). Other factors as leaf nitrogen content (HIKOSAKA, 2005), Leaf quantity (i.e., canopy leaf area index, LAI), quality (i.e., per-area photosynthetic capacity), and longevity all influence the photosynthetic seasonality of tropical evergreen forests (WU et al., 2017). The study by Albert et al. (2018) revealed that stomatal conductance and biochemical parameters of photosynthesis were higher for recently matured leaves than for old leaves.

Studies of photosynthetic temperature acclimation of planted forests in Brazil are still incipient. Evaluating the response of photosynthetic capacity of planted trees under environmental conditions is essential to provide reliable estimates of the parameters V_{cmax} and J_{max} for the genus *Eucalyptus* and *Pinus*. In this study we evaluated photosynthetic parameters from experiments under field environmental conditions planted in different locations in Brazil,

with different species/ genotypes of the genus *Eucalyptus* and *Pinus*, and with different ages. Our specific aim were to determine the role of stand age, the climatic origin of genotypes *Eucalyptus*, differ among species of *Pinus* and prevailing climatic conditions (growth temperature and precipitation) on V_{cmax} , J_{max} in planted forests of *Eucalyptus* and *Pinus* in Brazil. For this, we test three hypotheses: Our first hypothesis is that short-term environmental variables as growth temperature and precipitation have a significant effect on photosynthetic capacity of forests of *Eucalyptus* and *Pinus* in Brazil. These results can provide parameters for a robust representation of photosynthetic acclimation in GVMs and also to provide parameters for parameterization of process-based models such as MAESTRA/MAESPA (DUURSMA; MEDLYN, 2012) used in ecophysiological modeling studies. Our second hypothesis was the age of the stand influences the parameters V_{cmax} and J_{max} , as the morphological characteristics change along the plant's growth cycle, which can consequently alter the photosynthetic capacity. Finally, our third hypothesis was that species of cool-origin of genus eucalypts have greater photosynthetic than species of warm-origin.

2. Material and Methods

2.1 Dataset

We compiled a database consisting of leaf photosynthetic CO₂ response measurements (A-C_i curves hereafter) evaluated at different climatic conditions. The database covers species or genotypes of the genus *Eucalyptus* and species of the genus *Pinus* from 11 experiments conducted in different locations in Brazil. Each experiment was carried out independently, with different planting densities, fertilization regimes and specific silvicultural treatments (references in Table 1). All A-C_i curves were measured under field conditions.

We obtained 535 A-C_i curves measurements of upper canopy leaves from eucalypt and pine. The A-C_i curves of eucalypt species were obtained from 8 different experiments. In three experiments (1, 6 and 7) two campaigns were carried out in the same stand but at different stand ages (Table 1).

The genotypes of eucalypt were classified into two climatic groups (subtropical and tropical). The genotypes were classified according to the climate of the genotype origin region in Brazil and on the Köppen climate classification (ALVARES et al., 2013). This climatic

classification was based on the classification proposed by BINKLEY et al., 2017 on the TECHS Brazil project (table 2).

A-Ci curves for species in the genus pine were obtained in 3 experiments (ID12 to 14). Datasets ID12 and ID13 are part of the same experiment, but as the species are different (*P. taeda* e *P. caribaea*), we described with different IDs. The age of eucalypt ranged from 12 to 84 months. For species of pine, the age ranged from 36 to 60 months. All data that are part of the database are original data. The distribution of the experiments in Brazil is on the map (Figure 1).

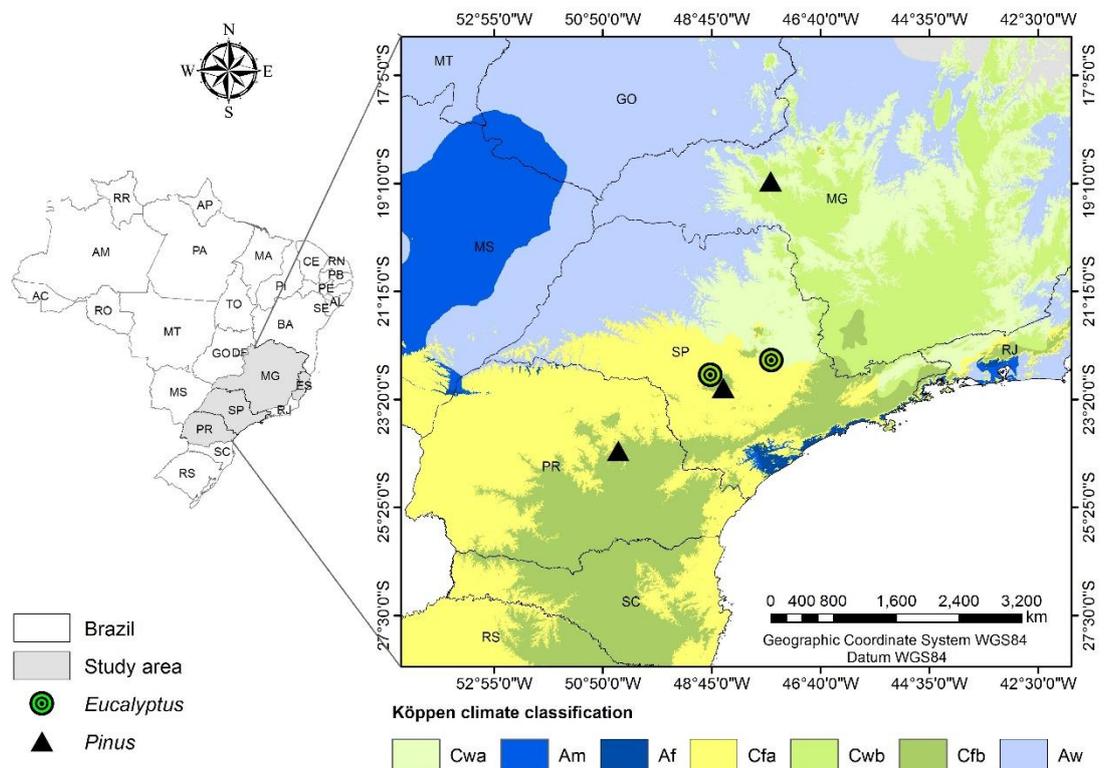


Figure1. Map showing the location of experiments in Brazil where photosynthetic parameters were determined.

Table 1. Experimental metadatasets used in this study.

Species/genotype	Experiment ID	Age (months)	N° of curves	Site of Location (city and state)	Lat. (°S)	Long. (°W)	Tmean (C°)	Rainfall (mm)	Reference
<i>E.grandis</i>	1	64	7	Itatinga-SP	-22.97	-48.73	19.5	1268	Campoe <i>et al.</i> (2013)
<i>E.grandis</i>	2	78.7	30	Itatinga-SP	-22.97	-48.73	20.5	1903	Campoe <i>et al.</i> (2013)
<i>Eucalyptus sp</i>	3	10	15	Piracicaba-SP	-22.7	-47.64	19.5	1098	Binkley <i>et al.</i> (2017)
<i>E.urophylla</i>	4	12	7	Itatinga-SP	-22.97	-48.73	19.5	2063	Unpublished data
<i>E. grandis x E. urophylla</i>	5	84	8	Itatinga-SP	-22.97	-48.73	19	1568	Unpublished data
<i>E.grandis</i>	6	30	35	Itatinga-SP	-22.97	-48.73	18.5	912	Christina <i>et al.</i> (2016)
<i>E.grandis</i>	7	20	66	Itatinga-SP	-23.03	-48.63	18.5	912	Christina <i>et al.</i> (2015)
<i>E.grandis</i>	8	32	65	Itatinga-SP	-23.03	-48.63	18.5	1075	Christina <i>et al.</i> (2015)
<i>E.grandis</i>	9	12	21	Itatinga-SP	-23.03	-48.63	21.7	1713	Battie-Laclau <i>et al.</i> (2014)
<i>E.grandis</i>	10	22	24	Itatinga-SP	-23.03	-48.63	19.0	1568	Battie-Laclau <i>et al.</i> (2014)
<i>Eucalyptus spp.</i>	11	16	50	Piracicaba-SP	-22.71	-47.63	21.6	1070	Marrichi <i>et al.</i> (2005)
<i>P.taeda</i>	12	60	47	Itatinga-SP	-23.05	-48.64	18.5	912	Carneiro, (2013)
<i>P.caribaea</i>	13	60	56	Itatinga-SP	-23.05	-48.64	18.5	912	Carneiro, (2013)
<i>P.taeda</i>	14	36	4	Telêmaco Borba-PR	-24.05	-50.07	18.5	1597	Carneiro, (2013)
<i>P.caribaea</i>	15	60	12	Nova Ponte-MG	-19.03	-47.13	21.4	1517	Carneiro, (2013)

ID: identification of each experiment

Age: months after planting of each experiment.

N° of curves: number of A-Ci curves measured in each experiment.

Lat e long: latitude (South) and longitude (west) of the experiment location in decimal degrees

Tmean: observed mean annual temperature during the year of data sampling

Rainfall: observed accumulated rainfall during the year of data sampling

Table 2. Climatic type, genotypes of *Eucalyptus* and climatic type of the breeding region.

Climatic type	Species or genotypes	Climate of the clone origin region*
Subtropical	<i>E.dunnii</i>	Temperate oceanic climate (Cfb)
	<i>E.grandis</i>	Temperate oceanic climate (Cfb)
	<i>E.grandis</i>	Tropical with dry-winter (Aw)
	<i>E.saligna</i>	Temperate oceanic climate (Cfb) humid subtropical with dry winter and hot summer (Cwa)
	<i>E.urophylla</i>	Tropical with dry-winter (Aw)
Tropical	<i>E.urophylla</i>	Tropical with dry-winter (Aw)
	<i>E.grandis</i> x <i>E.urophylla</i> ,	Tropical with dry-winter (Aw)
	<i>Eucalyptus</i> spp.	Tropical with dry-winter (Aw)
	<i>E.grandis</i>	Tropical without dry season (Af)
	<i>E.grandis</i> x <i>E. camaldulensis</i>	Tropical with dry summer (As)

*Köppen climatic classification (ALVARES et al., 2013b).

2.2. Estimation of apparent V_{max} , J_{max} from traditional response curves (A-Ci-TRAD)

The response of net CO₂ assimilation rate (A_{net}) ($\mu\text{mol m}^{-2} \text{s}^{-1}$) at a predetermined set of CO₂ various concentrations ($\mu\text{mol mol}^{-1}$) under saturating light intensity (photosynthetic photon flux density (PPFD) using portable photosynthesis systems are known as photosynthetic-CO₂ response curves or A-ci curves. The A-Ci curves are used to estimate the maximum rate of Rubisco carboxylation (V_{max}) and the maximum rate of electron transport (J_{max}) according to Farquhar *et al.* (1980).

The traditional method for completing one A-Ci curve begins with a measurement of A_{net} at ambient CO₂ concentration (400 $\mu\text{mol mol}^{-1}$), which activates Rubisco (LONG; BERNACCHI, 2003). The measurements then progress through a series of stepwise changes in CO₂ concentration spanning subambient (usually ranges from 40 to 400 $\mu\text{mol mol}^{-1}$) to superambient CO₂ concentration (usually 400-2000 ppm $\mu\text{mol mol}^{-1}$) (LONG; BERNACCHI, 2003; COURSOLE et al., 2019). Changes in atmospheric CO₂ are accomplished by triggering step changes in the reference CO₂ concentration. Measurements must be conducted in saturating irradiance conditions between 1000 and 2000 $\mu\text{mol m}^{-2} \text{s}^{-1}$ (DE KAUWE *et al.*, 2015)

At each reference CO₂ concentration, the atmospheric CO₂ (sample) outside the leaf and the intercellular CO₂ (C_i) are recorded once A_{net} has reached a predetermined level of stability; usually when the stability coefficient is reduced to less than 0.5%. The time required to reach stability varies but is usually between 4 and 10 minutes. The time required to complete one Aci-

curve can take from 30 min to more than 60 min (depending on the number of CO₂ concentrations measured and the system used) (COURSOLLE et al., 2019).

In this study we used the traditional A–C_i method for all datasets. Measurements were taken on fully expanded upper canopy (sun-lit) leaves, healthy and free of pathogens. Measurements were taken in the morning with RH higher than 50% aiming to avoid stomatal open limitation. Measurements were made at saturating irradiance conditions (photosynthetic photon flux density-PPFD) between 1600 and 2000 μmol m⁻² s⁻¹, using a portable photosynthesis system with standard 2x3 cm leaf chamber with a red-blue LED light source (LI-6400, Li-Cor Biosciences, Lincoln, NE, USA). The concentrations of CO₂ used ranged between 400 and 1500 ppm of CO₂ (400, 300, 250, 200, 150, 100, 75, 50 ppm and then 400, 600, 800, 1000, 1300 ppm). The A-C_i curves measured at leaf temperatures ranging from 12 to 38°C. To access the canopy of trees and take measurements, we installed scaffolding towers located between the rows of trees within the stand.

2.3 Data analyses

2.3.1 Model Farquhar (1980) – FvCB

We used the model of Farquhar, Caemmerer & Berry (1980) to characterize photosynthetic biochemical component processes. The widely used formulation and parameterization of the FvCB model is of the form:

$$A_n = \min (A_c, A_j) - R_d \quad (1)$$

$$A_c = V_{CMAX} \frac{C_i - \Gamma^*}{C_i + K_c(1 + \frac{O_i}{K_o})} \quad (2)$$

$$A_j = J \frac{C_i - \Gamma^*}{4(C_i + 2\Gamma^*)} \quad (3)$$

where A_c and A_j (μmol m⁻² s⁻¹) are the assimilation rate limited by Rubisco activity and by electron transport (regeneration of ribulose-1,5-bisphosphate, RuBP), respectively, R_d (μmol m⁻² s⁻¹) is the mitochondrial respiration under illumination condition, V_{CMAX} (μmol m⁻² s⁻¹) is the maximum rate of Rubisco carboxylation, C_i and O_i are the CO₂ and O₂ concentrations in the intercellular space (μmol mol⁻¹), Γ^* is the CO₂ compensation point in the absence of

mitochondrial respiration ($\mu\text{mol mol}^{-1}$); K_C and K_O are the Michaelis–Menten coefficients for CO_2 and O_2 , respectively ($\mu\text{mol mol}^{-1}$), and J (c) is the potential rate of electron transport, related to the incident photosynthetically active photon flux density (Q) by:

$$\theta J^2 - (\alpha Q + J_{MAX})J + \alpha Q J_{MAX} = 0 \quad (4)$$

where J_{MAX} is the maximum rate of electron transport for RuBP regeneration electron ($\mu\text{mol m}^{-2} \text{s}^{-1}$), θ is the curvature of the light response curve (unitless) and α the quantum yield of electron transport ($\text{mol e}^- \text{mol}^{-1}$).

We parameterized Eqns 1–4 using the *fitacis* function within the *PLANTECOPHYS* package (DUURSMA, 2015) in R version 4.1.0 (R Development Core Team, 2012), with the default settings. We standardized V_{cmax} and J_{max} estimates to 25 °C. R_d value was estimated from the fit to the A-Ci curve. We did not measure mesophyll conductance and rely on the simplifying assumption that C_i equals the $[\text{CO}_2]$ in the chloroplasts (as in Farquhar *et al.*, 1980). Therefore, our estimates of V_{cmax} and J_{max} are ‘apparent’ rates that reflect both biochemical limitations of photosynthesis and mesophyll conductance (e.g., SALMON *et al.*, 2020).

For each curve, we calculated the ratio of J_{max} to V_{cmax} at 25 °C (J_{max}/V_{cmax}) by dividing J_{max} by V_{cmax} . To assess the quality of the data, we assessed all A-Ci curves using the selection criteria, described in the topic below (DUURSMA, 2015; DE KAWUE *et al.*, 2015).

2.3.2 Curve selection criteria

Before fitting FvCB model we checked the dataset in two steps. First, we analyzed the raw data to identify possible errors made during measurements. Second, we analyzed the data after fitting the A-ci curves. In the first step we eliminated data that were outside the range of reasonable values and deleted measurements negative C_i values and eliminated incomplete curves with only a few observations. We selected only data where measurements were first conducted at ambient CO_2 concentration ($400 \mu\text{mol mol}^{-1}$) and saturating irradiance conditions ($1500 - 1800 \mu\text{mol m}^{-2} \text{s}^{-1}$).

In the second phase of data checking, after fitting the FvCB model, we analyzed the ACi curves. We check if the photosynthesis saturates with C_i and if C_i reaches high enough values for reasonable estimates of J_{max} ($> 800 \text{ ppm}$) (Duursma, 2015). When there is no CO_2

saturation, the J_{max} estimate may be underestimated, i.e. where there is no clear photosynthesis plateau at high C_i values, the J_{max} estimates should be excluded from the dataset. The curves used to estimate parameters (V_{cmax} and J_{max}) were screened to exclude ‘bad’ measurement curves based on the traditional $A-C_i$ fitting approach, ‘bad’ being defined according to the following criteria of De Kauwe et al. (2015) with adaptations. The R^2 was reduced to 0.8 in some dataset containing small samples. Follow all the criteria used in this study:

- (i) The first obtained measurement was at an ambient CO_2 concentration < 300 or $> 400 \mu\text{mol mol}^{-1}$?
- (ii) The FvCB model did not fit?
- (iii) The fitted function had $R^2 < 0.8$?
- (iv) The RMSE was greater than 20?
- (v) Parameter values are > 500 ?
- (vi) Are parameter values negative?

All curves that followed the criteria above were eliminated from this study. As a metric for evaluating the error of the $A-C_i$ curves, we used the RMSE (root mean square error) and the R^2 (coefficient of determination). We only used curves with $RMSE < 20$ and $R^2 > 0.8$. Curves with negative parameters and with very high values (greater than > 500) were considered as outliers and were eliminated. After screening, the dataset contained a total of 447 $A-C_i$ curves measured at leaf temperatures ranging from 12 to 38°C. A total of 88 curves were eliminated using the criteria (ii), (iii) and (iv), (v), (vi) which corresponded respectively 13%, 2%, $< 1\%$, $< 1\%$.

2.3.3 Meteorological data

Meteorological data were obtained from automatic weather stations located close to the experiments (approximately 500 meters). To determine the influence of plant growth temperature on photosynthetic parameters we used the mean air temperature for 10 (10d) and 30 days (30d) before gas exchange measurements. Previous studies that have evaluated the influence of prevailing growth temperature have calculated mean growth temperature for time periods ranging from 3 to 30 days. The 10d and 30d mean provides information about the average temperature close to the measurements and over the previous month (KATTGE; KNORR, 2007; KUMARATHUNGE et al., 2019). The 10d and 30 d growth temperatures were

based on previous studies that investigated the influence of short-term climate on plants. (MEDLYN et al., 2002, KATTGE; KNOOR 2007; SMITH; DUKES, 2018; KUMARATHUNGE et al., 2019). We also analyzed the influence of total precipitation for 10 and 30 days before gas exchange measurements on parameters.

2.2 Analyses of age, climate and origin effects

Initially, we analyzed the effects of the functional group (eucalypt vs. pine), age, and prevailing air temperature ($T_{\text{mean}10}$ and $T_{\text{mean}30}$, respectively) and total precipitation at 10 and 30 dias before gas exchange measurements (Prec_{10} and Prec_{30} , respectively) on parameters V_{cmax} , J_{max} and $J_{\text{max}}/V_{\text{cmax}}$ (all standardized at 25 °C) using mixed generalized linear models (GLMM).

First, we build a global model in the form: $Y \sim \text{Group} * (\text{t_mean}10 + \text{tmean}30 + \text{tmean_day} + \text{prec_10} + \text{prec_30}) + \text{age} + (1|\text{Experiment}) + (1|\text{Site})$, with all continuous variables interacting with the categorical variable “Group”. We include "Experiment" and "Site" as the random variables to control dependence between curve measurements performed in the same experiment and at the same collection site. From this global model, we obtained all submodels with combinations of uncorrelated variables ($r < |0.6|$) using the dredge function of the MuMIN package (Bartón, 2020).

We selected the best models based on the AIC (Akaike Information Criterion), considering a difference criterion of 4 in relation to the best model (AICc - Burnham et al., 2011), and then were submitted to the multi-model inference (BURNHAM et al., 2011) using the model.avg function of the MuMIn package (BARTÓN, 2020) to obtain the average coefficients of the explanatory variables and their significance. The three variables were worked on in the Gaussian family of residue distribution (ln transformation for the two first), also meeting the criteria of homoscedasticity and normality of residues, in addition to not showing spatial autocorrelation by the correlog function of the ncf package (BJORNSTAD, 2008).

After obtaining the significance of the variables, the models obtained for each variable were submitted to a Least Square means (Lsmeans) test using the lsmeans function from the lsmeans package (LENTH, 2018), to compare means between functional groups at the significance level of 0.05.

Then, we made a subset of the data corresponding to each of the functional groups (eucalypt vs. pine) for internal comparisons in relation to the climatic groups (tropical and

subtropical) and *Pinus* species (*P. taeda* and *P. caribaea*) for each variable physiological. In each case, we build a generalized linear model in the form $y \sim \text{category} + (1|\text{Experiment}) + (1|\text{Site})$, where “category” refers to the categorical explanatory variable of each functional group (climate group for eucalypt and species for pine), also including the experiment and the site as random factors to control the possible dependence between curves performed in the same experiment and on the same sites. The model was then submitted to a Least Square means (Lsmeans) test using the `lsmeans` function from the `lsmeans` package (LENTH, 2018), to compare means between categories in each functional group and their combinations at a significance level of 0.05. All analyzes were performed in R software (R Core Team, 2020).

3. Results

3.1 Climatic and age influence on parameters

We found significant differences between the functional groups in V_{cmax} and J_{max} , with significantly higher values observed for eucalypt, but with no significant difference for the ratio of the two variables (J_{max}/V_{cmax}) (Table 4). For all parameters, no significant interactions were found between group and climatic variables, indicating that groups responded similarly with climatic variables. The relationship between J_{max} and V_{cmax} (both at 25 °C) of the pine and eucalypt planted forests under the environmental conditions of Brazil is show in Figure 2.

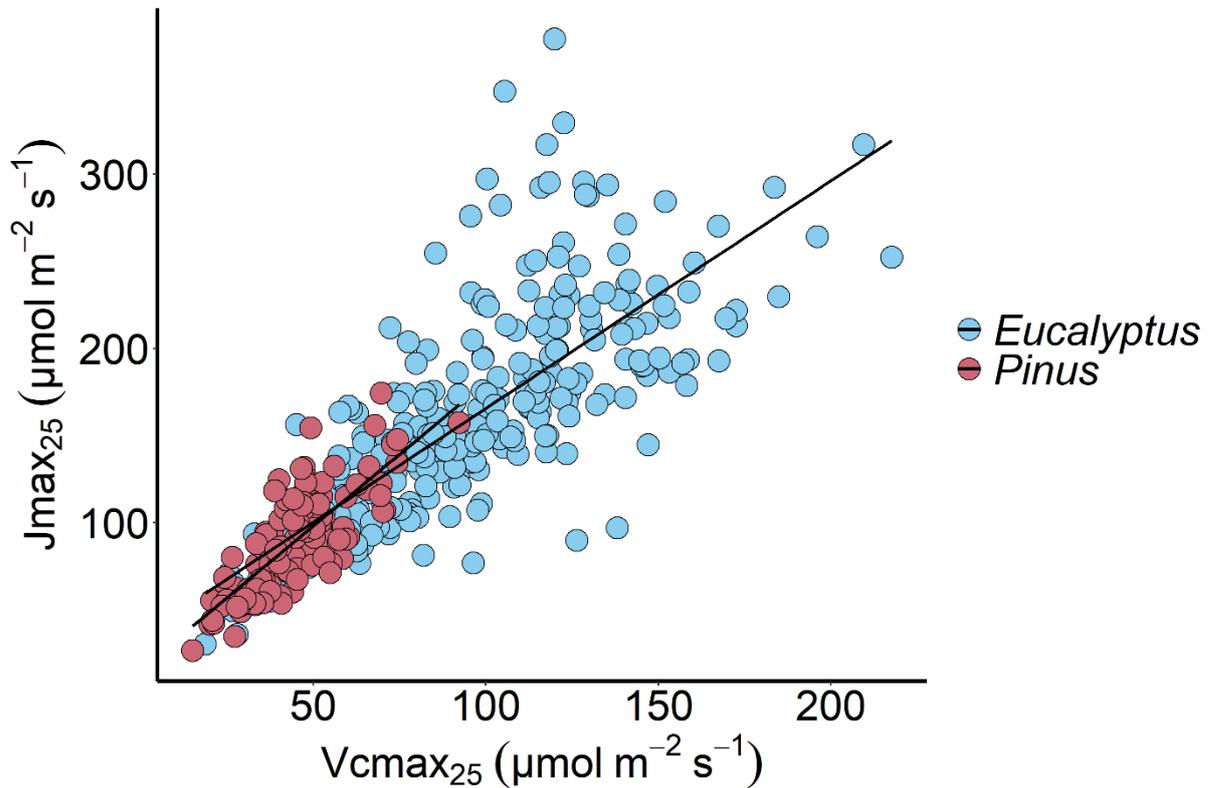


Figure 2: Relation between J_{max} ($\mu\text{mol m}^{-2} \text{s}^{-1}$) and V_{cmax} ($\mu\text{mol m}^{-2} \text{s}^{-1}$) values standardized at 25 °C across *Eucalyptus* and *Pinus* species in Brazil. The black line does not represent a statistical analysis, it is only a visual resource.

V_{cmax} was positively associated only by $Prec_{10}$ (Fig 3-a), while J_{max} was significantly positively influenced by all climatic variables ($Prec_{10}$, $Prec_{30}$, T_{mean10} and T_{mean30}) (Fig 4) and by age (Fig 3-b). Thus, J_{max} values are higher in older trees and when collected in warmer and humid climates (Table 5). The J_{max}/V_{cmax} ratio was positively associated with T_{mean30} (Fig 5 - b; Table 5) and significantly negatively influenced by $Prec_{10}$ (Fig 5-a; Table 5). Thus, J_{max}/V_{cmax} had higher values at high temperatures, but with lower precipitation rates. We found no significant effect of the variable mean temperature of the day before collection (T_{mean_day}) in the model.

Table 4: Average values and standard errors obtained by *Lsmeans* for physiological variables in each functional group. Treatments followed by the same letter within rows are not significantly different according to *LsMeans* test at 0.05 of significance level. Original data of V_{cmax} J_{max} were transformed by natural logarithm to be analyzed, but the estimated means were transformed back to be present in this table

Variables	<i>Eucalyptus</i>	<i>Pinus</i>
Vcmax ($\mu\text{mol m}^{-2} \text{s}^{-1}$)	89.5 ± 9.86 a	43.7 ± 8.17 b
Jmax ($\mu\text{mol m}^{-2} \text{s}^{-1}$)	153.3 ± 15.9 a	79.2 ± 13.9 b
Jmax/Vcmax	2.12 ± 0.19 a	1.83 ± 0.12 a

Table 5: Estimates and p-values of significance for the continuous variables with significant effects on physiological variables. Note that the first value before “/” is the estimate of relation and the second value is p-value of significance. The interaction between functional group and continuous variables is not included due to not being significant for any variable. Empty cell represents variables with no significant influence and/or were not selected in the final result.

Variables	Age	Prec 10	Prec 30	T mean 10	T mean 30
Vcmax		0.17 / <0.001			
Jmax	0.15 / 0.03	0.06 / 0.007	0.06 / 0.03	0.07 / <0.001	0.11 / <0.001
Jmax/Vcmax		- 0.17 / 0.001			0.11 / <0.001

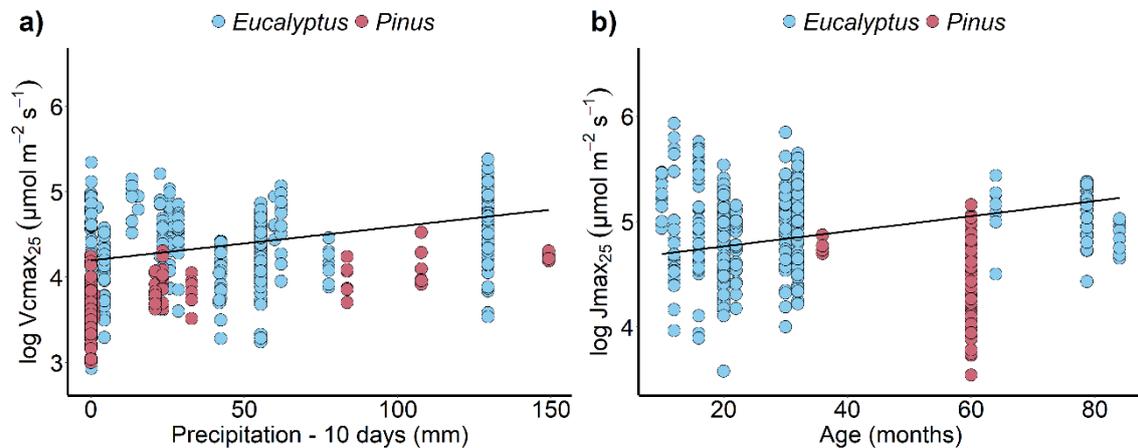


Figure 3: Relation between natural logarithm of V_{cmax} ($\mu\text{mol m}^{-2} \text{s}^{-1}$) standardized at 25 °C and the precipitation (mm) in the 10 days before the collection (a); and relation between natural logarithm of J_{max} ($\mu\text{mol m}^{-2} \text{s}^{-1}$) and the age (months) of plants in the collection time (b). The black line represents the estimate of relation between variables obtained by generalized linear models. The different colors of functional groups (*Eucalyptus* and *Pinus*) are just for better views. No significant differences between the functional groups.

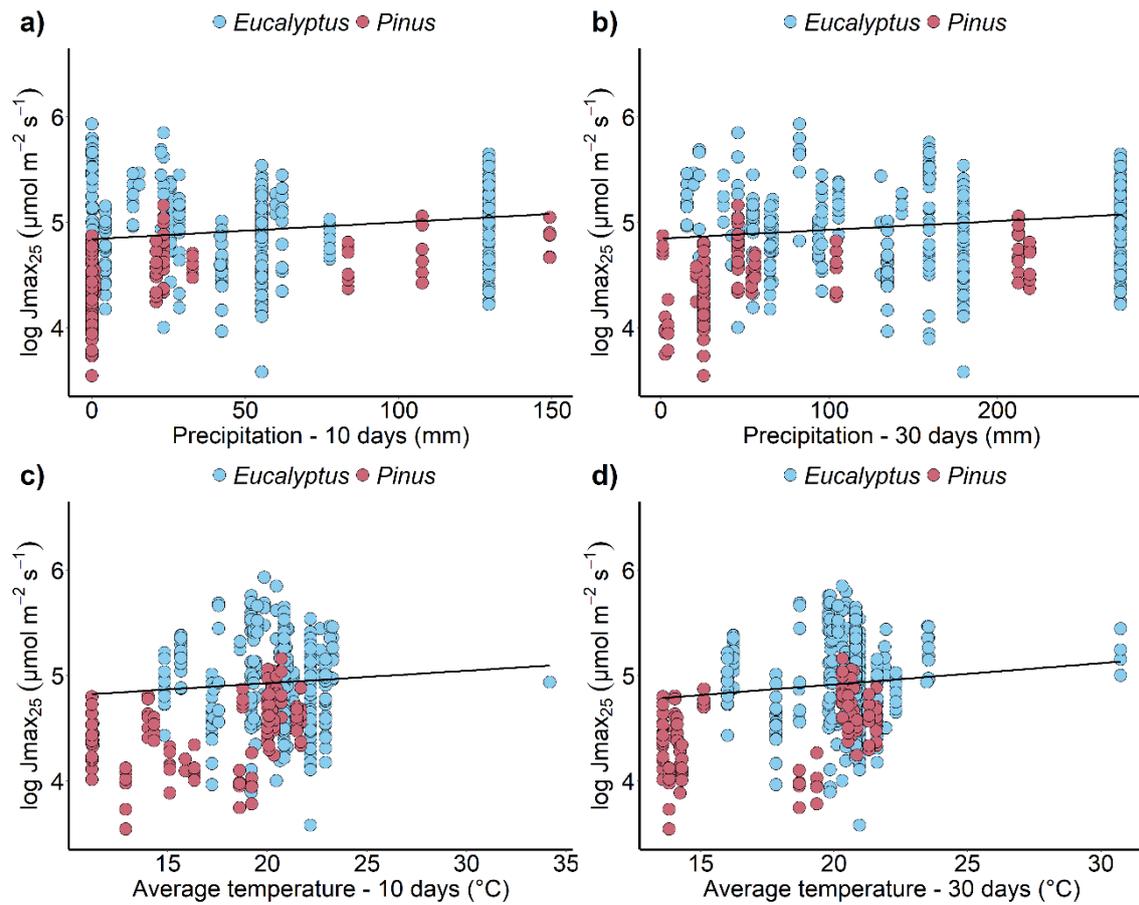


Figure 4: Relation between natural logarithm of J_{max} ($\mu\text{mol m}^{-2} \text{s}^{-1}$) standardized at 25 $^{\circ}\text{C}$ and the precipitation (mm) in the 10 days before the collection (a), precipitation (mm) in the 30 days before the collection (b), average temperature ($^{\circ}\text{C}$) in the 10 days before the collection (c) and average temperature ($^{\circ}\text{C}$) in the 30 days before the collection (d). The black line represents the estimate of relation between variables obtained by generalized linear models. The different colors of functional groups (*Eucalyptus* and *Pinus*) are just for better views. No significant differences between the functional groups.

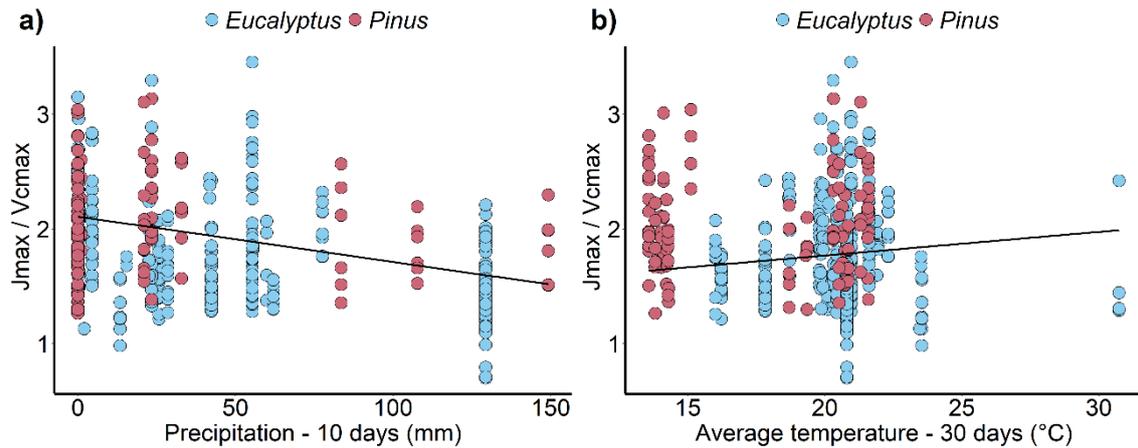


Figure 5: Relation between natural J_{max}/V_{cmax} and the precipitation (mm) in the 10 days before the collection (a); and average temperature ($^{\circ}\text{C}$) in the 30 days before the collection (b). The black line represents the estimate of relation between variables obtained by generalized linear models. The different colors of functional groups (*Eucalyptus* and *Pinus*) are just for better views. No significant differences between the functional groups.

3.3 Climatic group and species influence on physiological variables

Comparing the physiological parameters in relation to climatic groups of eucalypt genotypes (subtropical and tropical) no significant differences were found (V_{cmax} , J_{max} and J_{max}/V_{cmax}). For species of the genus *Pinus* (*P. taeda* and *P. caribaea*), we found significant differences for the parameters. The parameters V_{cmax} , J_{max} and J_{max}/V_{cmax} were higher in *P.taeda* than *P caribaea* (Table 6).

Table 6: Average values and standard errors obtained by *Lsmeans* for physiological variables in in categories of each functional group. Treatments followed by the same letter in the columns are not significantly different according to *LsMeans* test at 0.05 of significance level. Original data of V_{cmax} and J_{max} were transformed by natural logarithm to be analyzed, but the estimated means were transformed back to be present in this table.

Group	Category	V_{cmax} ($\mu\text{mol m}^{-2} \text{s}^{-1}$)	J_{max} ($\mu\text{mol m}^{-2} \text{s}^{-1}$)	J_{max} / V_{cmax}
Eucalyptus	Subtropical	99.0 ± 16.96 a	186 ± 28.2 a	1.86 ± 0.18 a
	Tropical	84.2 ± 7.61 a	146 ± 10.6 a	1.82 ± 0.11 a
Pinus	<i>P. taeda</i>	43.8 ± 5.04 a	101.5 ± 11.7 a	2.22 ± 0.21 a
	<i>P. caribea</i>	34.9 ± 4.00 b	73.1 ± 1.99 b	2.04 ± 0.21 b

4. Discussion

4.1 Intergroup differences in photosynthetic biochemistry

We investigated the photosynthetic capacity of the eucalypt and pine group in a dataset from several experiments under field conditions in Brazil, and found clear differences in parameters V_{cmax} , J_{max} and J_{max}/V_{cmax} between groups. There are several factors that correlate with variations in photosynthetic parameters, including temperature (KATTGE; KNORR, 2007), CO_2 concentration (AINSWORTH; LONG, 2005), light gradient (Niinemets et al., 1999), phenology (WU et al., 2017), leaf age (ALBERT et al., 2018) and characteristics of plant functional groups, for example genotype or species (MEDLYN et al., 2002; LIN et al., 2013). These factors are typically associated with variation in leaf nitrogen content (LIN et al., 2013; ROGERS, 2013; MEDLYN et al., 1999), leaf physiology of each functional group and photosynthetic capacity, which can be altered by enzyme activation states and other processes (REICH et al., 1991, STINZIANO et al., 2017; VON CAEMMERER, 2000).

The eucalypt group had an average of $V_{cmax} = 89.5 \mu\text{mol m}^{-2} \text{s}^{-1}$ and $J_{max} = 153.3 \mu\text{mol m}^{-2} \text{s}^{-1}$, values higher than the pine group ($V_{cmax} = 43.7 \mu\text{mol m}^{-2} \text{s}^{-1}$ and $J_{max} = 79.2 \mu\text{mol m}^{-2} \text{s}^{-1}$) (Table 2). The differences in the parameters of the eucalypt and pine groups confirm the need to always use specific parameters for functional groups in the modeling of planted forests. Differences between functional groups have also been observed in other studies (KATTGE; KNORR, 2009, MEDLYN et al., 2002).

The higher rates in eucalypt group parameters are likely explained by differences in leaf nitrogen content. V_{cmax} and J_{max} have positive correlations with soil nutrients P and N, widely used in *Eucalyptus* planted forests (BAHAR et al., 2016; WALKER et al., 2014). Higher rates of V_{cmax} and J_{max} were found in *Eucalyptus* species with higher leaf nitrogen (LIN et al., 2013, HÉROULT et al., 2013).

The variations in leaf and soil P play a key role in modulating the photosynthetic capacity. Studies shows reduced V_{cmax} and reduced N allocation to Rubisco under P-limited conditions (WARREN; ADAMS, 2002; BAHAR et al., 2016). Differences in leaf traits such as leaf chlorophyll concentration and leaf mass per area also are related to photosynthetic capacity (SONG et al., 2021).

Conifers and angiosperms differ in a variety of vegetative traits, for example, stomatal densities and gas exchange (LUSK et al., 2003). Lusk et al. (2003) revealed that when

angiosperms and conifers were compared to a common leaf nitrogen concentration, a large difference in photosynthetic capacity per unit leaf mass was found, indicating that the angiosperms obtained a higher rate of photosynthetic return per unit of biomass or mole of nitrogen invested in leaf tissue. The differences in photosynthetic performance of evergreen angiosperms and conifers were partly attributable to variation in stomatal conductance. Conifer xylem typically has a lower specific conductivity than angiosperm xylem, as a result of greater hydraulic resistance in narrow-diameter tracheids than in vessels (WANG et al., 1992; CASTRO-DIEZ et al., 1998; LUSK et al. 2003). Evergreen conifers and angiosperms therefore do appear to show co-ordinated differences in photosynthetic, stomatal and vascular traits (LUSK et al., 2003). According to the authors although photosynthetic differences can be partly explained by differences in leaf thickness, they may also be linked to greater hydraulic capacity of vessels, enabling angiosperms to develop higher stomatal conductance and sustain higher transpiration rates

4.2 Climatic influence on physiological variables

The parameter V_{cmax} was positively associated $Prec_{10}$, and J_{max} was associated positively with all climatic variables ($Prec_{10}$, $Prec_{30}$, T_{mean10} and T_{mean30}). Despite both parameters was influenced by $Prec_{10}$, the J_{max} was more sensitive to climate variables. These results indicated an increase in photosynthetic capacity by J_{max} with an increase in growth temperature and an increase in the precipitation rate before gas exchange measurements ($Prec_{10}$). Environmental variables including temperature, water availability, and light influence the photosynthesis process (SMITH; DUKE, 2018). Therefore, it is essential to understand how biotic and abiotic factors can be incorporated into global modeling studies. Previous studies show that temperature and water availability influence plant physiological performance at multiple spatial and temporal scales (STEFANSKI et al., 2019; SMITH; DUKE, 2018; KUMARATHUNGE et al., 2018; WANG et al., 2017).

The higher rates of V_{cmax} and J_{max} in response to $Prec_{10}$ suggest that photosynthesis capacity were affected by changes in short-term climatic variables. It is known that photosynthetic rates are not only determined by biochemical processes, but also by the stomatal conductance to CO_2 (MEDLYN et al., 2002). The higher rates of V_{cmax} and J_{max} in response to increased precipitation is likely explained by water availability that resulted in lower water stress and consequently greater stomatal opening, even at high temperatures. Some studies indicating that drought decreases both V_{cmax} and J_{max} (GE et al., 2012; SMITH; DUKES,

2018) and others showing that plants in both wet and dry conditions showed that J_{max} and V_{cmax} decrease with subsequent soil drying (MARTIN-ST.PAUL et al., 2012)

Reich et al. (2018), studied effects of climate warming on photosynthesis in boreal tree species revealed that in moist soils, the angiosperm species showed higher maximum carboxylation capacity at 25 °C ($V_{cmax-25}$) when grown at increased temperature compared to ambient temperatures. This higher maximum carboxylation capacity in well-watered, warmed angiosperms assessed at a standardized temperature is indicative of an acclimation response (upregulation of $V_{cmax-25}$) to growth in elevated temperatures. In moist soils, the species had strong increases in A_{net} and g_s in warmed conditions likely because of both higher carboxylation capacity (greater $V_{cmax-25}$) and higher carbon demand for photosynthate and warmed plants had a photosynthetic advantage because of less biochemical limitation (that is, higher V_{cmax}). Overall, warming stimulates photosynthesis in moist soils, but not otherwise. The likely mechanisms suggest that warmed plants did not have greater stomatal sensitivity to soil water deficits as such.

With changes in growth temperature many plants show considerable phenotypic plasticity in their photosynthetic characteristics (HIKOSAKA et al., 2005). What must be understood is that the interaction between water availability must be considered when assessing the photosynthetic capacity response to acclimation (SMITH; Duke, 2018). In our study, we did not evaluate photosynthesis under drought conditions, we investigated the influence of short-term climatic variables, growth temperature and precipitation as a metric of water availability on the photosynthetic capacity of the eucalypt and pine functional groups. Evidence that changes in the temperature response of photosynthesis are mainly driven by the acclimation of photosynthetic biochemistry to growth temperature was provided in the studies by KUMARATHUNGE et al. (2019). However, these authors, found no detectable correlation between T° growth and rate of V_{cmax} , but the rate of J_{max} showed a strong decrease.

Smith and Duke (2018) revealed that warmer temperatures could decrease photosynthetic capacity, especially during times of low water availability. Our analyzes contrarian this result, revealing higher values of J_{max} at higher temperatures and under higher precipitation rates. Our hypothesis is that the increase of J_{max} was influenced by the natural association of the growth temperature and water availability variables, since the parameters responded positively to the increase in precipitation ($Prec_{10}$, $Prec_{30}$) (Fig. 4a; 4b)

Higher temperatures increase transpirational demand for water, which can only be met if water is available (SMITH; DUKE, 2018; HATFIELD; PRUEGER 2015). Dry conditions

lead to greater downregulation under high temperatures resulting in decrease photosynthetic capacity (SMITH; DUKE, 2018). Our results revealed that there was no down-regulation of photosynthetic capacity under warmer temperatures, because precipitation before gas exchange measurements (10 and 30 days) influenced soil moisture and water availability for plants. Thus, the higher growth temperatures together with the high precipitation showed an up-regulation, reflecting in greater photosynthetic capacity.

The J_{\max}/V_{\max} ratio was negatively influenced by $Prec_{10}$ and positively influenced by $T_{\text{mean}30}$ (Figure 5; Table 5). The increase in the J_{\max}/V_{\max} ratio in response to growth temperature ($T_{\text{mean}30}$) was driven by the increase in J_{\max} at higher growth temperatures. A higher J_{\max}/V_{\max} ratio suggests a greater allocation of resources for electron transport in relation to carboxylation (SMITH; DUKE, 2018).

The reduction of J_{\max}/V_{\max} at higher precipitation values is correlated with the increase in photosynthetic capacity by V_{\max} in response to water availability. The precipitation positively influenced both V_{\max} and J_{\max} (Fig. 3 - a; Fig. 4 - a and b). However, the reduction of J_{\max}/V_{\max} in response to precipitation may have been more impacted by the V_{\max} parameter (see coefficients in Table 5).

Water availability influences stomatal processes, favoring the transport of CO_2 , which may have resulted in higher in Rubisco carboxylation (V_{\max}) in relation to electron transport (J_{\max}). Probably, V_{\max} did not experience a non-biochemical limitation, for example, stomatal closure, in conditions with greater precipitation. Rubisco carboxylation (V_{\max}) is limited by the supply of CO_2 , for which the stomata are primarily responsible (STENFANSKI et al., 2019). The J_{\max} is mainly limited by the rate of electron transport regulated by the light intensity (STENFANSKI et al., 2019; SHARKEY et al., 2007).

There is a discrepancy between our results and studies that found a decrease in the J_{\max}/V_{\max} ratio at higher growth temperatures (KATTGE; KNORR, 2009, MEDLYN et al., 2002). Photosynthetic acclimation to temperature appears to be species-specific and plant functional type (PFTs) (SCAFARO et al., 2017). Although photosynthesis is highly sensitive to temperature changes, which is driven by the temperature sensitivity of V_{\max} and J_{\max} and the large body of research on this subject, the effect of increasing temperature in both the short and long term on the biochemical limitations of photosynthesis is not yet fully clear or generalizable (KATTGE; KNORR, 2007; STENFANSKI et al., 2019).

4.3 Age influence

We found evidence that age positively influences the photosynthetic parameters of pine and eucalypt group. Older forests showed an increasing trend in J_{max} ((Fig. 3–b; Table 5). These differences can be attributed to nutrient content in leaves and differences in light availability within the stand. In addition to nitrogen being strongly correlated with photosynthetic capacity as previously mentioned (STINZIANO et al., 2017), other nutrients such as potassium also demonstrated a positive effect on the photosynthetic parameters of planted forests (CHRISTINA et al., 2015; BATTIE-LACLAU et al., 2013).

Increased photosynthetic capacity is also related to canopy and stand scale variables (BINKLEY et al., 2010). The plant's architecture changes throughout the development cycle with variation in the canopy and consequently in gas exchange. Modifications in leaf size, leaf area per tree, leaf area index, spatial distribution of leaf area in the canopy, leaf inclination angles, optical properties and crown dimensions result in different light and carbon absorption capacities (LE MAIRE et al., 2019; TARVAINEN et al., 2016). These differences result in variations in APAR and LUE, and influence the photosynthetic capacity of plants. Canopy-scale variables like leaf area index in conjunction with the V_{cmax} parameter have already been incorporated into vegetation models, aiming to more accurately estimate carbon and water fluxes (WANG *et al.*, 2019).

Studies in eucalypt stands showed that LUE increased with age (Le Maire et al., 2019). Older Forests probably acquired strategies that resulted in a higher LUE, so they tended to increase in J_{max} . Our results corroborate the study by Smith and Duke (2018), when evaluating the drivers of photosynthesis, also reported that adult trees tend to have greater photosynthetic capacity than juvenile trees, possibly as a result of differences in light availability. Plants or leaves grown in high light environments have greater photosynthetic capacity than those grown in low light environments (BOARDMAN, 1977; NIINEMETS et al., 2014; SMITH; DUKES, 2018).

On the other hand, our results diverge from those found by Delzon et al. (2005). When evaluating the photosynthetic capacity in conifer stands at different ages (10, 32, 54 and 91 years), they reported that the parameters V_{cmax} and J_{max} did not show any change with increasing age, however, the authors observed that the 32 years stand old had higher V_{cmax} , suggesting that photosynthetic capacity may be higher at younger stages due to initial fertilization. Although our results suggest that age is a variable that influences the tree's photosynthetic capacity in the forest stand, further studies should be conducted to investigate

whether the variable should be considered in terrestrial system models. Although our results suggest that age is a variable that influences photosynthetic capacity, more studies should be conducted to investigate whether the variable should be considered in Earth system models.

Our dataset has data from eucalypt experiments with age ranges ranging from 12 months to 84 months, whereas the dataset for the pine group has only two ages 36 and 60 months (Table 1). Although both groups responded in a similar way (positive age influence) more studies should be conducted in the pine group with different ages. In order to have more conclusive results with the conifer group, it is ideal that the data have a greater range of ages. Assessing the photosynthetic capacity along a growth rotation in planted forests deserves attention to understand the mechanisms that drive the variability in photosynthetic parameters.

4.4 Climatic group and species influence on parameters

We found no significant differences between subtropical and tropical climate types for genotypes of the eucalypt group (Table 6). Based on evidence that suggests many species are adapted to their thermal environment of origin, (BERRY; BJORKMAN, 1980), our hypothesis was that species of cool-origin of genus eucalypt have greater photosynthetic than species of warm-origin. However, our hypothesis was not confirmed for eucalyptus genotypes of tropical origin planted under environmental conditions in Brazil.

Although the species are adapted to the climate of origin, these species too exhibit the capacity to adjust the temporal variations in the temperature of their environment (KUMARATHUNGE et al., 2019; VALLADARES et al., 2014). Therefore, it is essential to study the acclimatization and adaptation processes and their contribution to vegetation modeling studies. In contrast to our studies, which revealed that genotypes of subtropical origin had photosynthetic capacity similar to tropical genotypes, Lin et al. (2013) found significantly higher V_{cmax} and J_{max} rates in species originating from warm climates than in species from cold weather.

The non-significant difference in photosynthetic capacity between tropical and subtropical groups of the eucalypt may be related to short-term acclimatization processes, as well as long-term processes, such as genetic adaptation of species (KUMARATHUNGE et al., 2019; YAMORI et al., 2014;). Could be a thermal adaptation of the tropical group to the environmental conditions of Brazil, resulting in a photosynthetic capacity similar to the subtropical group. Since adaptation is a process that takes many generations to occur

(Kumarathunge et al., 2019). Given the complexity of the photosynthesis temperature response and little information on a global scale (MERCADO et al., 2018; STINZIANO et al., 2017b) we suggest a better investigation of the acclimation and adaptation process of genotypes of eucalyptus in Brazil.

We testes differ among species of pine and found significant differences in the photosynthetic capacity of species from the pine group (*P. taeda* and *P. caribaea*) (Table 6). The parameters V_{cmax} , J_{max} and the J_{max}/V_{cmax} ratio were higher for *P. taeda* (Table 6). The rates of V_{cmax} ($43.8 \mu\text{mol m}^{-2} \text{s}^{-1}$) and J_{max} ($101.5 \mu\text{mol m}^{-2} \text{s}^{-1}$) for *P. taeda* in Brazilian stands were higher than the values found by Aspinwall et al. (2011) in forests in North Carolina (V_{cmax} : $19.1 \mu\text{mol m}^{-2} \text{s}^{-1}$ and J_{max} : $23.0 \mu\text{mol m}^{-2} \text{s}^{-1}$). The V_{cmax} and J_{max} values of *P. taeda* (V_{cmax} : $43.8 \mu\text{mol m}^{-2} \text{s}^{-1}$; J_{max} $101.5 \mu\text{mol m}^{-2} \text{s}^{-1}$) and *P. caribaea* (V_{cmax} : $34.9 \mu\text{mol m}^{-2} \text{s}^{-1}$; J_{max} : $73.1 \mu\text{mol m}^{-2} \text{s}^{-1}$) found in this study, also differed from the values of other species of the genus *Pinus*, for example *Pinus densiflora* (V_{cmax} : $61.6 \mu\text{mol m}^{-2} \text{s}^{-1}$; J_{max} : $91.0 \mu\text{mol m}^{-2} \text{s}^{-1}$), *Pinus sylvestris* (V_{cmax} : $87 \mu\text{mol m}^{-2} \text{s}^{-1}$; J_{max} : $146 \mu\text{mol m}^{-2} \text{s}^{-1}$); *Pinus radiata* (V_{cmax} : $34.4 \mu\text{mol m}^{-2} \text{s}^{-1}$; J_{max} : $75.4 \mu\text{mol m}^{-2} \text{s}^{-1}$) (HAN, 2011; TAVAINEN et al., 2016; BOWN et al., 2009). As mentioned above, the species have different photosynthetic characteristics, so it is essential for studies to make available data on forest species, to expand databases of parameters used in terrestrial system models.

Studies suggest that anatomical changes such as needle length and number of needles per fascicle are correlated with the physiological capacity of the leaves of species of the genus *Pinus* (INGWERS et al., 2016; WANG et al., 2019b). *Pinus taeda* usually has 3 needles per fascicle, however fascicles with two, four and five needles are also found (INGWERS et al., 2016). Investigating the photosynthetic capacity of needles in *P. taeda*, Ingwers et al. (2016) reported that V_{cmax} was significantly higher in needles of fascicles that had four needles than needles that belonged to fascicles with three leaves. These differences in V_{cmax} can be explained by the higher concentration of nitrogen in the leaf, although these relationships still remain uncertain (HAN, 2011; INGWERS et al., 2016). Assessing the influence of morphological characteristics of species of the *Pinus* genus on photosynthetic capacity should be better represented in modeling studies.

5. Conclusion

Our results suggest that the photosynthetic capacity of planted forests in Brazil has differences between functional groups. The parameters V_{cmax} , J_{max} , and the J_{max}/V_{cmax} ratio were higher in eucalypt than pine. The differences in photosynthetic capacity between groups can be related to differences in vegetative traits, for example, stomatal densities and gas exchange and leaf traits such as leaf chlorophyll concentration and leaf mass per area. The short-term climate through the variables growth temperature and precipitation at 10 and 30 days before data collection influenced the photosynthetic parameters, suggesting acclimation of leaf photosynthesis. Although the age of the population influences the photosynthetic capacity along the rotation, we suggest that more studies be carried out, mainly for the conifer group. We found evidence that the climatic groups of eucalypt do not show differences in photosynthetic capacity, demonstrating an adaptation of genotypes from the tropical group to environmental conditions in Brazil. *Pinus taeda* showed superiority in relation to *Pinus caribaea*. The values of parameters V_{cmax} , J_{max} and J_{max}/V_{cmax} found in this work expand the database of photosynthetic parameters and can be widely used in modeling studies of planted forests in Brazil.

6. Acknowledgements

To Federal University of Lavras (UFLA) and Coordination for the Improvement of Higher Education Personnel (CAPES) for all the support.

7. References

AINSWORTH, E. A.; LONG, S. P. What have we learned from 15 years of free-air CO₂ enrichment (FACE)? A meta-analytic review of the responses of photosynthesis, canopy properties and plant production to rising CO₂. **New Phytologist**, v. 165, n. 2, p. 351-372, 2004. <http://dx.doi.org/10.1111/j.1469-8137.2004.01224.x>.

ALBERT, L. P. et al. Age-dependent leaf physiology and consequences for crown-scale carbon uptake during the dry season in an Amazon evergreen forest. **New Phytologist**, v. 219, n. 3, p. 870-884, 2018. <http://dx.doi.org/10.1111/nph.15056>.

ALVARES, C. A. et al. 2013. Köppen's climate classification map for Brazil. **Meteorol. Z.** 22, 711–728.

ASPINWALL, M. J. et al. Convergent acclimation of leaf photosynthesis and respiration to prevailing ambient temperatures under current and warmer climates in *Eucalyptus tereticornis*. **New Phytologist**, v. 212, n. 2, p. 354-367, 2016. <https://doi.org/10.1111/nph.14035>

- ASPINWALL, M. J. et al. Adaptation and acclimation both influence photosynthetic and respiratory temperature responses in *Corymbia calophylla*. **Tree Physiology**, v. 37, n. 8, p. 1095-1112, 2017. <https://doi.org/10.1093/treephys/tpx047>
- ASPINWALL, M. J. et al. Leaf-level gas-exchange uniformity and photosynthetic capacity among loblolly pine (*Pinus taeda* L.) genotypes of contrasting inherent genetic variation. **Tree Physiology**, v. 31, n. 1, p. 78-91, 2011. <http://dx.doi.org/10.1093/treephys/tpq107>
- BAHAR, N. H. A. et al. Leaf-level photosynthetic capacity in lowland Amazonian and high-elevation Andean tropical moist forests of Peru. **New Phytologist**, v. 214, n. 3, p. 1002-1018, 2016. <http://dx.doi.org/10.1111/nph.14079>.
- BARTÓN, K., 2020. MuMIn: Multi-Model Inference. R package version 1.42.1. Retrieved from <https://cran.r-project.org/package=MuMIn>.
- BATTAGLIA, M. et al. Prediction of leaf area index in eucalypt plantations: effects of water stress and temperature. **Tree Physiology**, v. 18, n. 8-9, p. 521-528, 1998. <http://dx.doi.org/10.1093/treephys/18.8-9.521>.
- BATTIE-LACLAU, P. et al. Photosynthetic and anatomical responses of *Eucalyptus grandis* leaves to potassium and sodium supply in a field experiment. **Plant, Cell & Environment**, v. 37, n. 1, p. 70-81, 2013. <http://dx.doi.org/10.1111/pce.12131>.
- BATTIE-LACLAU, P. et al. Influence of potassium and sodium nutrition on leaf area components in *Eucalyptus grandis* trees. **Plant And Soil**, v. 371, n. 1-2, p. 19-35, 2013. <http://dx.doi.org/10.1007/s11104-013-1663-7>.
- BATTIE-LACLAU, P. et al. Effects of potassium and sodium supply on drought-adaptive mechanisms in *Eucalyptus grandis* plantations. **New Phytologist**, v. 203, n. 2, p. 401-413, 2014. <http://dx.doi.org/10.1111/nph.12810>.
- BEER, C. et al. Terrestrial gross carbon dioxide uptake: global distribution and covariation with climate. **Science**, v. 329, n. 5993, p. 834-838, 2010. <https://doi.org/10.1126/science.1184984>
- BERRY, J.; BJORKMAN, O. Photosynthetic Response and Adaptation to Temperature in Higher Plants. **Annual Review Of Plant Physiology**, v. 31, n. 1, p. 491-543, 1980. Annual Reviews. <http://dx.doi.org/10.1146/annurev.pp.31.060180.002423>.
- BINKLEY, D et al. The interactions of climate, spacing and genetics on clonal *Eucalyptus* plantations across Brazil and Uruguay. **Forest Ecology And Management**. v. 405, n. 1, p. 271–283, 2017. <https://doi.org/10.1016/j.foreco.2017.09.050>
- BINKLEY, D. et al. Explaining growth of individual trees: light interception and efficiency of light use by eucalyptus at four sites in Brazil. **Forest Ecology And Management**, v. 259, n. 9, p. 1704-1713, 2010. <http://dx.doi.org/10.1016/j.foreco.2009.05.037>.
- BJORNSTAD, O. N. 2018. ncf: Spatial Covariance Functions. R package version 1.2-6. Retrieved from <https://cran.r-project.org/package=ncf>.
- BOARDMAN, N. K. Comparative photosynthesis of sun and shade plants. Annual Review of **Plant Physiology**, v. 28, p. 355-377, 1977. <https://doi.org/10.1146/annurev.pp.28.060177.002035>

- BOWN, H. E. et al. The influence of nitrogen and phosphorus supply and genotype on mesophyll conductance limitations to photosynthesis in *Pinus radiata*. **Tree Physiology**, v. 29, n. 9, p. 1143-1151, 2009. <http://dx.doi.org/10.1093/treephys/tpp051>
- BURNHAM, K.P.; ANDERSON, D.R.; HUYVAERT, K. P. AIC model selection and multimodel inference in behavioral ecology: some background, observations, and comparisons. **Behavioral Ecology and Sociobiology**, v.65, n.1, p. 23-35, 2011. <https://doi.org/10.1007/s00265-010-1029-6>
- CAMPOE, O. C. et al. Stem production, light absorption and light use efficiency between dominant and non-dominant trees of *Eucalyptus grandis* across a productivity gradient in Brazil. **Forest Ecology Management**, v. 288, n. 15, 14–20. 2013. <https://doi.org/10.1016/j.foreco.2012.07.035>.
- CASTRO-DÍEZ, P. et al. Stem anatomy and relative growth rate in seedlings of a wide range of woody plant species and types. **Oecologia**, v. 116, n. 1, p. 57-66, 1998. <https://doi.org/10.1007/s004420050563>
- CARNEIRO, R. L. **Caracterização da capacidade fotossintética e da condutância estomática em árvores de *Pinus caribaea* var. *hondurensis* e de *Pinus taeda* em Itatinga, São Paulo**. 2013. 84 p. Dissertação de mestrado em Recursos Florestais - Escola Superior de Agricultura “Luiz de Queiroz”, Universidade de São Paulo, Piracicaba, 2012.
- CHRISTINA, M. et al. Sensitivity and uncertainty analysis of the carbon and water fluxes at the tree scale in Eucalyptus plantations using a metamodeling approach. **Canadian Journal Forest Research**. 46, p. 297–309. 2015. <https://doi.org/10.1139/cjfr-2015-0173>
- CHRISTINA, M. et al. Measured and modeled interactive effects of potassium deficiency and water deficit on gross primary productivity and light-use efficiency in Eucalyptus grandis plantations. **Global Change Biology**, v. 21, n. 5, p. 2022-2039, 2015. <http://dx.doi.org/10.1111/gcb.12817>.
- COURSOLLE, C. et al. Nathalie. Measuring Rapid A–Ci Curves in Boreal Conifers: black spruce and balsam fir. **Frontiers In Plant Science**, v. 10, p. 1-9, 2019. **Frontiers Media SA**. <http://dx.doi.org/10.3389/fpls.2019.01276>.
- DRAKE, J. E. et al. Hydraulic limitation not declining nitrogen availability causes the age-related photosynthetic decline in loblolly pine (*Pinus taeda* L.). **Plant, cell & environment**, v. 33, n. 10, p. 1756-1766, 2010. <https://doi.org/10.1111/j.1365-3040.2010.02180.x>
- DELZON, S. et al. Variation of the photosynthetic capacity across a chronosequence of maritime pine correlates with needle phosphorus concentration. **Annals Of Forest Science**, v. 62, n. 6, p. 537-543, 2005. <http://dx.doi.org/10.1051/forest:2005046>.
- DE KAUWE, M. G. et al. Test of the ‘one-point method’ for estimating maximum carboxylation capacity from field-measured, light-saturated photosynthesis. **New Phytologist**, v. 210, n. 3, p. 1130-1144, 2015a. <http://dx.doi.org/10.1111/nph.13815>.
- DE KAUWE, M.G et al. A test of an optimal stomatal conductance scheme within the CABLE land surface model. **Geoscientific Model Development**, v. 8, p. 431-452, 2015b.
- DUURSMA, R. A. Plantecophys - An R Package for Analysing and Modelling Leaf Gas Exchange Data. **Plos One**, v.10, n.11, 2015.

- DUURSMA, R. A.; MEDLYN, B. E. MAESPA: A model to study interactions between water limitation, environmental drivers and vegetation function at tree and stand levels, with an example application to [CO₂] × drought interactions. **Geoscientific Model Development Discussions**, v. 5, n.4, p. 919–940, 2012. <https://doi.org/10.5194/gmd-5-919-2012>
- ELLSWORTH, D. S. et al. Phosphorus recycling in photorespiration maintains high photosynthetic capacity in woody species. **Plant, Cell & Environment**, v. 38, n. 6, p. 1142–1156, 2015. <http://dx.doi.org/10.1111/pce.12468>.
- FARQUHAR, G. D.; CAEMMERER, S. V.; BERRY, J. A. A biochemical model of photosynthetic CO₂ assimilation in leaves of C3 species. **Plant**, n. 149, p.78–90, 1980.
- FERREIRA, V. et al. A global assessment of the effects of eucalyptus plantations on stream ecosystem functioning. **Ecosystems**, v. 22, n. 3, p. 629–642, 2019.
- FRIEDLINGSTEIN, P. et al. Uncertainties in CMIP5 Climate Projections due to Carbon Cycle Feedbacks. *Journal Of Climate*, v. 27, n. 2, p. 511–526, 2014. **American Meteorological Society**. <http://dx.doi.org/10.1175/jcli-d-12-00579.1>.
- GE, Z. M. et al. Acclimation of photosynthesis in a boreal grass (*Phalaris arundinacea* L.) under different temperature, CO₂, and soil water regimes. *Photosynthetica*, v. 50, n. 1, 141–151, 2012. <https://doi.org/10.1007/s11099-012-0014-x>
- HAN, Q. Height-related decreases in mesophyll conductance, leaf photosynthesis and compensating adjustments associated with leaf nitrogen concentrations in *Pinus densiflora*. **Tree Physiology**, v. 31, n. 9, p. 976–984, 2011. <http://dx.doi.org/10.1093/treephys/tpr016>.
- HATFIELD, J. L.; PRUEGER, J. H. Temperature extremes: effect on plant growth and development. **Weather And Climate Extremes**, v. 10, p. 4–10, 2015. <http://dx.doi.org/10.1016/j.wace.2015.08.001>.
- HÉROULT, A. et al. Optimal stomatal conductance in relation to photosynthesis in climatically contrasting Eucalyptus species under drought. **Plant, Cell & Environment**, v. 36, n. 2, p. 262–274, 2012. <http://dx.doi.org/10.1111/j.1365-3040.2012.02570.x>.
- HIKOSAKA, K. et al. Temperature acclimation of photosynthesis: mechanisms involved in the changes in temperature dependence of photosynthetic rate. **Journal Of Experimental Botany**, v. 57, n. 2, p. 291–302, 2005. <http://dx.doi.org/10.1093/jxb/erj049>.
- IBÁ - Indústria Brasileira de produtores de Árvores. **Relatório anual IBÁ 2021**, ano base 2020. Instituto Brasileiro de Economia - FGV: 2021. 93p. Disponível em:< <https://iba.org/datafiles/publicacoes/relatorios/relatorioiba2021-compactado.pdf>>. Acesso em: 10 de março, 2021.
- INGWERS, M. W. et al. Physiological attributes of three- and four-needle fascicles of loblolly pine (*Pinus taeda* L.). **Trees**, v. 30, n. 6, p. 1923–1933, 2016. <http://dx.doi.org/10.1007/s00468-016-1421-6>.
- IGLESIAS-TRABADO G.; WILSTERMANN D. 2009. **Eucalyptus Universalis. Global cultivated eucalypt forests map 2009**. GIT Forestry Consulting's Eucalyptologies: Information resources on Eucalyptus cultivation worldwide.
- IPCC. **Climate Change 2014: Synthesis Report. Contribution of Working Groups I, II and III to the Fifth Assessment Report of the Intergovernmental Panel on Climate Change**. Geneva, Switzerland, 2014.

- KATTGE, J.; KNORR, W. Temperature acclimation in a biochemical model of photosynthesis: a reanalysis of data from 36 species. **Plant, Cell & Environment**. v. 30, n. 9, p. 1176-1190. 2007. <http://dx.doi.org/10.1111/j.1365-3040.2007.01690.x>.
- KUMARATHUNGE, D. P. et al. Acclimation and adaptation components of the temperature dependence of plant photosynthesis at the global scale. **New Phytologist**, v. 222, n. 2, p. 768-784, 2019. <http://dx.doi.org/10.1111/nph.15668>.
- LANDSBERG, J. J.; SANDS, P. J. **Physiological ecology of forest production: Principles, processes, and models**. London: Academic Press, 2011. 331p.
- LE MAIRE, G. et al. Light absorption, light use efficiency and productivity of 16 contrasted genotypes of several Eucalyptus species along a 6-year rotation in Brazil. **Forest Ecology And Management**, v. 449, p. 117-143, 2019. <http://dx.doi.org/10.1016/j.foreco.2019.06.040>.
- LENTH, Russell. Package 'lsmeans'. *The American Statistician*, v. 34, n. 4, p. 216-221, 2018.
- LIN, Y.-S. et al. Biochemical photosynthetic responses to temperature: how do interspecific differences compare with seasonal shifts? **Tree Physiology**, v. 33, n. 8, p. 793-806, 2013. <http://dx.doi.org/10.1093/treephys/tpt047>.
- LONG, S.; BERNACCHI, C. Gas exchange measurements, what can they tell us about the underlying limitations to photosynthesis? Procedures and sources of error. **Journal of Experimental Botany** v. 54, p. 2393–2401, 2003.
- LUSK, C. H.; WRIGHT, I.; REICH, P. B. Photosynthetic differences contribute to competitive advantage of evergreen angiosperm trees over evergreen conifers in productive habitats. **New Phytologist**, v. 160, n. 2, p. 329-336, 2003. <https://doi.org/10.1046/j.1469-8137.2003.00879.x>
- MARRICHI, A. H. C. **Caracterização da capacidade fotossintética e da condutância estomática em sete clones comerciais de Eucalyptus e seus padrões de resposta ao déficit de pressão de vapor**. 2009. 104 p. Dissertação de Mestrado em Recursos Florestais – Escola Superior de Agricultura “Luiz de Queiroz”, Universidade de São Paulo, Piracicaba, 2009.
- MARTIN-STPAUL, N. K. et al. Photosynthetic sensitivity to drought varies among populations of *Quercus ilex* along a rainfall gradient. **Functional Plant Biology**, v. 39, n. 1, p. 25–37, 2012. <https://doi.org/10.1071/FP11090>
- MEDLYN, B. E. et al. Effects of elevated [CO₂] on photosynthesis in European forest species: a meta-analysis of model parameters. **Plant, Cell & Environment**, v. 22, n. 12, p.1475-1495, 1999. <https://doi.org/10.1046/j.1365-3040.1999.00523.x>
- MEDLYN, B. E. et al. Temperature response of parameters of a biochemically based model of photosynthesis. II. A review of experimental data. **Plant, Cell & Environment**, v. 25, n. 9, p. 1167-1179, 2002. <http://dx.doi.org/10.1046/j.1365-3040.2002.00891.x>.
- MEDLYN, B. E. et al. Reconciling the optimal and empirical approaches to modelling stomatal conductance. **Global Change Biology**, v. 17, n. 6, p. 2134-2144, 2011. <http://dx.doi.org/10.1111/j.1365-2486.2010.02375.x>.
- MERCADO, L. M. et al. Large sensitivity in land carbon storage due to geographical and temporal variation in the thermal response of photosynthetic capacity. **New Phytologist**, v. 218, n. 4, p. 1462-1477, 2018. <http://dx.doi.org/10.1111/nph.15100>.

- NIINEMETS, U. Differences in chemical composition relative to functional differentiation between petioles and laminas of *Fraxinus excelsior*. **Tree Physiology**, v. 19, n. 1, p. 39-45, 1999. <http://dx.doi.org/10.1093/treephys/19.1.39>.
- NIINEMETS, Ülo. Optimization of foliage photosynthetic capacity in tree canopies: towards identifying missing constraints. **Tree physiology**, v. 32, n. 5, p. 505-509, 2012. <https://doi.org/10.1093/treephys/tps045>
- NIINEMETS, Ü.; KEENAN, T. F.; HALLIK, L. A worldwide analysis of within-canopy variations in leaf structural, chemical and physiological traits across plant functional types. **New Phytologist**, v. 205, n. 3, p. 973-993, 2014. <http://dx.doi.org/10.1111/nph.13096>.
- OLEKSYN J. et al. Growth and physiology of *Picea abies* populations from elevational transects: common garden evidence for altitudinal ecotypes and cold adaptation. **Functional Ecology**, v.12 p. 573–590, 1998.
- PAQUETTE, A.; MESSIER, C. The role of plantations in managing the world's forests in the Anthropocene. **Frontiers in Ecology and the Environment**, v. 8, n. 1, p. 27-34, 2010.
- PRENTICE, I. C et al. (2001) The carbon cycle and atmospheric carbon dioxide. In: Houghton JT, Ding Y, Griggs DJ, Noguer M, van der Linden PJ, Dai X, Maskell K, Johnson CA, eds. **Climate Change 2001: the scientific basis**. Contribution of Working Group I to the third assessment report of the Intergovernmental Panel on Climate Change. Cambridge, UK: Cambridge University Press, 183–237.
- R Core Team, 2020. R: A Language and Environment for Statistical Computing. R Foundation for Statistical Computing, Vienna. ISBN 3-900051-07-0. URL <http://www.R-project.org>.
- REICH, P. B.; WALTERS, M. B.; ELLSWORTH, D. S. Leaf age and season influence the relationships between leaf nitrogen, leaf mass per area and photosynthesis in maple and oak trees. **Plant, Cell And Environment**, v. 14, n. 3, p. 251-259, 1991. <http://dx.doi.org/10.1111/j.1365-3040.1991.tb01499.x>.
- REICH, P. B. et al. Effects of climate warming on photosynthesis in boreal tree species depend on soil moisture. **Nature**, v. 562, n. 7726, p. 263-267, 2018. <https://doi.org/10.1038/s41586-018-0582-4>.
- ROGERS, A. The use and misuse of V_{cmax} in Earth System Models. **Photosynthesis Research**, v. 119, n. 1-2, p. 15-29, 2013. **Springer Science and Business Media LLC**. <http://dx.doi.org/10.1007/s11120-013-9818-1>.
- ROGERS, A. et al. A roadmap for improving the representation of photosynthesis in Earth system models. **New Phytologist**, v. 213, n. 1, p. 22-42, 2016. <http://dx.doi.org/10.1111/nph.14283>.
- SALMON, Y. et al. Leaf carbon and water status control stomatal and nonstomatal limitations of photosynthesis in trees. **New Phytologist**, 26, p. 690-703, 2020. <http://dx.doi.org/10.1111/nph.16436>.
- SCAFARO, A. P. et al. Strong thermal acclimation of photosynthesis in tropical and temperate wet-forest tree species: the importance of altered rubisco content. **Global Change Biology**, v. 23, n. 7, p. 2783-2800, 2017. <http://dx.doi.org/10.1111/gcb.13566>.

- SHARKEY, T. D. Photosynthesis in intact leaves of C3 plants: physics, physiology and rate limitations. **The Botanical Review**, v. 51, n. 1, p. 53-105, 1985. Springer Science and Business Media LLC. <http://dx.doi.org/10.1007/bf02861058>.
- SHARKEY, T. D. et al. Fitting photosynthetic carbon dioxide response curves for C3leaves. **Plant, Cell & Environment**, v. 30, n. 9, p. 1035-1040, 2007. <http://dx.doi.org/10.1111/j.1365-3040.2007.01710.x>
- SILIM S. N.; RYAN, N.; KUBIEN D. S. Temperature responses of photosynthesis and respiration in *Populus balsamifera* L.: acclimation versus adaptation. **Photosynth Res**, v. 104, p.19–30, 2010.
- SMITH, N. G.; DUKES, J. S. Drivers of leaf carbon exchange capacity across biomes at the continental scale. **Ecology**, v. 99, n. 7, p. 1610-1620, 2018. <http://dx.doi.org/10.1002/ecy.2370>.
- SONG, G.; WANG, Q.; JIN, J. Including leaf trait information helps empirical estimation of j_{max} from v_{cmax} in cool-temperate deciduous forests. **Plant Physiology and Biochemistry**, v. 166, p. 839-848, 2021. <https://doi.org/10.1016/j.plaphy.2021.06.055>
- STEFANSKI, A. et al. Surprising lack of sensitivity of biochemical limitation of photosynthesis of nine tree species to open-air experimental warming and reduced rainfall in a southern boreal forest. **Global Change Biology**, v. 26, n. 2, p. 746-759, 2019. <http://dx.doi.org/10.1111/gcb.14805>.
- STINZIANO, J. R.; WAY, D. A.; BAUERLE, W. L. Improving models of photosynthetic thermal acclimation: which parameters are most important and how many should be modified?. **Global Change Biology**, v. 24, n. 4, p. 1580-1598, 2017b. <http://dx.doi.org/10.1111/gcb.13924>.
- STINZIANO, J. R.; WAY, D. A. Autumn photosynthetic decline and growth cessation in seedlings of white spruce are decoupled under warming and photoperiod manipulations. **Plant, Cell & Environment**, v. 40, n. 8, p. 1296-1316, 2017a. Wiley. <http://dx.doi.org/10.1111/pce.12917>.
- TARVAINEN, L. et al. Increased Needle Nitrogen Contents Did Not Improve Shoot Photosynthetic Performance of Mature Nitrogen-Poor Scots Pine Trees. **Frontiers In Plant Science**, v. 7, p. 1-17, 2016. <http://dx.doi.org/10.3389/fpls.2016.01051>.
- VALLADARES, F. et al. The effects of phenotypic plasticity and local adaptation on forecasts of species range shifts under climate change. **Ecology Letters**, v. 17, n. 11, p. 1351-1364, 2014. <http://dx.doi.org/10.1111/ele.12348>.
- VON CAEMMERER, S. (2000) **Biochemical Models of Leaf Photosynthesis**, p. 1–165. CSIRO Publishing, Collingwood, Victoria, Australia.
- WALKER, A. P. et al. The relationship of leaf photosynthetic traits – V_{cmax} and J_{max} - to leaf nitrogen, leaf phosphorus, and specific leaf area: a meta-analysis and modeling study. **Ecology And Evolution**, v. 4, n. 16, p. 3218-3235, 2014. <http://dx.doi.org/10.1002/ece3.1173>.
- WANG, H. et al. Towards a universal model for carbon dioxide uptake by plants. **Nature Plants**, v. 3, n. 9, p. 734-741, 2017. <http://dx.doi.org/10.1038/s41477-017-0006-8>.

WANG, R. et al. Seasonality of leaf area index and photosynthetic capacity for better estimation of carbon and water fluxes in evergreen conifer forests. **Agricultural And Forest Meteorology**, v. 279, p. 1-15, 2019. <http://dx.doi.org/10.1016/j.agrformet.2019.107708>.

WANG, R. et al. Seasonality of leaf area index and photosynthetic capacity for better estimation of carbon and water fluxes in evergreen conifer forests. **Agricultural and Forest Meteorology**, v. 279, p. 107708, 2019b.

WANG, J.; IVES, N. E.; LECHOWICZ, M. J. The relation of foliar phenology to xylem embolism in trees. **Functional Ecology**, p. 469-475, 1992. <https://doi.org/10.2307/2389285>

WAY, D. A.; YAMORI, W. Thermal acclimation of photosynthesis: on the importance of adjusting our definitions and accounting for thermal acclimation of respiration. *Photosynthesis research*, v. 119, n. 1, p. 89-100, 2014. <https://doi.org/10.1007/s11120-013-9873-7>

WARREN, C. R.; ADAMS, M. A. Phosphorus affects growth and partitioning of nitrogen to Rubisco in *Pinus pinaster*. **Tree Physiology**, v. 22, n. 1, p. 11-19, 2002. <https://doi.org/10.1093/treephys/22.1.11>.

WU, J. et al. The phenology of leaf quality and its within-canopy variation is essential for accurate modeling of photosynthesis in tropical evergreen forests. **Global Change Biology**, v. 23, n. 11, p. 4814-4827, 2017. <http://dx.doi.org/10.1111/gcb.13725>.

YAMORI, W.; HIKOSAKA, K.; WAY, D. A. Temperature response of photosynthesis in C3, C4, and CAM plants: temperature acclimation and temperature adaptation. **Photosynthesis research**, v. 119, p. 101–117, 2014. <https://doi.org/10.1007/s11120-013-9874-6>

8. Supplementary material

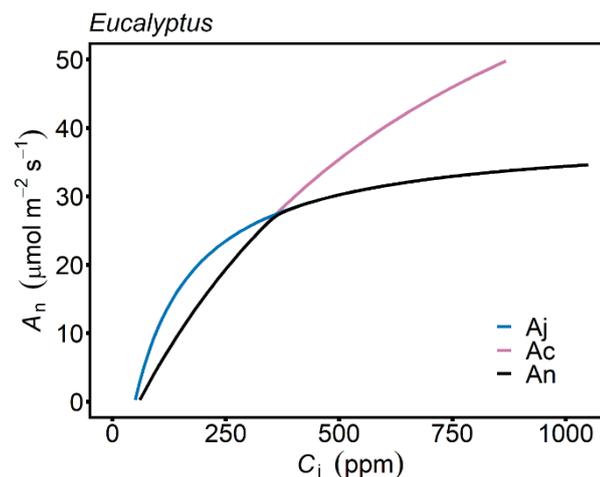


Figure 6: CO₂ response curve as modelled with the FvCB model to *Eucalyptus* genus. No significant differences were found between climatic groups (tropical and subtropical) **An**: Net rate of CO₂ assimilation; **Ac**: The assimilation rate limited by Rubisco activity, **Aj**: The

assimilation rate limited by electron transport (regeneration of ribulose-1,5-bisphosphate, RuBP).

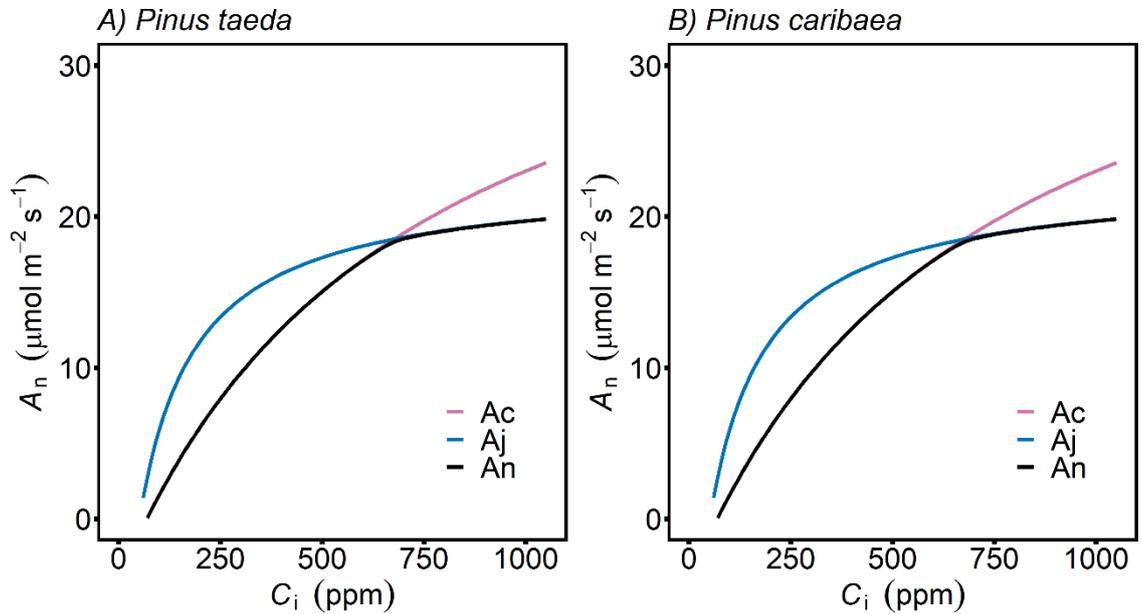


Figure 7: CO₂ response curve as modelled with the FvCB model to *Pinus* species. a) *Pinus taeda*; b) *Pinus caribaea*. **An:** Net rate of CO₂ assimilation; **Ac:** The assimilation rate limited by Rubisco activity, **Aj:** The assimilation rate limited by electron transport (Regeneration of ribulose-1, 5-bisphosphate, RuBP).

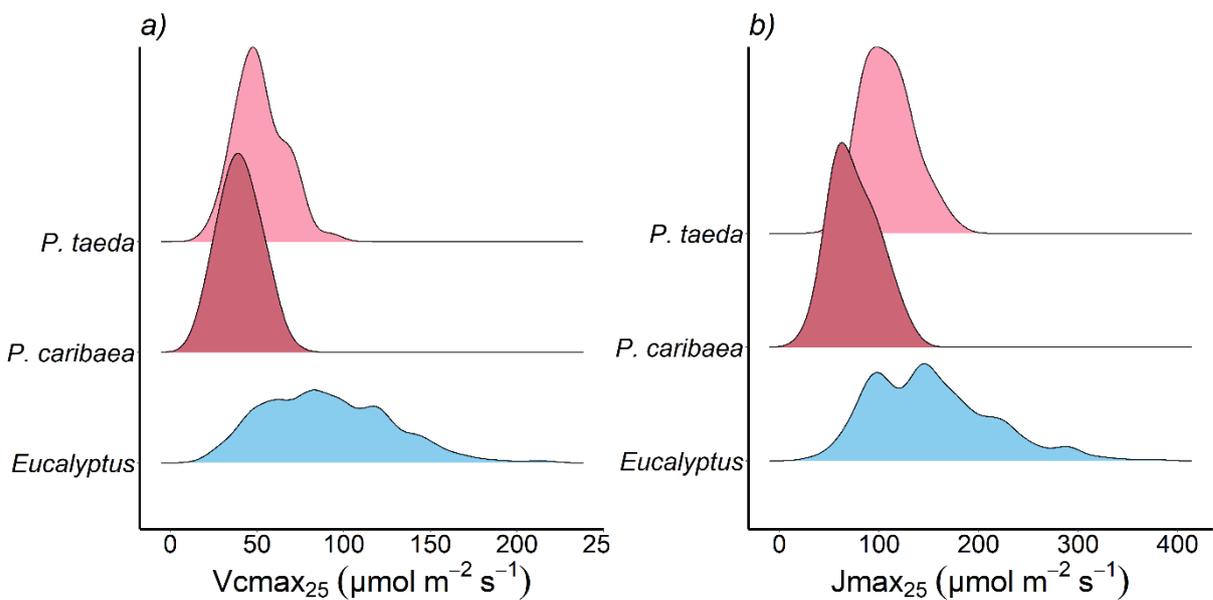


Figura 8. a) Distribution of the V_{cmax} for *Pinus taeda*, *Pinus caribaea* and *Eucalyptus*. b) Distribution of the J_{max} for *Pinus taeda*, *Pinus caribaea* and *Eucalyptus*. V_{cmax} e J_{max} standardized at 25 °C.

Tabela 7. Details of the number of curves in each data set, fitted curves and curves eliminated by verification criteria

ID	Genotype	Initial curves	Adjusted curves	Eliminated curves	(%)
1	<i>E.grandis</i>	37	30	7	19
2	<i>E.grandis</i>	7	7	0	0
3	<i>E.spp</i>	49	15	34	69
4	<i>E. grandis x E. urophylla</i>	8	7	1	12
5	<i>E.grandis</i>	9	8	1	11
6	<i>E.grandis</i>	36	35	1	3
7	<i>E.grandis</i>	72	66	6	8
8	<i>E.grandis</i>	72	65	7	10
9	<i>E.grandis</i>	28	21	7	25
10	<i>E. spp</i>	24	24	0	0
11	<i>Eucalyptus</i>	57	50	7	12.
12	<i>P.taeda</i>	48	47	1	2
13	<i>P.caribaea</i>	56	56	0	0
14	<i>P.taeda</i>	7	4	3	43
15	<i>P.caribaea</i>	25	12	13	52
Total		535	447	88	16

ID: identification of each experiment

V_{cmax} : maximum carboxylation rate of the Rubisco enzyme

J_{max} : maximum electron transport rate

SE: error estimate of V_{cmax} and J_{max} parameters

Range: range of parameters for the dataset

J_{max}/V_{cmax} : J_{max} and V_{cmax} ratio

Table 8. Estimates of the parameters V_{cmax} , J_{max} standardized at 25 °C the error estimate (SE), data range and the J_{max}/V_{cmax} ratio for each dataset that make up the database.

ID	N° of curves	Genotype	V_{cmax}	$SE_{(V_{cmax})}$	Range(V_{cmax})	J_{max}	$SE_{(J_{max})}$	Range (J_{max})	J_{max}/V_{cmax}
1	7	<i>E.grandis</i>	97.12	3.25	49.64 - 140.61	170.53	3.83	90.27 - 230.31	1.79
2	30	<i>E.grandis</i>	105.99	5.46	47.94 - 153.24	168.32	8.68	84.15 - 217.64	1.63
3	15	<i>E.spp</i>	132.50	34.84	91.97 - 172.55	183.72	16.50	139.58 - 237.01	1.42
4	7	<i>E. grandis x E. urophylla</i>	113.39	17.15	70.72 - 141.62	277.11	32.60	124.59 - 377.44	2.43
5	8	<i>E.grandis</i>	64.53	5.80	48.73 - 86.62	129.52	6.35	104.72 - 152.56	2.03
6	35	<i>E.grandis</i>	93.30	6.32	36.71 - 158.87	153.70	4.21	54.79 - 347.29	1.65
7	66	<i>E.grandis</i>	75.75	7.83	25.64 - 130.00	134.18	4.23	35.91 - 254.53	1.80
8	65	<i>E.grandis</i>	110.09	19.96	34.41 - 217.64	157.70	3.11	68.00 - 284.09	1.47
9	21	<i>E.grandis</i>	60.38	17.39	26.63 - 83.51	95.59	10.09	52.78 - 150.51	1.64
10	24	<i>E. spp</i>	61.50	3.71	26.97 - 97.14	122.29	4.03	65.22 - 173.32	2.07
11	50	<i>Eucalyptus</i>	90.18	3.91	18.76 - 209.51	180.30	5.67	30.35 - 316.91	2.04
12	47	<i>P.taeda</i>	52.39	2.34	24.89 - 92.36	108.24	2.88	61.10 - 174.33	2.12
13	56	<i>P.caribaea</i>	42.00	4.04	20.14 - 69.58	80.69	3.52	34.62 - 132.31	1.96
14	4	<i>P.taeda</i>	44.16	1.04	38.93 - 46.82	118.17	3.14	109.96 - 130.91	2.69
15	12	<i>P.caribaea</i>	30.85	3.54	15.10 - 54.98	51.50	3.28	26.68 - 71.36	1.74

**ARTIGO 2 - COMPARING OF STOMATAL CONDUCTANCE MODELS IN
BRAZILIAN FOREST PLANTATIONS**

Comparing of stomatal conductance models in Brazilian forest plantations

Abstract: Several leaf-level models have been developed to model stomatal conductance (g_s) in response to environmental factors such as CO₂, light, temperature, vapor pressure deficit. We studied the applicability of three common stomatal conductance models including Ball-Woodrow-Berry (BB), Ball-Berry-Leuning (BBL) and unified stomatal optimization (USO) models to identify the best model using data obtained from planted forests in Brazil, in addition to analyzing how stomatal conductance and water use efficiency vary between functional groups (angiosperm and gymnosperm) and between eucalyptus genotypes. The BBL and USO models performed better comparing to BB model. Both the USO model and the BBL model showed good fits (R^2 ranging from 0.41 to 0.95) with the evaluated metrics. From 22 genotypes tested, three did not fit the BBL model. The USO model had good metrics and fit all datasets. The species of the pine group had the highest slope parameter of g_s model (g_1) and, consequently, the lowest efficiency in water use when compared to eucalyptus group. Eucalyptus genotypes showed differences in stomatal responses, indicating that in addition to the genotype characteristics, local climatic conditions may also have influenced the variation in g_1 .

1. Introduction

Stomata regulate the exchange of carbon and water between plants and the atmosphere (COWAN; FARQUHAR, 1977; WU et al., 2019; MEDLYN et al., 2011; BUCKLEY, 2019), and play a critical role in leaf physiology, balancing the need for photosynthetic CO₂ uptake against the need to control water loss from leaves (HÉROULT et al., 2013; KATUL, LEUNING; OREN 2003). Additionally, at large scales, control of stomatal aperture regulates regional and global biogeochemical cycles of carbon, water, and energy, and influences the climate through vegetation-mediated climate feedbacks (LIN et al., 2015; WU et al., 2019). Stomatal conductance has been a topic of plant ecophysiological research because it affects water use efficiency (WUE), plant growth, vegetation distribution and ecosystem function and ultimately plant productivity (MEDLYN et al., 2011; WANG et al., 2018).

Understanding the WUE is helpful to forecasting the responses of terrestrial vegetation to global climate change and to the adoption of adaptive strategies (LI et al., 2019). Models that simulate stomatal conductance have become the most effective and appropriate tools for

studying this important physiological process activity (MEDLYN *et al.*, 2011). Several leaf-level models have been developed to model stomatal conductance (g_s) in response to environmental factors such as CO₂, light, temperature (Jarvis, 1976), relative humidity (BALL *et al.*, 1987), VPD (LEUNING, 1995), and soil hydraulic potential (TUZET *et al.*, 2003). A review conducted by Damour *et al.* (2010) highlighted more than 30 stomatal conductance models developed. The g_s models are basically divided into three approaches: empirical (data-based); mechanistic (process-based); and economic optimization (optimization-based) (DAMOUR *et al.*, 2010; BUCKLEY; MOTT, 2013; LU *et al.*, 2018).

Three previously models of g_s are widely used in forestry research (FRANK *et al.*, 2018; LIN *et al.*, 2013; BONAN *et al.*, 2014; MEDLYN *et al.*, 2017). These include the phenomenological Ball–Berry (BB; BALL; WOODROW; BERRY, 1987), Ball–Berry–Leuning (BBL; LEUNING, 1995) models, and the optimality-based unified stomatal optimization model (USO; MEDLYN *et al.*, 2011). Ball *et al.* (1987) developed one of the most commonly used models of g_s , known as BB or BWB (DAMON *et al.*, 2010). The BB method assumes that stomatal conductance is strongly correlated with assimilation rate (WONG *et al.*, 1979) because stomata open and close to keep a nearly constant ratio between intercellular and ambient CO₂ concentration (HOSHIKA *et al.*, 2017). This ratio may vary with atmospheric humidity. Therefore, Ball *et al.* (1987) elaborated a model that links stomatal conductance to leaf photosynthesis, vapor pressure deficit, and CO₂ concentration at the leaf surface (Hoshika *et al.*, 2017). The BB model is classified as a semi-empirical model approach i.e. built on physiological hypotheses but still combined with empirical functions (DAMOUR *et al.*, 2010).

The BBL model was developed from modifications to the BB model equation. Leuning (1995) modified the equation incorporating an empirical dependence on leaf-to-air vapor pressure deficit (VPD) to a proxy for transpiration. An alternative to the BB and BBL semi-empirical approach models is the optimal stomatal conductance model (USO) proposed by Medlyn *et al.* (2011). The USO model is based on a theory of optimal stomatal behavior was developed by Cowan & Farquhar (1977). This theory postulates that stomata should act to maximize carbon gain (photosynthesis, A) while minimizing water loss (transpiration, E). These models are widely used because they are straightforward to parameterize from leaf-scale data, are easy to implement at large scales (MEDLYN *et al.*, 2011).

The representation of stomatal conductance (g_s) is a fundamental component of Earth system models (ESMs) and Process-based models (PBMs). Earth system models (ESMs) are essential tools for understanding and predicting the global implications of large-scale

environmental perturbations (FRANKS et al., 2018; BONAN; DONEY, 2018). These models integrate biogeochemical and biogeophysical land-surface processes with physical climate models. Within the biogeophysical components of land-surface processes, *gs* plays a pivotal role because it is a key feedback route for carbon and water exchange between the atmosphere and terrestrial vegetation. Process-based models (PBMs) are used to understand how plants respond to environmental change and can be used as a research tool to clarify interactions among environmental drivers, plant and canopy structure, leaf physiology, and soil water availability and their combined effects on water use and carbon uptake (MEDLYN et al., 2012; WILLIAMS et al., 2001). The BB, BBL and USO models are the most used in ESMs and PBMs, however each model prefers a stomatal conductance model based on the approach.

Many ESMs at present use an empirical stomatal model to predict *gs*, for example, the CABLE model (WANG et al., 2011) uses the empirical stomatal model of Ball-Berry-Leuning (1995) but has been tested with the USO model (DE KAUWE et al., 2015b), the CLM 4.0 (OLESON et al., 2013) model uses the empirical stomatal model of Ball et al. (1987), the MAESPA (DUURSMA; MEDLYN, 2012) has the option to use the three models (BB, BBL and USO). Moreover, Studies have revealed that the accuracy of stomatal conductance models is affected by the plant species, test regions, environmental conditions, and time scales (GAO et al., 2016; WU et al., 2019, WANG et al., 2014; HÉROULT et al., 2013). Thus, selecting an appropriate stomatal conductance model based on the existing research data can be problematic (WANG et al., 2014; WANG et al., 2018).

Brazil is a world reference for forest plantation productivity, with high annual production volumes of wood per area and a short cycle. In 2020, the total area of planted trees totaled 9.55 million hectares, with the majority of planted trees were eucalyptus species, with 78% of the area and 7.47 million hectares, and 18% pine species with 1.7 million hectares (IBA, 2021). However, studies of modeling the stomatal conductance of planted forests in Brazil are still incipient, so it is necessary and fundamental to develop studies that aim to obtain physiological parameters explaining the stomatal behavior and water use efficiency under environmental conditions in Brazil.

In this study, we compiled a database of eucalypt and pine measurements of *gs* and photosynthesis suitable for estimating model parameters. We employed models of stomatal conductance to obtain parameters that can be used in ESMS and PBMs models. The goal of this study was to compare the performance of three stomatal conductance models (BB, BBL and

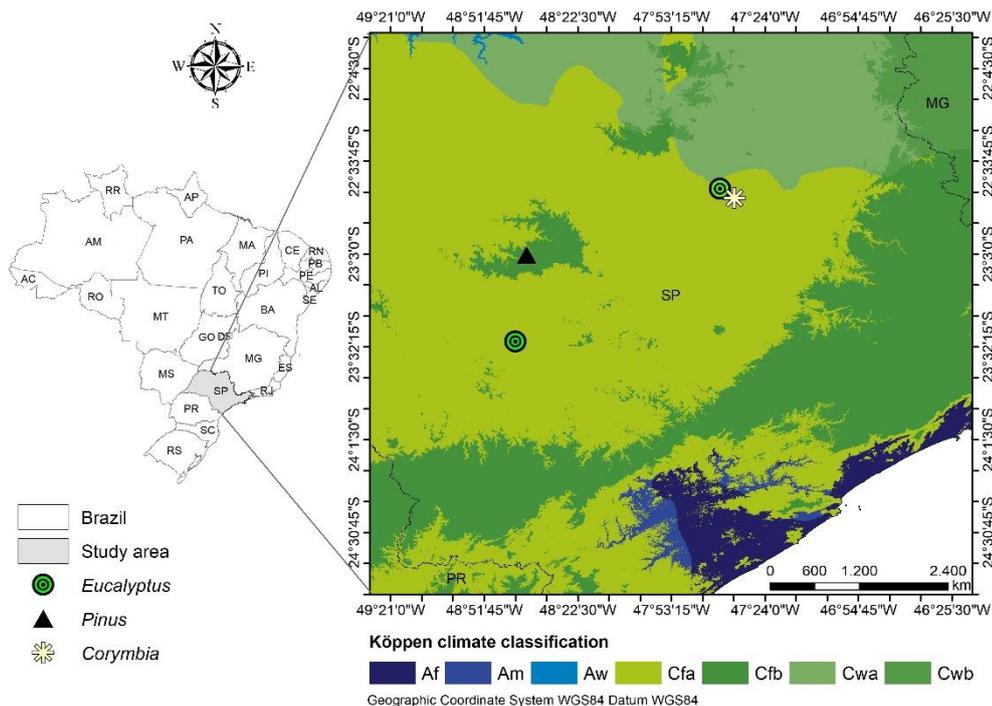
USO), and explore the underlying response of stomatal conductance should vary between functional groups (pine and eucalypt) in Brazilian forest plantations.

2. Material and Methods

2.1 Datasets

We combined leaf level gas exchange measurements from 22 genotypes covering 20 genotypes of *Eucalyptus* and 2 species of *Pinus* in Brazilian forest plantations. These data were taken from 4 experiments in São Paulo state, Brazil. Each experiment was carried independently, with different spacings, fertilization and specific silvicultural treatments. The Distribution of the experiments is on the map (Figure 1). The age of eucalypt genotypes ranged from 6 to 36 months. The age of pine species were 60 months. In most cases, measurements were under ambient field conditions except for one dataset obtained in nursery conditions (ID 3). These datasets were obtained through partnerships with projects that aim to study the ecophysiology of planted forests in Brazil.). Each genetic material was described by a clone code and sites/experiments were describes as ID. For more details on these sites as historic mean annual air temperature, rainfall, latitude, longitude see table 1.

Figure1. Map showing the location and distribution of experiments in São Paulo state - Brazil



2.2 Measurements of leaf gas exchange

Measurements of leaf stomatal conductance response to VPD (vapor pressure deficit) were made using the LI-6400 portable photosynthesis system (Li-Cor Inc., Lincoln, NE, USA). These data are measurements on upper-canopy leaves during the growing season. The 3–5 individuals for each clone were selected to measure leaf stomatal conductance response, with fully developed and sun-exposed leaves. The measurements were carried out between 8:00 am and 3:00pm in order to capture VPD variation throughout the day. The measurements were made under a wide range of environmental conditions on sunny days, with leaf temperatures ranging 18–36°C and VPD ranging from <1 to 5kPa.

2.3 Stomatal conductance models

The parameter g_1 was estimated from leaf gas exchange data using three common models to describe the coupled g_s – A relationship to environmental variables. The g_s models fitted were describe as BB, BBL e USO. We chose these models because they are the most used in ecophysiology studies, in addition to their simplicity, versatility, and broad success in LSMs.

The BB model (BALL et al., 1987) is formulated as follows:

(1)

$$g_s = g_0 + g_1 \left(\frac{A_n H_s}{C_a} \right)$$

where g_0 and g_1 are fitted parameters, A_n is net assimilation rate ($\mu\text{mol m}^{-2} \text{s}^{-1}$), H_s is relative humidity at the leaf surface (dimensionless) and C_a is atmospheric CO_2 concentration at the leaf surface ($\mu\text{mol mol}^{-1}$).

The BBL model (LEUNING, 1995) is an alternative way to relate g_s to the environment incorporating an empirical dependence on leaf-to-air vapor pressure deficit (D , kPa) as follows:

(2)

$$g_s = g_0 + g_1 \frac{A_n}{(C_a - \Gamma^*) \left(1 + \frac{D}{D_0} \right)}$$

where Γ is the CO₂ compensation point of assimilation in the presence of dark respiration. This model has three empirically fitted parameters, g_0 , g_1 and D_0 .

The USO model as follows is an optimality model developed by Medlyn et al. (2011), with the slope parameter of g_1 .

(3)

$$g_s^* \approx 1.6 \left(1 + \frac{g_1}{\sqrt{D}} \right) \frac{A}{C_a} + g_0$$

Where A is the net assimilation rate ($\mu\text{mol m}^{-2} \text{s}^{-1}$), and C_a ($\mu\text{mol mol}^{-1}$) and D (kPa) are the CO₂ concentration and VPD at the leaf surface, respectively. The model parameter g_1 ($\text{kPa}^{0.5}$) represents normalized plant WUE.

2.4 Statistical analyses

We first tested each dataset for each of the three models of stomatal conductance (BB, BBL e USO) to estimate the parameter g_1 . We fitted these g_s models using the *fitBB* function within the PLANTECOPHYS package (DUURSMA, 2015) in R version 4.1.0 (R Development Core Team, 2012). The *fitBB* function provides an interface to non-linear or linear regression to fit one of three stomatal conductance models. The R² (coefficient of determination), root mean square error (RMSE) and Akaike information criterion (AIC) were used to evaluate the performance of models. The RMSE reflects the difference between simulated and measure. The smaller the value, the better the model's performance. The AIC can be used to compare the overall performance of the models with different numbers of parameters and give the ranking of the model simulation results. A smaller AIC value means a better simulation performance of model.

We selected model USO model to analyze the stomatal behavior across genotypes and the water use efficiency. The parameter g_1 by USO model is a proxy for the efficiency of water use. We also calculated the slope parameter of the unified stomatal optimization model (USO; MEDLYN et al., 2011) for each genotype of dataset.

The regression slope between stomatal conductance (g_s) and the USO model index ($1.6 \times (A/C_a \times \sqrt{D})$) is almost linearly proportional to the stomatal slope of the USO model. For a given CO₂ assimilation rate (A), atmospheric CO₂ concentration (C_a), and leaf-to-air vapor

pressure deficit (D) a higher regression slope (and thus stomatal slope) means that plants maintain a higher g_s to keep the same photosynthetic rate. As such, the stomatal slope parameter is an indicator of intrinsic plant water use efficiency, and a greater stomatal slope equates to a lower intrinsic water use efficiency (WU et al., 2019)

Table 1. Details of experimental data sets used in this study

Species/genotype	Clone	Experiment ID	Site of Location (city and state)	Age (months)	Condition	Tmean (C°)	Rainfall (mm)	Lat. (°S)	Long. (°W)	Reference
<i>Eucalyptus</i> sp	E1	1	Piracicaba- SP	36	Field	21.1	1253	-22,71	-47,63	Marrichi et al. (2005)
<i>Eucalyptus</i> sp	E2	1	Piracicaba- SP	36	Field	21.1	1253	-22,71	-47,63	Marrichi et al. (2005)
<i>Eucalyptus</i> sp	E3	1	Piracicaba- SP	36	Field	21.1	1253	-22,71	-47,63	Marrichi et al. (2005)
<i>E.grandis</i> x <i>E.urophylla</i>	UG1	1	Piracicaba- SP	36	Field	21.1	1253	-22,71	-47,63	Marrichi et al. (2005)
<i>E. urophylla</i>	U1	1	Piracicaba- SP	36	Field	21.1	1253	-22,71	-47,63	Marrichi et al. (2005)
<i>E.grandis</i>	G1	1	Piracicaba- SP	36	Field	21.1	1253	-22,71	-47,63	Marrichi et al. (2005)
<i>E.grandis</i>	G2	1	Piracicaba- SP	36	Field	21.1	1253	-22,71	-47,63	Marrichi et al. (2005)
<i>E. grandis</i> x <i>E. camaldulensis</i>	GC	2	Buri-SP	14,7	Field	20.5	1180	-23,51	-48,7	Binkley et al. (2017)
<i>E. grandis</i> x <i>E. sp</i>	GS	2	Buri-SP	14,7	Field	20.5	1180	-23,51	-48,7	Binkley et al. (2017)
<i>E. grandis</i> x <i>E.urophylla</i>	UG2	2	Buri-SP	14,7	Field	20.5	1180	-23,51	-48,7	Binkley et al. (2017)
<i>E. grandis</i> x <i>E.urophylla</i>	UG3	2	Buri-SP	14,7	Field	20.5	1180	-23,51	-48,7	Binkley et al. (2017)
<i>E. urophylla</i>	U2	2	Buri-SP	14,7	Field	20.5	1180	-23,51	-48,7	Binkley et al. (2017)
<i>E. urophylla</i>	U3	2	Buri-SP	14,7	Field	20.5	1180	-23,51	-48,7	Binkley et al. (2017)
<i>E. urophylla</i> x <i>E. brassiana</i>	UB	2	Buri-SP	14,7	Field	20.5	1180	-23,51	-48,7	Binkley et al. (2017)
<i>E.urophylla</i> x <i>E.grandis</i>	UG4	3	Buri-SP	14,7	Field	20.5	1180	-23,51	-48,7	Binkley et al. (2017)
<i>E.urophylla</i>	U4	3	Piracicaba- SP	6	Nursery	21.1	1253	-22,71	-47,63	Unpublished data
<i>C. citriodora</i>	CC	3	Piracicaba- SP	6	Nursery	21.1	1253	-22,71	-47,63	Unpublished data
<i>E.crebra</i>	CB	3	Piracicaba- SP	6	Nursery	21.1	1253	-22,71	-47,63	Unpublished data
<i>E. grandis</i>	G3	3	Piracicaba- SP	6	Nursery	21.1	1253	-22,71	-47,63	Unpublished data
<i>E.longirostrata</i>	LG	3	Piracicaba- SP	6	Nursery	21.1	1253	-22,71	-47,63	Unpublished data
<i>P. caribaea</i>	PC	4	Itatinga -SP	60	Field	22,5	1350	-23,05	-48,64	Carneiro, (2013)
<i>P. taeda</i>	PT	4	Itatinga -SP	60	Field	22,5	1350	-23,05	-48,64	Carneiro, (2013)

3. Results

3.1 Leaf gas exchange

Stomatal conductance (g_s) and photosynthesis (A) was coupled with VpdL for 20 *Eucalyptus* genotypes and 2 species of *Pinus* (Figure 1 and 2). The leaf gas exchange showed a clear decline in both A and g_s with increasing VpdL. The prevailing pattern regarding the relationship between g_s and atmospheric water content is that increasing vapor pressure deficit (VPD) leads to reduction of stomatal conductance (LI et al., 2019). These correlation between g_s /VpdL reveals the different behaviors of the genotypes. We observed in figure 1 that at low VpdL values there was a reduction in g_s for pine (PC, PT) indicating a lower stomatal control. This stomatal sensitivity at higher VpdL resulted in the highest slope between the g_s and Medlyn index, indicating a low water use efficiency as shown in Figure 4.

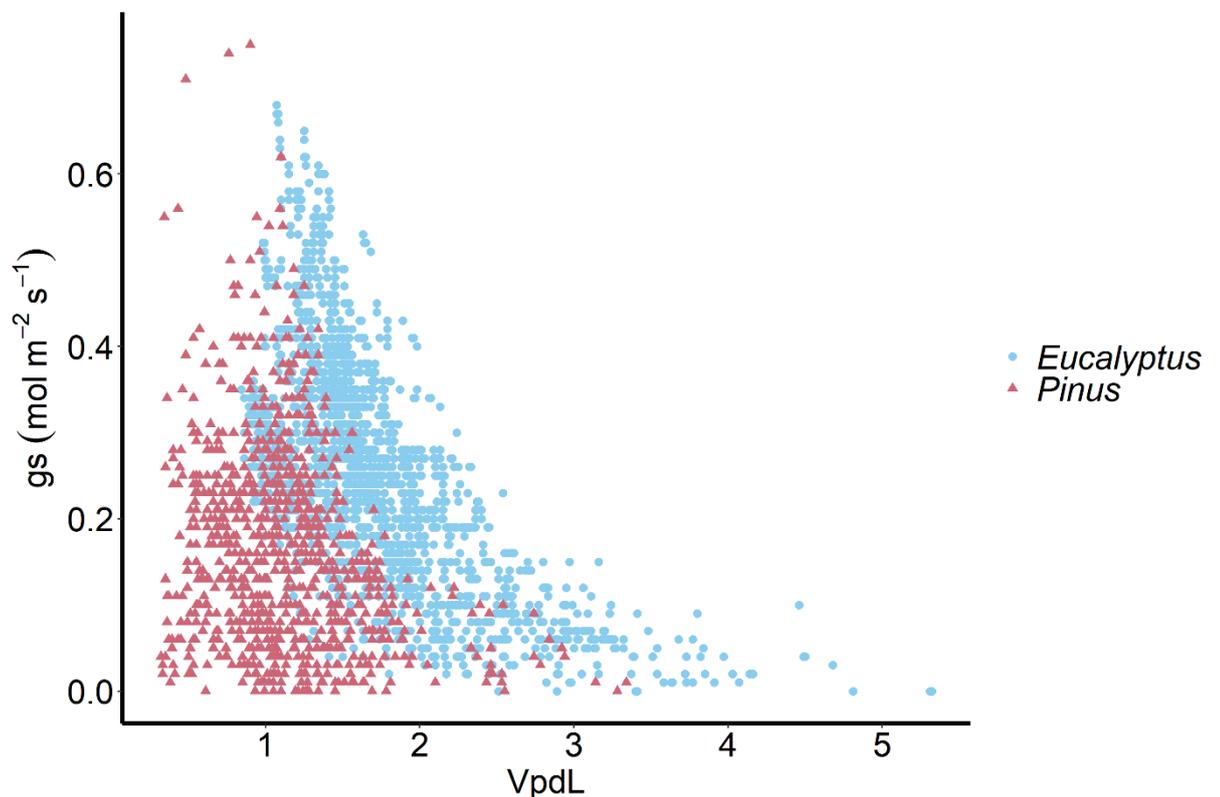


Figure 1. Relationship between stomatal conductance to water (g_s) with (leaf-air vapor pressure deficit - VpdL) for functional groups (pine and eucalypt) in Brazil forest.

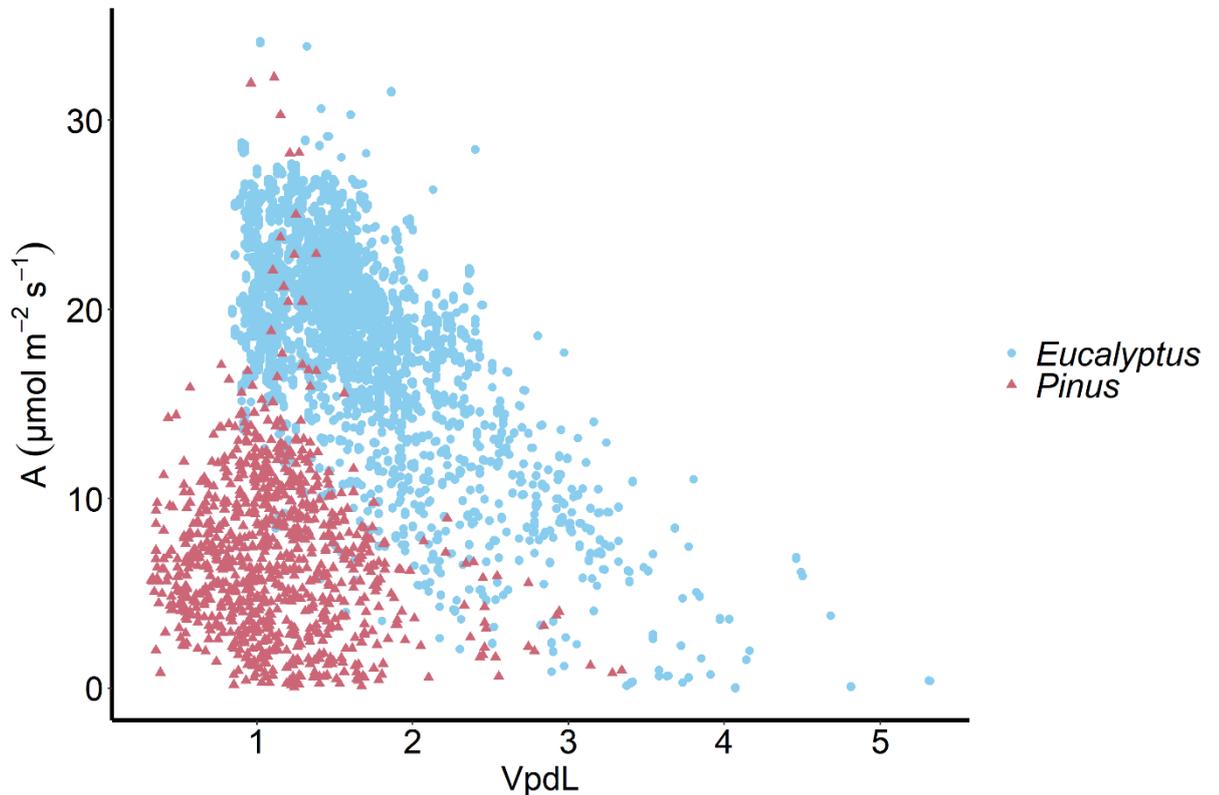


Figure 2. Relationship between photosynthesis (A) with (leaf-air vapor pressure deficit ($VpdL$)) for functional groups (pine and eucalypt) in Brazil forest.

3.2 Fits derived from the BB, BBL, and USO models

Values of g_1 estimated using the three g_s models (BB, BBL and USO) for each clone and metrics calculated are describe in Table 2. Both the USO model and the BBL model showed good fits (R^2 ranging from 0.41 to 0.95) with the evaluated metrics. The BBL model was the best fit for some datasets (E1, E3, G1, UG2, GC, U2, UG3, GS, U4, LG, CB and PT). From 22 genotypes, three did not fit the BBL model (U3, CC, and G3). The USO model had good metrics and fit all datasets. The R^2 value fitted by the BBL model ranged 0.47 to 0.95. The five genotypes (E3, U1, GC, UG3, and UB) had R^2 less than 0.6.

The R^2 value fitted by the USO model ranged from 0.43 to 0.95, and five genotypes also had R^2 less than 0.6 (E3, U1, GC, UG3 and GS). From five genotypes with R^2 less than 0.6 by model USO, four (E3, U1, GC, UG3) are the same genotypes that had R^2 less than 0.6 fitted by model BBL.

Although the BB model presented good fits for some datasets (R^2 ranged 0.31 to 0.86, eight genotypes E3, U1, UG2, GC, UB, GS, PC, PT had R^2 less than 0.6) the performance was inferior to the BBL and USO model. Among these models, the BB formulations use relative

humidity (RH) while the BBL and USO formulations represent g_s responses to vapor pressure deficit (VPDL). (Table 2)

Table 2. Fitted coefficients (g1) of the Ball-Berry (BB), Ball-Berry-Leuning (BBL) and Medlyn (USO) stomatal conductance models for 20 *Eucalyptus* genotypes and 2 species of *Pinus*. The model results are shown below including the statistic metrics for model performance (R², RMSE, and AIC).

Genotype	Clone	ID	Condition	Age (months)	gs models	g1± SE	R ²	RMSE	AIC
<i>Eucalyptus</i> sp	E1	1	field	36	BBL	7.19 ± 0.92***	0,94	0,016	-281
<i>Eucalyptus</i> sp	E1	1	field	36	BB	9.31 ± 0.22***	0,87	0,025	-236
<i>Eucalyptus</i> sp	E1	1	field	36	USO	1.85 ± 0.05***	0,94	0,017	-280
<i>E. grandis</i> x <i>E. urophylla</i>	UG1	1	field	36	BBL	4.16 ± 0.34 ***	0,95	0,012	-305
<i>E. grandis</i> x <i>E. urophylla</i>	UG1	1	field	36	BB	7.59 ± 0.12***	0,94	0,014	-289
<i>E. grandis</i> x <i>E. urophylla</i>	UG1	1	field	36	USO	1.42 ± 0.04***	0,95	0,012	-304
<i>Eucalyptus</i> sp	E2	1	field	36	BBL	16. 6 ± 15.18ns	0,85	0,057	-138
<i>Eucalyptus</i> sp	E2	1	field	36	BB	8.62 ± 0.39***	0,70	0,081	-103
<i>Eucalyptus</i> sp	E2	1	field	36	USO	2.67 ± 0.12 ***	0,87	0,053	-145
<i>Eucalyptus</i> sp	E3	1	field	36	BBL	8.36 ± 2.91**	0,47	0,066	-128
<i>Eucalyptus</i> sp	E3	1	field	36	BB	6.26 ± 0.23***	0,31	0,076	-114
<i>Eucalyptus</i> sp	E3	1	field	36	USO	1.85 ± 0.094***	0,46	0,067	-127
<i>E. urophylla</i>	U1	1	field	36	BBL	10.56 ± 2.20***	0,55	0,045	-170
<i>E. urophylla</i>	U1	1	field	36	BB	16 ± 0.28***	0,41	0,052	-156
<i>E. urophylla</i>	U1	1	field	36	USO	4.87 ± 0.10***	0,57	0,044	-173
<i>E. grandis</i>	G1	1	field	36	BBL	13.05 ± 3.97**	0,78	0,067	-96,6
<i>E. grandis</i>	G1	1	field	36	BB	10 ± 0.36***	0,69	0,079	-82,9
<i>E. grandis</i>	G1	1	field	36	USO	3.3 ± 0.12	0,77	0,068	-94,8
<i>E. grandis</i>	G2	1	field	36	BBL	3.30 ± 0.12***	0,41	0,05	-156
<i>E. grandis</i>	G2	1	field	36	BB	10.88 ± 0.42***	0,62	0,086	-92,9
<i>E. grandis</i>	G2	1	field	36	USO	3.21 ± 0.12***	0,83	0,056	-133
<i>E. urophylla</i> x <i>E. grandis</i>	UG2	2	field	14,7	BBL	8.21 ± 0.47***	0,73	0,039	-2421

<i>E.urophylla</i> x <i>E.grandis</i>	UG2	2	field	14,7	BBL	10.11 ± 0.06***	0,57	0,049	-2117
<i>E.urophylla</i> x <i>E.grandis</i>	UG2	2	field	14,7	USO	2.54 ± 0.021***	0,72	0,040	-2401
<i>E. grandis</i> x <i>E. camaldulensis</i>	GC	2	field	14,7	BBL	18.4 ± 2.61***	0,58	0,075	-1413
<i>E. grandis</i> x <i>E. camaldulensis</i>	GC	2	field	14,7	BB	13.16 ± 0.10***	0,56	0,077	-1374
<i>E. grandis</i> x <i>E. camaldulensis</i>	GC	2	field	14,7	USO	3.89 ± 0.03***	0,57	0,076	-1396
<i>E. urophylla</i>	U2	2	field	14,7	BBL	15.82 ± 1.99***	0,86	0,021	-2401
<i>E. urophylla</i>	U2	2	field	14,7	BB	8.99 ± 0.09***	0,77	0,027	-2124
<i>E. urophylla</i>	U2	2	field	14,7	USO	2.03 ± 0.03***	0,84	0,023	-2305
<i>E. urophylla</i>	U3	2	field	14,7	BBL	-	-		
<i>E. urophylla</i>	U3	2	field	14,7	BB	10.84 ± 0.08***	0,79	0,047	-1485
<i>E. urophylla</i>	U3	2	field	14,7	USO	3.48 ± 0.03***	0,87	0,037	-1699
<i>E. grandis</i> x <i>E.urophylla</i>	UG3	2	field	14,7	BBL	7.05 ± 8.03	0,55	0,031	-2561
<i>E. grandis</i> x <i>E.urophylla</i>	UG3	2	field	14,7	BB	8.32 ± 0.05 ***	0.23	0,041	-2214
<i>E. grandis</i> x <i>E.urophylla</i>	UG3	2	field	14,7	USO	2.35 ± 0.01***	0,43	0,035	-2406
<i>E. grandis</i> x <i>E.urophylla</i>	UG4	2	field	14,7	BBL	6.55 ± - 0.43***	0,72	0,031	-1996
<i>E. grandis</i> x <i>E.urophylla</i>	UG4	2	field	14,7	BB	9.19 ± 0.06***	0.60	0.037	-1987
<i>E. grandis</i> x <i>E.urophylla</i>	UG4	2	field	14,7	USO	2.20 ± 0.021***	0.71	0,031	-1991
<i>E. urophylla</i> x <i>E. brassiana</i>	UB	2	field	14,7	BBL	8.41 ± 0.38***	0,60	0,046	-2082
<i>E. urophylla</i> x <i>E. brassiana</i>	UB	2	field	14,7	BB	11.46 ± 0.10***	0,39	0,059	-1788
<i>E. urophylla</i> x <i>E. brassiana</i>	UB	2	field	14,7	USO	3 ± 0.02***	0,60	0,046	-2058
<i>E. grandis</i> x <i>E.sp</i>	GS	2	field	14,7	BBL	3.00 ± 0.02	0,60	0,047	-2058
<i>E. grandis</i> x <i>E.sp</i>	GS	2	field	14,7	BB	9.68 ± 0.10***	0,51	0,054	-1260
<i>E. grandis</i> x <i>E.sp</i>	GS	2	field	14,7	USO	2.92 ± 0.04***	0,51	0,054	-1260
<i>E.urophylla</i>	U4	3	nursery	6	BBL	9.27± 2.38***	0,8	0,028	-593
<i>E.urophylla</i>	U4	3	nursery	6	BB	7.09± 0.20 ***	0,7	0,036	-530
<i>E.urophylla</i>	U4	3	nursery	6	USO	1.82 ± 0.07***	0,78	0,030	-578
<i>C.citriodora</i>	CC	3	nursery	6	BBL	-			
<i>C.citriodora</i>	CC	3	nursery	6	BB	8.86 ± 0.23***	0,62	0.66	-375

<i>C.citriodora</i>	CC	3	nursery	6	USO	2.36 ± 0.08 ***	0,73	0,05	-428
<i>E.crebra</i>	CB	3	nursery	6	BBL	10.01 ± 2.01***	0,90	0,027	-422
<i>E.crebra</i>	CB	3	nursery	6	BB	8.34 ± 0.19 ***	0,86	0,033	-386
<i>E.crebra</i>	CB	3	nursery	6	USO	2.35 ± 0.07***	0,90	0,029	-408
<i>E. grandis</i>	G3	3	nursery	6	BBL	-			
<i>E. grandis</i>	G3	3	nursery	6	BB	8.25 ± 0.33***	0,6	0,042	-515
<i>E. grandis</i>	G3	3	nursery	6	USO	2.43 ± 0.12***	0,72	0,035	-570
<i>E.longirostrata</i>	LG	3	nursery	6	BBL	11.4 ± 2.07***	0,9	0,033	-588
<i>E.longirostrata</i>	LG	3	nursery	6	BB	7.66 ± 0.15***	0,83	0,044	-502
<i>E.longirostrata</i>	LG	3	nursery	6	USO	1.92 ± 0.05***	0,9	0,035	-571
<i>P. caribaea</i>	PC	4	field	60	BBL	12.20 ± 0.87***	0,65	0,055	-1345
<i>P. caribaea</i>	PC	4	field	60	BB	11.87 ± 0.25***	0,59	0,059	-1268
<i>P. caribaea</i>	PC	4	field	60	USO	4.30 ± 0.10***	0,66	0,057	-1325
<i>P. taeda</i>	PT	4	field	60	BBL	23.44 ± 3.31***	0,67	0,07	-1135
<i>P. taeda</i>	PT	4	field	60	BB	13.28 ± 0.24***	0,56	0,082	-991
<i>P. taeda</i>	PT	4	field	60	USO	4.96 ± 0.09***	0,66	0,071	-1121

***: (p < 0.001)

_ : Data no fitted

3.3 Comparison of stomatal responses across genotypes (g1 - USO model)

The table 3 and figure 3 shows the coefficients g1 fitted by only model USO for 20 genotypes of *Eucalyptus*, 2 species of *Pinus* in Brazilian forest plantations. The USO model had the highest slope parameter for species *Pinus Taeda* ($g1 = 4.96 \pm 0.09$) and the lowest slope parameter for genotype *E. grandis x E. urophylla* (1.42 ± 0.04). The parameter g1 of the eucalypt group ranged from 1.42 to 4.87. The group pine ranged from 4.30 to 4.96. Overall, the species of the pine had higher slope parameter than the eucalypt group. Only one genotype from the eucalypt (*E. urophylla*) had g1 close to pine values (Table 3)

The USO model had the highest slope parameter for the genotypes UB, G2, G1, U3, GC, U1, PC and PT ($g1 > 3$) and the lowest slope parameter for the genotypes UG1, U4, E1, E3, LG ($g1 < 2$), with intermediate slopes for other genotypes (U2, UG4, UG3, UG2, GS). We observed that within datasets the parameter g1 varied between the genotypes (Figure 3).

We also identified that for the same genotype, the parameter g1 varies between experiments: *Eucalyptus grandis*, genotypes G2 (3.21 ± 0.12) and G3 ($g1 = 2.43 \pm 0.12$) present in ID 1 and 3, *E. grandis x E. urophylla*, genotype UG1 ($g1 = 1.42 \pm 0.04$) and UG4 ($g1 = 2.20 \pm 0.021$) present in ID 1 and 2 and the *E. urophylla*, genotype U2 ($g1 = 2.03 \pm 0.03$), U3 (3.48 ± 0.03) and U4 (1.82 ± 0.07) present in ID 2 and 3. (Table 3).

Table 3. Fitted coefficients (g1) of the Medlyn (USO) stomatal conductance model and statistics

Genotype	Clone	ID	Location (site)	Age (months)	g1± SE	R²	RMSE
<i>E.grandis x E.urophylla</i>	UG1	1	Piracicaba- SP	36	1.42 ± 0.04***	0.95	0.012
<i>Eucalyptus</i> sp	E1	1	Piracicaba- SP	36	1.85 ± 0.05***	0.94	0.017
<i>Eucalyptus</i> sp	E3	1	Piracicaba- SP	36	1.85 ± 0.094***	0.46	0.067
<i>Eucalyptus</i> sp	E2	1	Piracicaba- SP	36	2.67 ± 0.12 ***	0.87	0.053
<i>E. grandis</i>	G2	1	Piracicaba- SP	36	3.21 ± 0.12***	0.83	0.056
<i>E. grandis</i>	G1	1	Piracicaba- SP	36	3.3 ± 0.12	0.77	0.068
<i>E. urophylla</i>	U1	1	Piracicaba- SP	36	4.87 ± 0.10***	0.57	0.044
<i>E. urophylla</i>	U2	2	Buri-SP	14.7	2.03 ± 0.03***	0.84	0.023
<i>E. grandis x E.urophylla</i>	UG4	2	Buri-SP	14.7	2.20 ± 0.021***	0.71	0.031
<i>E. grandis x E.urophylla</i>	UG3	2	Buri-SP	14.7	2.35 ± 0.01***	0.43	0.035
<i>E.urophylla x E.grandis</i>	UG2	2	Buri-SP	14.7	2.54 ± 0.021***	0.72	0.04
<i>E. grandis x E.sp</i>	GS	2	Buri-SP	14.7	2.92 ± 0.04***	0.51	0.054
<i>E. urophylla x E. brassiana</i>	UB	2	Buri-SP	14.7	3 ± 0.02***	0.60	0.046
<i>E. urophylla</i>	U3	2	Buri-SP	14.7	3.48 ± 0.03***	0.87	0.037
<i>E. grandis x E. camaldulensis</i>	GC	2	Buri-SP	14.7	3.89 ± 0.03***	0.57	0.076
<i>E.urophylla</i>	U4	3	Piracicaba- SP	6	1.82 ± 0.07***	0.78	0.03
<i>E.longirostrata</i>	LG	3	Piracicaba- SP	6	1.92 ± 0.05***	0.9	0.035
<i>E.crebra</i>	CB	3	Piracicaba- SP	6	2.35 ± 0.07***	0.9	0.029
<i>C.citriodora</i>	CC	3	Piracicaba- SP	6	2.36 ± 0.08 ***	0.73	0.05
<i>E. grandis</i>	G3	3	Piracicaba- SP	6	2.43 ± 0.12***	0.72	0.035
<i>P. caribaea</i>	PC	4	Itatinga -SP	60	4.30 ± 0.10***	0.66	0.057
<i>P. taeda</i>	PT	4	Itatinga -SP	60	4.96 ± 0.09***	0.66	0.071

***: (p < 0.001)

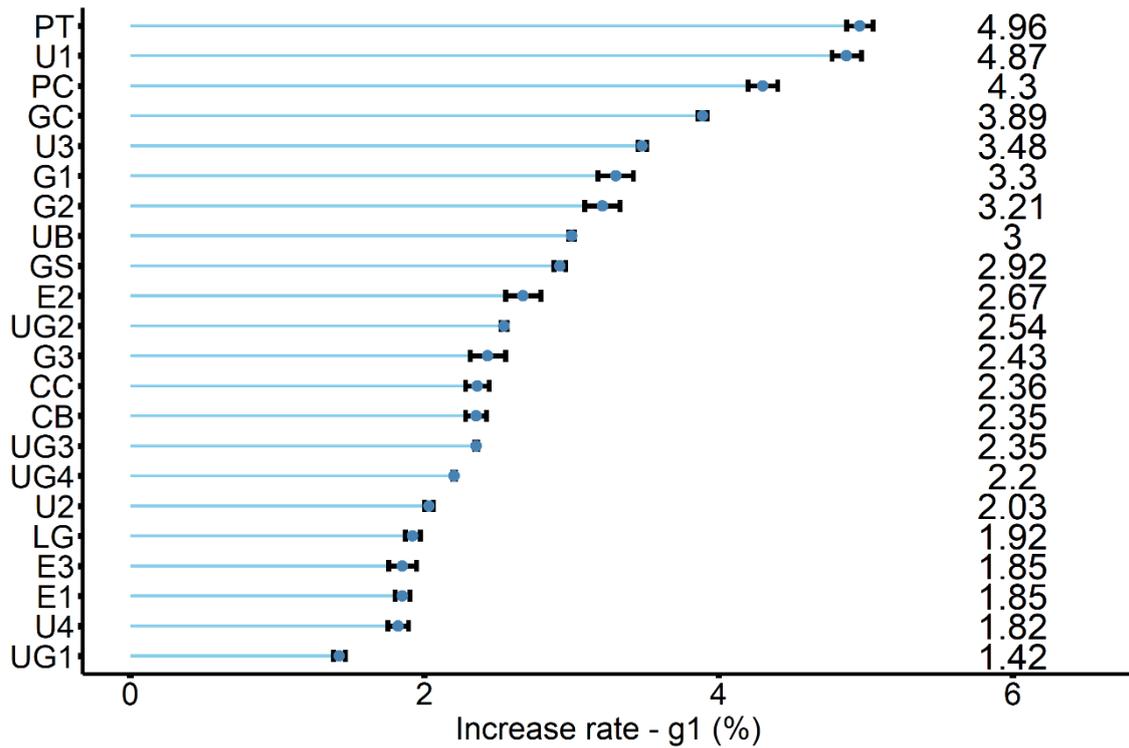


Figure 3. USO model coefficients ($g1$) derived from leaf-level measurements on from 20 *Eucalyptus* genotypes and 2 species of *Pinus* in Brazilian forest plantations.

3.3 USO model index

The Stomatal conductance (g_s) was coupled with USO model index for all genotypes of dataset (Figure 4). The relationship between USO model index of group pine and g_s has higher regression slope (and thus stomatal slope) than the group of eucalypt. As such, the stomatal slope parameter is an indicator of intrinsic plant water use efficiency, and a greater stomatal slope equates to a lower intrinsic water use efficiency. This type of plot can therefore be used as a simple way of visualizing the fit of USO model.

The slope of this plot varies principally with $g1$, although it also depends slightly on the range of DPV in the measurements. Differences in slope can be used to help visualize differences in $g1$ among datasets. The figure 4 shows that the slope of the relationship (and therefore $g1$) clearly differs among functional groups (pine and eucalypt).

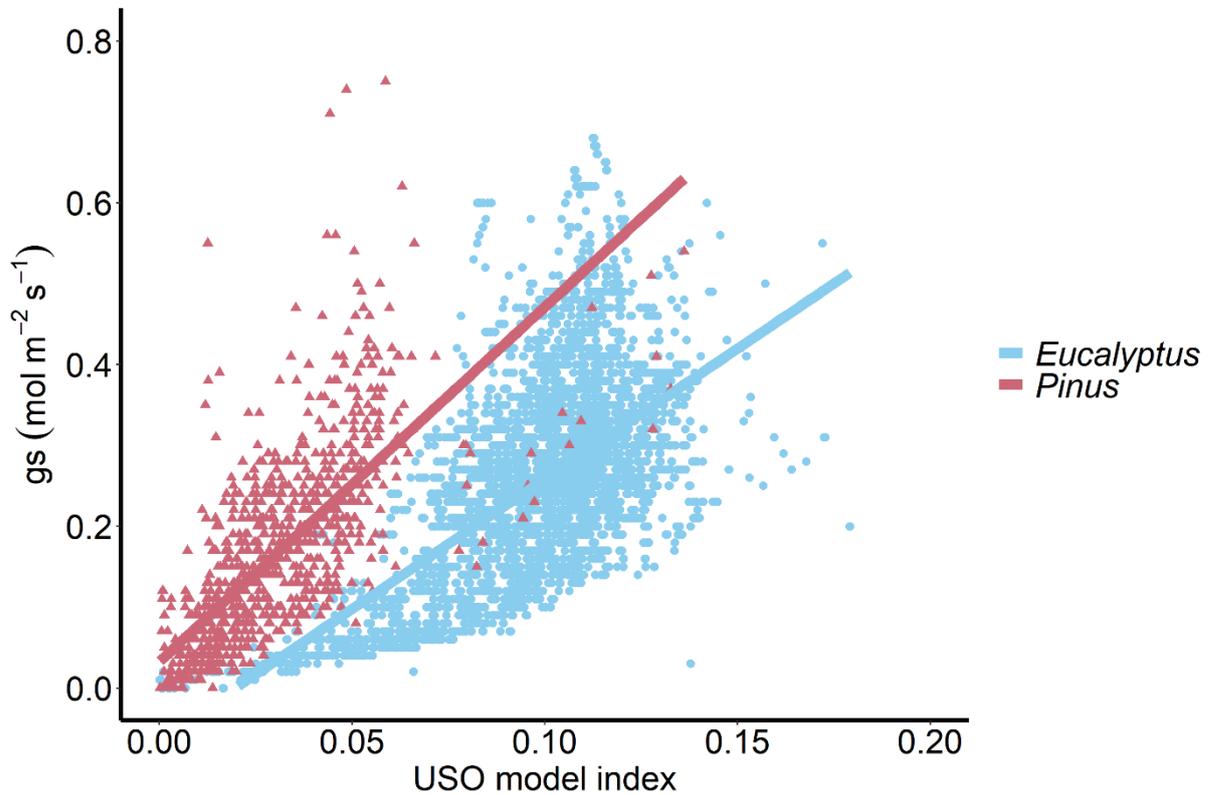


Figure 4. Relationship between stomatal conductance with the slope parameter of the unified stomatal optimization model (USO model index) for functional groups (pine and eucalypt) in Brazil forest.

4. Discussion

Understanding abiotic and biotic controls of g_s and exploring accurate representation of g_s in ESMs and PBMs has been a core focus in plant physiology ecology. In this study, we investigated the modeling of g_s using data from 20 genotypes of *Eucalyptus* and 2 species of *Pinus* in the Brazil forest. We demonstrated that in planted forests the models that represent g_s response to vapor pressure deficit (i.e. models, BBL and USO) performed better than the model based on RH (i.e. BB). Additionally, we demonstrated variation in the slope parameter (g_1 by model USO) across genotypes, indicating differences in water use efficiency. We also estimated the USO model index as an indicator of intrinsic plant water use efficiency.

4.1 Modelling stomatal conductance - BB, BBL, and USO models

The stomatal conductance is influenced by multiple environmental factors, and the dominant factors are different depending on the environmental conditions, which affects the performance of stomatal conductance models (WANG et al., 2018). In our study, the performance of BB model was inferior to the BBL and USO model. Several studies revealed the differences on responses of conductance models (WANG et al., 2018, ANDEREGG *et al.*, 2017, WU et al., 2019, HÉROULT et al., 2013).

Unlike the BB model that g_s response to relative humidity, the BBL and USO model represents g_s response to the vapor pressure deficit. Despite the different approaches, these models are derived from leaf-level physiological theory and their simplicity, versatility, and broad success observations in simulating leaf gas exchange have encouraged their use in LSMs.

The study of Frank et al. (2018), evaluated empirical and optimal approaches to modeling g_s in ESMs by undertaking a detailed comparison of BB and USO model at multiple scales (leaf to land surface), in forest sites in North America, revealed that the BB and USO models both exhibit high-quality fits to leaf gas exchange data in a coupled leaf photosynthesis-conductance model and also in the land surface model - CLM5. Accord to authors, the absence of any significant difference in the performance of BB or MED in the coupled photosynthesis-conductance leaf model or the CLM5 model is consistent with the similarities in their capacity to describe the fundamental correlation between g_s and photosynthesis in leaf gas exchange measurements.

The inclusion of environmental factors has been studied in several studies aiming to improve the accuracy of models (WANG et al., 2018; WU et al., 2019, ZHANG et al., 2017; JI et al., 2016). The study carried out by Wu et al. (2019) in forests of Panama revealed that the inclusion of leaf water potential did not improve model performance and that the models that represent the response of g_s to steam pressure deficit performed better than corresponding models that respond to relative humidity. Despite not including environmental variables in the models tested here, the results observed by Wu et al., 2019 were similar to those found in our study, the BBL and USO model were better performance than BB.

Our results also corroborate the study by Héroult et al. (2013), when evaluating the *Eucalyptus* species originating from different climate zones in Australia comparing the two g_s models (BBL and USO), showed that Goodness-of-fit was similar between the empirical BBL model and the USO model among the species.

Wang et al. (2018), also studied the inclusion of variables for improves the prediction of different stomatal conductance models (BB, BBL, USO, and Jarvis), and showed that, the incorporating water response function improved the performance of the Jarvis, BB, and USO models, but negatively affected the BBL model under varying moisture conditions. These results reveal that models of stomatal responses are complex, and that the accuracy of these models can be affected by different factors, such as different species, test regions, environmental conditions, and time scales (ANDEREGG et al., 2017; HÉROULT et al., 2013; WANG et al., 2018).

Several studies show different results using stomatal conductance models (WANG *et al.*, 2016; WANG et al., 2018; HOSHIKA *et al.*, 2017; LU and WANG et al., 2018). Therefore, it is essential to assess the accuracy of models for a particular study region. The performance of these models can be affected by different factors, such as different species, test regions, environmental conditions and time scales (GAO et al., 2016; WANG et al., 2018). Providing a database of g_1 from planted forests in Brazil, well-fitted by three models will expand the possibilities of studies with models ESMs and PBMs.

4.2 Stomatal responses across PFTs (Gymnosperm and Angiosperms)

The stomatal responses varied across genotypes of this study and between PFTs (Pine and eucalypt). The USO model had the highest slope parameter (g_1) for the gymnosperm group (*Pinus* sp). Studies performed by Lin et al. (2015), evaluating the optimal stomatal behavior around the world found a clear pattern of g_1 variation among different PFTs, with trees angiosperms (3.97) having the largest g_1 than gymnosperm (2.35). Although there are differences in g_1 of PFTs found by Lin et al. (2015) meta-analysis and our results, the g_1 range for the most genotypes in this study is within the range of g_1 for tropical forest (4.43). Angiosperm trees would have larger g_1 than gymnosperms due to their higher sapwood permeability, which yields a lower carbon cost of construction per unit water transported (Lin et al., 2015). This discrepancy between our study and the Lin et al. (2015) may be a consequence of the limited of gymnosperm data in our database of the 22 datasets, 20 are from the eucalypt group and only 2 from the pine group (Table 1).

On another hand, a study by Hasper et al. (2017), using 21 tree species surveyed in tropical central Africa, the g_1 for gymnosperms (3.45) was not lower than that for angiosperms

(3.33), similar to our study. One explanation for these results is that gymnosperm and angiosperm trees may have similar g_1 if measured in similar climates, at least in the tropics (HASPER et al., 2017). The g_1 parameter values for the *Pinus* species of our study (4.30 to 4.96) are close to those derived for *Pinus taeda* ($g_1 = 5.08 \pm 0.49$ - R2: 17%) in Medlyn et al. (2011). However, for two species here (*P. taeda* and *P. caribae* - R2: 66% - table 3), the USO model was better fitted than *Pinus taeda* in North Carolina, USA. These findings suggest that our results could be broadly applicable to other forests in the tropics.

The original optimization theory predicts that stomata are regulated so as to maximize photosynthesis minus the carbon cost of transpiration. From this premise, the model predicts that g_s should be related to photosynthesis, vapor pressure deficit, and atmospheric CO₂ concentration, with a single slope parameter, g_1 . The model also predicts that g_1 should be inversely related to plant water-use efficiency (WUE) (LIN et al., 2015; MEDLYN et al., 2011; MEDLYN et al., 2017). The parameter g_1 is then a measure of WUE that can be directly compared across datasets (MEDLYN et al., 2017). The differences in WUE between the eucalypt and pine groups can be easily visualized in Figure 4. As g_1 was highest in gymnosperms, consequently, this group had lower intrinsic water use efficiency (Figure 4).

4.3 Water-use efficiency and g_1 across genotypes of *Eucalyptus*

We observed a large variation in the slope parameter across 20 genotypes of eucalypt group ($g_1 = 1.42$ to 4.87) (Table 3). Our observed g_1 range is similar to the g_1 range (2.46 to 5.17) of *Eucalyptus* species in Australia (HÉROULT et al., 2013), and also encompasses g_1 (4.27) found by Gimeno et al. (2016) in native *Eucalyptus* woodland. On the other hand, our range of g_1 was lower than the values found by Medlyn et al. (2011) in *Eucalyptus delegatensis* ($g_1: 6.06$) and $g_1(5.67)$ in eucalypt forests found by Yang et al. (2019), both in Australia using the USO approach.

The stomatal behavior is known to vary with environmental factors and with plant traits associated with hydraulic function (LIN et al., 2015; HÉROULT et al., 2013, TUZET et al., 2003). The variation in the g_1 parameter across genotypes of eucalypt and among datasets can be associated by local condition climatic and adaptation of species to the climate of origin. Héroult et al. (2013) found differences among contrasting species in the same genus at the same site for species of eucalyptus. The USO model had the highest g_1 parameter for humid-zone

species and the lowest g_1 parameter for sub-humid climate species that are drought tolerant, suggesting implications for species selections for plantations in these climatic regions (HÉROULT et al., 2013).

Long-standing theory of stomatal behavior suggests that species from more arid habitats that experience frequent droughts are expected to have more conservative stomatal behavior and more efficient use of water per unit carbon gain than species adapted to moist habitats (HÉROULT et al., 2013; COWAN; FARQUHAR 1977; ORIAN; SOLBRIG 1977).

Among the genotypes UG1, U4, E1, E3, LG that had $g_1 < 2$, genotypes UG1 (*E. grandis* x *E. urophylla*) and U4 (*E. urophylla*) should be emphasized because they had the lowest values of g_1 of the dataset, so higher WUE. These genotypes were planted at the site of Piracicaba (ID 1) (Table 1). This result is compatible with recommended for planting. Under humid subtropical with dry winter and hot summer (Cwa climate type), the most recommended genetic materials are the hybrid *E. urophylla* x *grandis* (urograndis) and *E. urophylla* (GONÇALVES et al., 2013). The *E. urophylla* x *grandis* is the genetic material most planted in Brazil since its edaphoclimatic adaptation is compatible with the regions where the largest plantation areas are located. *E. urophylla* has high adaptability to several regions and has been widely hybridized with *E. grandis*, aiming to obtain materials tolerant to droughts and resistant to eucalypt canker (GONÇALVES et al., 2013)

Although the aim of this study was not to analyze changes in the parameter g_1 in response to climatic variables, we can observe differences in g_1 when the same genetic materials were planted in different locations. It is important to be clear that genetic materials do not correspond to the same genotypes. *Eucalyptus grandis* (G2 and G3) in ID1 and 3, *E. grandis* x *E.urophylla* (UG1 and UG4) in ID1 and 2, and the *E. urophylla* (U2, and U3, U4) in ID 2 and 3 (Table 3) had differences in g_1 . These results could be associated with the influence of the climatic variables of each location.

The variation in WUE, and therefore in g_1 in responses to climatic conditions as growth temperature water availability has been studied (LIN et al., 2015; GIMENO et al., 2016). Gimeno et al. (2016) analyzing the conserved stomatal behavior under variations conditions in *Eucalyptus* forest did not find a statistically significant trend of g_1 in response to changing water availability but suggest that g_1 could increase with temperature, entailing a greater marginal water cost of carbon gain under a warmer climate.

Lin et al. (2015) analyzed if low soil water availability should increase WUE, so lower g_1 , and if g_1 should increase with growth temperature. The results demonstrated different degrees of responses in g_1 between moisture index and temperature. In a warm/wet environment, g_1 is higher. However, in a warm/dry environment, g_1 would increase to a smaller degree than in a warm/wet environment. One of the reasons for the increase in g_1 with growth temperature is that the viscosity of water decreases with increasing temperature, making it less costly to transport water, leading to an increased g_1 (PRENTICE et al., 2014; LIN Et al., 2015)

Our results suggest that more studies should be carried out to investigate the influence of local climatic conditions on the g_1 parameter of Brazil forest. It is important to understand whether differences in g_1 were more influenced by the genotype or by local weather conditions.

5. Conclusion

The BBL and USO models had the best performance for the Brazilian forest plantations of eucalypt and pine. The genotypes of the eucalypt group had differences in stomatal responses, indicating that in addition to the genotype characteristics, the local climatic conditions may also have influenced the variation in g_1 . Our study made available a database of g_1 obtained by the three most used models in ESMS and PBMs models, making it possible to expand studies of stomatal conductance modeling in planted forests in Brazil.

6. Acknowledgements

To Federal University of Lavras (UFLA) and Coordination for the Improvement of Higher Education Personnel (CAPES) for all the support.

7. References

ANDEREGG, W. R. L. et al. Plant water potential improves prediction of empirical stomatal models. **Plos One**, v. 12, n. 10, p.1-17, 2017. Public Library of Science (PLoS). <http://dx.doi.org/10.1371/journal.pone.0185481>.

BALL, J. T.; WOODROW, I. E.; BERRY, J. A. A model predicting stomatal conductance and its contribution to the control of photosynthesis under different environmental conditions. In Progress in photosynthesis research (**ed. J Biggins**), v. 4, p. 221–224, 1987. Dordrecht, The Netherlands: Kluwer Academic Publishers.

BINKLEY, D. et al. Explaining growth of individual trees: light interception and efficiency of light use by eucalyptus at four sites in Brazil. **Forest Ecology And Management**, v. 259, n. 9, p. 1704-1713, 2010. <http://dx.doi.org/10.1016/j.foreco.2009.05.037>.

BONAN, G. B. et al. Modeling stomatal conductance in the earth system: linking leaf water-use efficiency and water transport along the soil-plant atmosphere continuum, **Geoscientific Model Development**, v. 7, p. 2193–2222, doi:10.5194/gmd-7-2193-2014, 2014.

BUCKLEY, T. N. How do stomata respond to water status? **New Phytologist**, v. 224, n. 1, p. 21-36, 2019. <http://dx.doi.org/10.1111/nph.15899>.

BUCKLEY, T. N.; MOTT, K. A. Modelling stomatal conductance in response to environmental factors. **Plant, Cell & Environment**, v. 36, n. 9, p.1691-1699, 2013. <http://dx.doi.org/10.1111/pce.12140>

CARNEIRO, R. L. **Caracterização da capacidade fotossintética e da condutância estomática em árvores de *Pinus caribaea* var. *hondurensis* e de *Pinus taeda* em Itatinga, São Paulo**. 2013. 84 p. Dissertação de mestrado em Recursos Florestais - Escola Superior de Agricultura “Luiz de Queiroz”, Universidade de São Paulo, Piracicaba, 2012.

COWAN I. R.; FARQUHAR G. D. Stomatal function in relation to leaf metabolism and environment. In: **Integration of Activity in the Higher Plant** (ed. Jennings DH), pp. 471–505, 1977, Cambridge University Press, Cambridge.

DAMOUR, G. et al. An overview of models of stomatal conductance at the leaf level. **Plant, Cell & Environment**, v. 33. p. 1419-1438, 2010. <http://dx.doi.org/10.1111/j.1365-3040.2010.02181.x>.

DE KAUWE, M. G. et al. Test of the ‘one-point method’ for estimating maximum carboxylation capacity from field-measured, light-saturated photosynthesis. **New Phytologist**, v. 210, n. 3, p. 1130-1144, 2015a. <http://dx.doi.org/10.1111/nph.13815>.

DE KAUWE, M.G et al. A test of an optimal stomatal conductance scheme within the CABLE land surface model. **Geoscientific Model Development**, v. 8, p. 431-452, 2015b.

DUURSMA, R. A. Plantecophys - An R Package for Analysing and Modelling Leaf Gas Exchange Data. **Plos One**, v.10, n.11, 2015.

DUURSMA, R. A.; MEDLYN, B. E. MAESPA: a model to study interactions between water limitation, environmental drivers and vegetation function at tree and stand levels, with an example application to [CO₂]× drought interactions. **Geoscientific Model Development**, v. 5, n. 4, p. 919-940, 2012. <https://doi.org/10.5194/gmd-5-919-2012>, 2012

FARQUHAR, G. D, von CAEMMERER S.; BERRY J. A. A biochemical model of photosynthetic CO₂ assimilation in leaves of C₃ species. **Planta**, v. 149, p. 78–90, 1980.

FRANKS, P. J. et al. Comparing optimal and empirical stomatal conductance models for application in Earth system models. **Global change biology**, v. 24, n. 12, p. 5708-5723, 2018. <https://doi.org/10.1111/gcb.14445>.

GAO, G. L. et al. Environmental response simulation and the up-scaling of plant stomatal conductance. **Acta Ecol. Sin.** v. 36, p.1491–1500, 2016.

GONÇALVES, J. L. M. et al. Integrating genetic and silvicultural strategies to minimize abiotic and biotic constraints in Brazilian eucalypt plantations. **Forest ecology and management**, v. 301, p. 6-27, 2013. <https://doi.org/10.1016/j.foreco.2012.12.030>

GIMENO, T. E. et al. Conserved stomatal behaviour under elevated CO₂ and varying water availability in a mature woodland. **Functional Ecology**, v. 30, n. 5, p. 700–709, 2015. <https://doi.org/10.1111/1365-2435.12532>.

HASPER, T. B. et al. Stomatal CO₂ responsiveness and photosynthetic capacity of tropical woody species in relation to taxonomy and functional traits. **Oecologia**, v. 184, n. 1, p. 43, 2017.

HÉROULT, A. et al. Optimal stomatal conductance in relation to photosynthesis in climatically contrasting Eucalyptus species under drought. **Plant, Cell & Environment**, v. 36, n. 2, p.262-274, 2012. <http://dx.doi.org/10.1111/j.1365-3040.2012.02570.x>.

HOSHIKA, Y. et al. Stomatal conductance models for ozone risk assessment at canopy level in two Mediterranean evergreen forests. **Agricultural And Forest Meteorology**, v. 234-235, p. 212-221, 2017. <https://doi.org/10.1016/j.agrformet.2017.01.005>

IBÁ - Indústria Brasileira de produtores de Árvores. Relatório anual IBÁ 2021, ano base 2020. Instituto Brasileiro de Economia - FGV: 2021. 93p. Disponível em:< <https://iba.org/datafiles/publicacoes/relatorios/relatorioiba2021-compactado.pdf>>. Acesso em: 10 de março, 2021.

JARVIS, P. G. The Interpretation of the Variations in Leaf Water Potential and Stomatal Conductance Found in Canopies in the Field. **Philosophical Transactions Of The Royal Society B: Biological Sciences**, v. 273, n. 927, p. 593-610, 1976. <http://dx.doi.org/10.1098/rstb.1976.0035>.

Jl, S. et al. A modified optimal stomatal conductance model under water-stressed condition. **Int. J. Plant Prod.** v. 11, p. 295–315. 2017.

KATUL G.; LEUNING R.; OREN R. Relationship between plant hydraulic and biochemical properties derived from a steady state coupled water and carbon transport model. **Plant, Cell & Environment**, v. 26, p. 339–350. 2003. <https://doi.org/10.1046/j.1365-3040.2003.00965.x>

LEUNING, R. A critical appraisal of a combined stomatal– photosynthesis model for C3 plants. **Plant, Cell & Environmental**, v. 18, p. 339–355, 1995.

LEUNING, R. Modelling stomatal behaviour and photosynthesis of *Eucalyptus grandis*. **Australian Journal of Plant Physiology** v. 17, p.159-175, 1990.

LI, J. et al. Seasonal change in response of stomatal conductance to vapor pressure deficit and three phytohormones in three tree species. **Plant Signaling & Behavior**, v. 14, n. 2, p. 1682341. 2019. <https://doi.org/10.1080/15592324.2019.1682341>.

LIN, Y. S. et al. Optimal stomatal behaviour around the world. **Nature Climate Change**, v. 5, n.5, p. 459-464. 2015. <https://doi.org/10.1038/nclimate2550>

LIN, Y.-S. et al. Biochemical photosynthetic responses to temperature: how do interspecific differences compare with seasonal shifts? **Tree Physiology**, v. 33, n. 8, p. 793-806, 2013. <http://dx.doi.org/10.1093/treephys/tpt047>.

LU, X.; WANG, L. Evaluating ecohydrological modelling framework to link atmospheric CO₂ and stomatal conductance. **Ecohydrology**, v. 12, n. 1, p.1-11, 2018. <http://dx.doi.org/10.1002/eco.2051>.

MARRICHI, A. H. C. **Caracterização da capacidade fotossintética e da condutância estomática em sete clones comerciais de *Eucalyptus* e seus padrões de resposta ao déficit de pressão de vapor**. 2009. 104 p. Dissertação de Mestrado em Recursos Florestais – Escola Superior de Agricultura “Luiz de Queiroz”, Universidade de São Paulo, Piracicaba, 2009.

MEDLYN, B. E. et al. How do leaf and ecosystem measures of water-use efficiency compare? **New Phytologist**, v. 216, n. 3, p.758-770, 2017. <http://dx.doi.org/10.1111/nph.14626>.

MEDLYN, B. E. et al. Reconciling the optimal and empirical approaches to modelling stomatal conductance. **Global Change Biology**, v. 17, n. 6, p.2134-2144, 2011. <http://dx.doi.org/10.1111/j.1365-2486.2010.02375.x>.

OLESON, K. et al. Technical description of version 4.5 of the Community Land Model (CLM) (No. NCAR/TN-503+STR). 2013. <https://doi.org/10.5065/D6RR1W7M>.

ORIAN G. H.; SOLBRIG O. T. A cost-income model of leaves and roots with special reference to arid and semiarid areas. **American Naturalist**, v. 111, n. 980, p.677–690, 1977. <https://www.jstor.org/stable/2460324>

PRENTICE, I. C. et al. Balancing the costs of carbon gain and water transport: Testing a new theoretical framework for plant functional ecology. **Ecology Letters**. v. 17, n.1, 82-91, 2014. <https://doi.org/10.1111/ele.12211>

TUZET, A.; PERRIER, A.; LEUNING, R. A coupled model of stomatal conductance, photosynthesis and transpiration. **Plant Cell Environmental**, v.26, p. 1097–1116, 2003. <http://dx.doi:10.1046/j.1365-3040.2003.01035>.

WANG, H. et al. Optimization of canopy conductance models from concurrent measurements of sap flow and stem water potential on Drooping Sheoak in South Australia. **Water**

Resources Research, v. 50, n. 7, p. 6154-6167, 2014.
<https://doi.org/10.1002/2013WR014818>.

WANG, Q.; HE, Q.; ZHOU, G. Applicability of common stomatal conductance models in maize under varying soil moisture conditions. **Science Of The Total Environment**, v. 628-629, p.141-149, 2018. <http://dx.doi.org/10.1016/j.scitotenv.2018.01.291>

WANG, Y. P. et al. Diagnosing errors in a land surface model (CABLE) in the time and frequency domains. **Journal of Geophysical Research: Biogeosciences**, v. 116, G01034. p. 1-18, 2011. <https://doi.org/10.1029/2010JG001385>.

WILLIAMS, M.; BOND, B.; RYAN, M. Evaluating different soil and plant hydraulic constraints on tree function using a model and sap flow data from ponderosa pine. **Plant Cell Environment**. v. 24, p. 679–690. 2001. <https://doi.org/10.1046/j.1365-3040.2001.00715.x>.

WONG, S. C.; COWAN, I. R.; FARQUHAR, G. D. Stomatal Conductance Correlates with photosynthetic capacity. **Nature**, v. 282, p. 424– 426, 1979. <https://doi.org/10.1038/282424a0>

WU, J. et al. The response of stomatal conductance to seasonal drought in tropical forests. **Global change biology**, v. 26, n. 2, p. 823-839, 2020. <https://doi.org/10.1111/gcb.14820>.

YANG, J. et al. Incorporating non-stomatal limitation improves the performance of leaf and canopy models at high vapour pressure deficit. **Tree Physiology**, p.1-14, 2019.
<http://dx.doi.org/10.1093/treephys/tpz103>

ZHANG, N. et al. Can the Responses of Photosynthesis and Stomatal Conductance to Water and Nitrogen Stress Combinations Be Modeled Using a Single Set of Parameters? **Frontiers In Plant Science**, v. 8, p.1-20, 2017. <http://dx.doi.org/10.3389/fpls.2017.00328>

3. CONSIDERAÇÕES FINAIS

Encontramos neste estudo parâmetros fotossintéticos V_{cmax} , J_{max} e parâmetros que explicam o comportamento estomático (g_1) a partir de um extenso conjunto de dados fisiológicos das florestas plantadas de eucalipto e pinus no Brasil. Nosso estudo amplia o banco de dados de parâmetros fisiológicos para as florestas plantadas do Brasil, possibilitando o uso destes parâmetros em estudos de modelagem ecofisiológica, que ainda são incipientes nas florestas brasileiras. Nós modelamos os parâmetros mais utilizados para parametrização dos modelos baseados em processos e para os modelos globais da vegetação que estudam o crescimento e a distribuição dos ecossistemas florestais nas condições climáticas atuais e em cenários futuros. Fornecemos aqui, parâmetros específicos para os dois gêneros (*Eucalyptus* e *Pinus*) mais plantados no Brasil, obtidos sob diferentes condições climáticas. O uso específico destes parâmetros para os gêneros *Eucalyptus* e *Pinus* fornece informações precisas sobre a capacidade fotossintética e a eficiência do uso da água e melhoram a simulação da produtividade florestal. Nós também fornecemos aqui, informações sobre a influência climática na capacidade fotossintética destas florestas, esclarecendo a importância de considerar as variáveis temperatura e precipitação ao modelar os processos fotossintéticos. Essas informações melhoram a compreensão sobre o comportamento dos diferentes genótipos nas diferentes condições climáticas, para desenvolver melhores estratégias de gestão das florestas plantadas.